

SRINIVASAN COLLEGE OF ARTS AND SCIENCE
(Affiliated to Bharathidasan University Trichy)
PERAMBALUR – 62121

DEPARTMENT OF CHEMISTRY

COURSE MATERIAL

II M.Sc., CHEMISTRY

PHYSICAL METHODS IN CHEMISTRY II

Subject Code : P16CH41

Prepared & Compiled

Mr. D. Madhan Kumar
Assistnat Professor in Chemistry
Srinivasan College of Arts & Science
Perambalur – 621 212

PHYSICAL METHODS IN CHEMISTRY II (syllabus)**UNIT I: Electronic Spectroscopy**

Microstates, terms and energy levels for d1 – d9 ions in cubic and square fields– intensity of bands – group theoretical approach to selection rules – effect of distortion and spin-orbit coupling on spectra – evaluation of $10Dq$ and β for octahedral complexes of cobalt and nickel – applications to simple coordination compounds – charge transfer spectra – electronic spectra of $[\text{Ru}(\text{bipy})_3]^{2+}$. Optical rotatory dispersion and circular dichroism and magnetic circular dichroism – applications to metal complexes.

UNIT II: Infrared and Raman Spectroscopy

Vibrations in simple molecules (H_2O , CO_2) and their symmetry notation for molecular vibrations – group vibrations and the limitations – combined uses of IR and Raman spectroscopy in the structural elucidation of simple molecules like N_2O , ClF_3 , NO_3^- , ClO_4^- – effect of coordination on ligand vibrations – uses of group vibrations in the structural elucidation of metal complexes of urea, thiourea, cyanide, thiocyanate and dimethyl sulfoxide. Effect of isotopic substitution on the vibrational spectra of molecules – vibrational spectra of metal carbonyls with reference to the nature of bonding – geometry and number of C-O stretching vibrations (group theoretical treatment) – applications of Raman spectroscopy – resonance Raman spectroscopy.

UNIT III: NMR Spectroscopy

Examples for different spin systems – chemical shifts and coupling constants (spin-spin coupling) involving different nuclei (^1H , ^{19}F , ^{31}P , ^{13}C) interpretation and applications to inorganic compounds – Effect of quadrupolar nuclei (^2H , ^{10}B , ^{11}B) on the ^1H NMR spectra. Systems with chemical exchange – evaluation of thermodynamic parameters in simple systems – study of fluxional behaviour of molecules – NMR of paramagnetic molecules – isotropic shifts contact and pseudo-contact interactions – lanthanide shift reagents.

UNIT IV: EPR Spectroscopy and Magnetic properties

Theory of EPR spectroscopy – spin densities and McConnell relationship – factors affecting the magnitude of g and A tensors in metal species – zero-field splitting and Kramers degeneracy – spectra of V(II), Mn(II), Fe(II), Co(II), Ni(II) and Cu(II) complexes – applications of EPR to a few biological molecules containing Cu(II) and Fe(III) ions. Magnetic properties – types of magnetism – dia-, para-, ferro- and antiferromagnetism – magnetic properties of free ions – first-order Zeeman effect – second-order Zeeman effect – states KT – states $\lll KT$ – determination of magnetic moments and their applications to the elucidation of structures of inorganic compounds – temperature independent paramagnetism – magnetic properties of lanthanides and actinides – spin crossover in coordination compounds.

UNIT V: Mossbauer Spectroscopy

Isomer shifts – quadrupole splitting – magnetic interactions – applications to iron and tin compounds. NQR spectroscopy – characteristics of quadrupolar nucleus – effects of field gradient and magnetic field upon quadrupolar energy levels – NQR transitions – applications of NQR spectroscopy.

Unit I

Electronic spectroscopy

spectroscopic term of the ground state of an atom

Hund's rule predicts the stable state of an atom to have large number of unpaired electrons (High spin configuration). The ground state is given by a term, $2S + 1LJ$,

Where, the superscript $(2S + 1)$ is the maximum multiplicity, L is the total orbital angular momentum and J is the total angular momentum arising out of coupling between the spin and orbital angular momentum.

J will be equal to $(L + S)$ for more than half-filled degenerate orbitals and $(L - S)$ for equal & less than half-filled degenerate orbitals.

ü For carbon with atomic number 6, electronic configuration is $1s^2 2s^2 2p^2$.

p-orbital is degenerate with three sub orbitals, with different magnetic quantum numbers. The two electrons can occupy these orbitals, in many ways, subjected to Pauli's exclusion principle.

There are three possible states corresponding to three positive 'L' values and among them the ground state has the term symbol of $3P_2$.

Number of unpaired electrons	S	2S + 1	L	J	Term	Ground state	
$\uparrow\downarrow$	0	0	1	2	1	1D1	3P2
$\uparrow \uparrow$	2	1	3	1	3P2		
$\uparrow \uparrow$	2	1	3	0	3	3S3	

Atomic Term Symbols

In electronic spectroscopy, an atomic term symbol specifies a certain electronic state of an atom (usually a multi-electron one), by briefing the quantum numbers for the angular momenta of that atom. The form of an atomic term symbol implies **Russell-Saunders** coupling. Transitions between two different atomic states may be represented using their term symbols, to which certain rules apply.

History

At the beginning, the spectroscopic notation for term symbols was derived from an obsolete system of categorizing spectral lines. In 1885, Johann Balmer, a Swiss mathematician, discovered the Balmer formula for a series of hydrogen emission lines.

$$\lambda = B(m^2 - 4n^2) \quad (1)$$

where

- B is constant, and M is an integer greater than 2.

Later it was extended by Johannes Rydberg and Walter Ritz.

Yet this principle could hardly explain the discovery of fine structure, the splitting of spectral lines. In spectroscopy, spectral lines of alkali metals used to be divided into categories: sharp, principal, diffuse and fundamental, based on their fine structures. These categories, or "term series," then became associated with atomic energy levels along with the birth of the old quantum theory. The initials of those categories were employed to mark the atomic orbitals with respect to their azimuthal quantum numbers. The sequence of "s, p, d, f, g, h, i, k..." is known as the spectroscopic notation for atomic orbitals.

By introducing spin as a nature of electrons, the fine structure of alkali spectra became further understood. The term "spin" was first used to describe the rotation of electrons. Later, although electrons have been proved unable to rotate, the word "spin" is reserved and used to describe the property of an electron that involves its intrinsic magnetism. LS coupling was first proposed by Henry Russell and Frederick Saunders in 1923. It perfectly explained the fine structures of hydrogen-like atomic spectra. The format of term symbols was developed in the Russell-Saunders coupling scheme.

Term Symbols

In the Russell-Saunders coupling scheme, term symbols are in the form of $^{2S+1}L_J$, where S represents the total spin angular momentum, L specifies the total orbital angular momentum, and

J refers to the total angular momentum. In a term symbol, L is always an upper-case from the sequence "s, p, d, f, g, h, i, k...", wherein the first four letters stand for sharp, principal, diffuse and fundamental, and the rest follow in an alphabetical pattern. Note that the letter j is omitted.

Angular momenta of an electron

In today's physics, an electron in a spherically symmetric potential field can be described by four quantum numbers all together, which applies to hydrogen-like atoms only. Yet other atoms may undergo trivial approximations in order to fit in this description. Those quantum numbers each present a conserved property, such as the orbital angular momentum. They are sufficient to distinguish a particular electron within one atom. The term "angular momentum" describes the phenomenon that an electron distributes its position around the nucleus. Yet the underlying quantum mechanics is much more complicated than mere mechanical movement.

- **The azimuthal angular momentum:** The azimuthal angular momentum (or the orbital angular momentum when describing an electron in an atom) specifies the azimuthal component of the total angular momentum for a particular electron in an atom. The orbital quantum number, l , one of the four quantum numbers of an electron, has been used to represent the azimuthal angular momentum. The value of l is an integer ranging from 0 to $n-1$, while n is the principal quantum number of the electron. The limits of l came from the solutions of the Schrödinger Equation.
- **The intrinsic angular momentum:** The intrinsic angular momentum (or the spin) represents the intrinsic property of elementary particles, and the particles made of them. The inherent magnetic momentum of an electron may be explained by its intrinsic angular momentum. In LS-coupling, the spin of an electron can couple with its azimuthal angular momentum. The spin quantum number of an electron has a value of either $\frac{1}{2}$ or $-\frac{1}{2}$, which reflects the nature of the electron.

Coupling of the electronic angular momenta

Coupling of angular momenta was first introduced to explain the fine structures of atomic spectra. As for LS coupling, S , L , J and M_J are the four "good" quantum numbers to describe electronic states in lighter atoms. For heavier atoms, jj coupling is more applicable, where J , M_J , M_L and M_s are "good" quantum numbers.

LS coupling

LS coupling, also known as Russell-Saunders coupling, assumes that the interaction between an electron's intrinsic angular momentum s and its orbital angular momentum L is small enough to be considered as a perturbation to the electronic Hamiltonian. Such interactions can be derived in a classical way. Let's suppose that the electron goes around the nucleus in a circular orbit, as

in Bohr model. Set the electron's velocity to be \mathbf{V}_e . The electron experiences a magnetic field \mathbf{B} due to the relative movement of the nucleus

$$\mathbf{B} = \frac{1}{4\pi\epsilon_0} \frac{Ze}{r^3} (\mathbf{E} \times \mathbf{p}) = \frac{Ze}{4\pi\epsilon_0} \frac{2\mathbf{L}}{r^3} \quad (2)$$

while \mathbf{E} is the electric field at the electron due to the nucleus, \mathbf{p} the classical momentum of the electron, and r the distance between the electron and the nucleus. The electron's spin \mathbf{s} brings a magnetic dipole moment $\boldsymbol{\mu}_s$

$$\boldsymbol{\mu}_s = -g_s \frac{e}{2m} \hbar \mathbf{s} \quad (3)$$

where g_s is the gyromagnetic ratio of an electron. Since the potential energy of the coulombic attraction between the electron and nucleus is⁶

$$V(r) = -\frac{Ze^2}{4\pi\epsilon_0 r} \quad (4)$$

the interaction between $\boldsymbol{\mu}_s$ and \mathbf{B} is

$$H^{so} = g_s \frac{e}{2m} \hbar \frac{Ze^2}{4\pi\epsilon_0 r^2} (\mathbf{L} \cdot \mathbf{s}) = g_s \frac{e}{2m} \hbar \frac{\partial V}{\partial r} (\mathbf{L} \cdot \mathbf{s}) \quad (5)$$

After a correction due to centripetal acceleration¹⁰, the interaction has a format of

$$H^{so} = \frac{1}{2} \mu_B \frac{\partial V}{\partial r} (\mathbf{L} \cdot \mathbf{s}) \quad (6)$$

Thus the coupling energy is

$$\langle \psi n l m | H^{so} | \psi n l m \rangle \quad (7)$$

In lighter atoms, the coupling energy is low enough to be treated as a first-order perturbation to the total electronic Hamiltonian, hence LS coupling is applicable to them. For a single electron, the spin-orbit coupling angular momentum quantum number j has the following possible values

$$j = |l-s|, \dots, l+s$$

if the total angular momentum \mathbf{J} is defined as $\mathbf{J} = \mathbf{L} + \mathbf{s}$. The azimuthal counterpart of j is m_j , which can be a whole number in the range of $[-j, j]$.

The first-order perturbation to the electronic energy can be deduced so⁶

$$\frac{\hbar^2}{4} [j(j+1) - l(l+1) - s(s+1)] \mu_B \int_0^\infty r^2 dr \frac{\partial V}{\partial r} R_{nl}^2(r) \quad (8)$$

Above is about the spin-orbit coupling of one electron. For many-electron atoms, the idea is similar. The coupling of angular momenta is

$$\mathbf{J}=\mathbf{L}+\mathbf{S}(9)$$

thereby the total angular quantum number

$$J = |L-S|, \dots, L+S$$

where the total orbital quantum number

$$L=\sum l_i(10)$$

and the total spin quantum number

$$S=\sum s_i(11)$$

While \mathbf{J} is still the total angular momentum, \mathbf{L} and \mathbf{S} are the total orbital angular momentum and the total spin, respectively. The magnetic momentum due to \mathbf{J} is

$$\mu_J = -g_J \mu_B \mathbf{J} / \hbar \quad (12)$$

wherein the Landé g factor is

$$g_J = 1 + \frac{J(J+1) + S(S+1) - L(L+1)}{2J(J+1)} \quad (13)$$

supposing the gyromagnetic ratio of an electron is 2.

jj coupling

For heavier atoms, the coupling between the total angular momenta of different electrons is more significant, causing the fine structures not to be "fine" any more. Therefore the coupling term can no more be considered as a perturbation to the electronic Hamiltonian, so that jj coupling is a better way to quantize the electron energy states and levels.

For each electron, the quantum number $j = l + s$. For the whole atom, the total angular momentum quantum number

$$J=\sum j_i(14)$$

Term symbols for an Electron Configuration

Term symbols usually represent electronic states in the Russell-Saunders coupling scheme, where a typical atomic term symbol consists of the spin multiplicity, the symmetry label and the total angular momentum of the atom. They have the format of

$$2S+1LJ(15)$$

such as 3D_2 , where $S = 1$, $L = 2$, and $J = 2$.

Here is a commonly used method to determine term symbols for an electron configuration. It requires a table of possibilities of different "micro states," which happened to be called "Slater's table".⁶ Each row of the table represents a total magnetic quantum number, while each column does a total spin. Using this table we can pick out the possible electronic states easily since all terms are concentric rectangles on the table.

The method of using a table to count possible "microstates" has been developed so long ago and honed by so many scientists and educators that it is hard to accredit a single person. Let's take the electronic configuration of d^3 as an example. In the Slater's table, each cell contains the number of ways to assign the three electrons quantum numbers according to the M_S and M_L values. These assignments follow Pauli's exclusion law. The figure below shows an example to find out how many ways to assign quantum numbers to d^3 electrons when $M_L = 3$ and $M_S = -1/2$.

		ml				ML	MS	
		+2	+1	0	-1			-2
	↓	↓	↑	↓			3	-1/2
	↓	↓	↓	↑			3	-1/2
	↑	↓	↓				3	-1/2
	↑↓				↓		3	-1/2

		MS			
		-3/2	-1/2	1/2	3/2
ML	5	0	1	1	0
	4	0	2	2	0
	3	1	4	4	1
	2	1	6	6	1

	1	2	8	8	2
	0	2	8	8	2
	-1	2	8	8	2
	-2	1	6	6	1
	-3	1	4	4	1
	-4	0	2	2	0
	-5	0	1	1	0

Now we start to subtract term symbols from this table. First there is a 2H state. And now it is subtracted from the table.

		M_s			
		$-3/2$	$-1/2$	$1/2$	$3/2$
M_L	5	0	0	0	0
	4	0	1	1	0
	3	1	3	3	1
	2	1	5	5	1
	1	2	7	7	2
	0	2	7	7	2
	-1	2	7	7	2
	-2	1	5	5	1
	-3	1	3	3	1
	-4	0	1	1	0
	-5	0	0	0	0

And now is a 4F state. After being subtracted by 4F , the table becomes

		M _s			
		-3/2	-1/2	1/2	3/2
M _L	5	0	0	0	0
	4	0	1	1	0
	3	0	2	2	0
	2	0	4	4	0
	1	1	6	6	1
	0	1	6	6	1
	-1	1	6	6	1
	-2	0	4	4	0
	-3	0	2	2	0
	-4	0	1	1	0
	-5	0	0	0	0

And now ²G.

		M _s			
		-3/2	-1/2	1/2	3/2
M _L	5	0	0	0	0
	4	0	0	0	0
	3	0	1	1	0
	2	0	3	3	0
	1	1	5	5	1
	0	1	5	5	1
	-1	1	5	5	1

	-2	0	3	3	0
	-3	0	1	1	0
	-4	0	0	0	0
	-5	0	0	0	0

Now 2F .

		M_s			
		$-3/2$	$-1/2$	$1/2$	$3/2$
M_L	5	0	0	0	0
	4	0	0	0	0
	3	0	0	0	0
	2	0	2	2	0
	1	1	4	4	1
	0	1	4	4	1
	-1	1	4	4	1
	-2	0	2	2	0
	-3	0	0	0	0
	-4	0	0	0	0
	-5	0	0	0	0

Here in the table are two 2D states.

		M _s			
		-3/2	-1/2	1/2	3/2
M _L	5	0	0	0	0
	4	0	0	0	0
	3	0	0	0	0
	2	0	0	0	0
	1	1	2	2	1
	0	1	2	2	1
	-1	1	2	2	1
	-2	0	0	0	0
	-3	0	0	0	0
	-4	0	0	0	0
	-5	0	0	0	0

⁴P.

		M _s			
		-3/2	-1/2	1/2	3/2
M _L	5	0	0	0	0
	4	0	0	0	0
	3	0	0	0	0
	2	0	0	0	0
	1	0	1	1	0
	0	0	1	1	0
	-1	0	1	1	0

	-2	0	0	0	0
	-3	0	0	0	0
	-4	0	0	0	0
	-5	0	0	0	0

And the final deduced state is 2P . So in total the possible states for a d^3 configuration are 4F , 4P , 2H , 2G , 2F , 2D , 2D and 2P . Taken J into consideration, the possible states are:

$4F24F34F44P04P14P22H922H1122G922G722F722F522D522D522D322D322P322P32(16)$

For lighter atoms before or among the first-row transition metals, this method works well.

Using group theory to determine term symbols

Another method is to use direct products in group theory to quickly work out possible term symbols for a certain electronic configuration. Basically, both electrons and holes are taken into consideration, which naturally results in the same term symbols for complementary configurations like p^2 vs p^4 . Electrons are categorized by spin, therefore divided into two categories, α and β , as are holes: α stands for +1, and β stands for -1, or vice versa. Term symbols of different possible configurations within one category are given. The term symbols for the total electronic configuration are derived from direct products of term symbols for different categories of electrons. For the p^3 configuration, for example, the possible combinations of different categories are e_α^3 , e_β^3 , $e_\alpha^2e_\beta$ and $e_\alpha e_\beta^2$. The first two combinations were assigned the partial term of S .⁶ As e_α^2 and e_β were given an P symbol, the combination of them gives their direct product

$$P \times P = S + [P] + D.$$

The direct product for e_α and e_β^2 is also

$$P \times P = S + [P] + D.$$

Considering the degeneracy, eventually the term symbols for p^3 configuration are 4S , 2D and 2P .

There is a specially modified version of this method for atoms with 2 unpaired electrons. The only step gives the direct product of the symmetries of the two orbitals. The degeneracy is still determined by Pauli's exclusion.

Determining the ground state

In general, states with a greater degeneracy have a lower energy. For one configuration, the level with the largest S , which has the largest spin degeneracy, has the lowest energy. If two levels have the same S value, then the one with the larger L (and also the larger orbital degeneracy) have the lower energy. If the electrons in the subshell are fewer than half-filled, the ground state should have the smallest value of J , otherwise the ground state has the greatest value of J .

Electronic transitions

Electrons of an atom may undergo certain transitions which may have strong or weak intensities. There are rules about which transitions should be strong and which should be weak. Usually an electronic transition is excited by heat or radiation. Electronic states can be interpreted by solutions of Schrödinger's equation. Those solutions have certain symmetries, which are a factor of whether transitions will be allowed or not. The transition may be triggered by an electric dipole momentum, a magnetic dipole momentum, and so on. These triggers are transition operators. The most common and usually most intense transitions occur in an electric dipolar field, so the selection rules are

1. $\Delta L = 0, \pm 1$ except $L = 0 \ddagger L' = 0$
2. $\Delta S = 0$
3. $\Delta J = 0; \pm 1$ except $J = 0 \ddagger J' = 0$

where a double dagger means not combinable. For jj coupling, only the third rule applies with an addition rule: $\Delta j = 0; \pm 1$.

Selection Rules for Electronic Spectra of Transition Metal Complexes

The Selection Rules governing transitions between electronic energy levels of transition metal complexes are:

1. $\Delta S = 0$ The Spin Rule
2. $\Delta l = \pm 1$ The Orbital Rule (or Laporte)

The first rule says that allowed transitions must involve the promotion of electrons without a change in their spin. The second rule says that if the molecule has a center of symmetry, transitions within a given set of p or d orbitals (i.e. those which only involve a redistribution of electrons within a given subshell) are forbidden.

Relaxation of these rules can occur through:

- **Spin-Orbit coupling:** this gives rise to weak spin forbidden bands
- **Vibronic coupling:** an octahedral complex may have allowed vibrations where the molecule is asymmetric. Absorption of light at that moment is then possible.
- **Mixing:** π -acceptor and π -donor ligands can mix with the d-orbitals so transitions are no longer purely d-d.

Selection rules and transition moment integral

In chemistry and physics, selection rules define the transition probability from one eigenstate to another eigenstate. In this topic, we are going to discuss the transition moment, which is the key to understanding the intrinsic transition probabilities. Selection rules have been divided into the electronic selection rules, vibrational selection rules (including Franck-Condon principle and vibronic coupling), and rotational selection rules.

Introduction

The transition probability is defined as the probability of particular spectroscopic transition to take place. When an atom or molecule absorbs a photon, the probability of an atom or molecule to transit from one energy level to another depends on two things: the nature of initial and final state wavefunctions and how strongly photons interact with an eigenstate. Transition strengths are used to describe transition probability. Selection rules are utilized to determine whether a transition is allowed or not. Electronic dipole transitions are by far the most important for the topics covered in this module.

Transition Moment

In an atom or molecule, an electromagnetic wave (for example, visible light) can induce an oscillating electric or magnetic moment. If the frequency of the induced electric or magnetic moment is the same as the energy difference between one eigenstate Ψ_1 and another eigenstate Ψ_2 , the interaction between an atom or molecule and the electromagnetic field is resonant (which means these two have the same frequency). Typically, the amplitude of this (electric or magnetic) moment is called the transition moment. In quantum mechanics, the transition probability of one molecule from one eigenstate Ψ_1 to another eigenstate Ψ_2 is given by $|\mathbf{M}^{\rightarrow} 21|^{21}$, and $\mathbf{M}^{\rightarrow} 21$ is called the transition dipole moment, or transition moment, from Ψ_1 to Ψ_2 . In mathematical form it can be written as

$$\mathbf{M}^{\rightarrow} 21 = \int \Psi_2 \mu^{\rightarrow} \Psi_1 d\tau$$

The Ψ_1 and Ψ_2 are two different eigenstates in one molecule, $M \rightarrow 21M \rightarrow 21$ is the electric dipole moment operator. If we have a system with n molecules and each has charge Q_n , and the dipole moment operator is can be written as

$$\vec{\mu} = \sum_n Q_n \vec{x}_n \rightarrow n \quad (2)(2) \mu \rightarrow = \sum_n Q_n \vec{x}_n \rightarrow n$$

the $\vec{x}_n \rightarrow n$ is the position vector operator.

Transition Moment Integral

Based on the Born-Oppenheimer approximation, the fast electronic motion can be separated from the much slower motion of the nuclei. As a result, the total wavefunction can be separated into electronic, vibrational, and rotational parts:

$$\Psi(r, R) = \psi_e(r, R_e) \psi_v(R) \psi_r(R) \quad \Psi(r, R) = \psi_e(r, R_e) \psi_v(R) \psi_r(R)$$

The Born-Oppenheimer approximation assumes that the electronic wavefunction, ψ_e , is approximated in all electronic coordinates at the equilibrium nuclear coordinates (R_e). Since mass of electrons is much smaller than nuclear mass, the rotational wavefunction, ψ_r , only depends on nuclear coordinates. The rotational wavefunction could provide important information for rotational selection rules, but we will not consider the rotational wavefunction any further for simplicity because most of the spectra are not rotationally resolved. With the rotational part removed, the transition moment integral can be expressed as

$$M = \iint \psi'_e(r, R_e) \cdot \psi'_v(R) (\mu_e + \mu_n) \psi''_e(r, R_e) \cdot \psi''_v(R) dr dR \quad M = \iint \psi'_e(r, R_e) \cdot \psi'_v(R) (\mu_e + \mu_n) \psi''_e(r, R_e) \cdot \psi''_v(R) dr dR$$

where the prime and double prime represent the upper and lower states respectively. Both the nuclear and electronic parts contribute to the dipole moment operator. The above equation can be integrated by two parts, with μ_n and μ_e respectively. A product of two integral is obtained:

$$M = \int \psi'_e(r, R_e) \cdot \mu_e \cdot \psi''_e(r, R_e) dr \int \psi'_v(R) \cdot \psi''_v(R) dR + \int \psi'_v(R) \cdot \mu_n \cdot \psi''_v(R) dR \int \psi'_e(r, R_e) \psi''_e(r, R_e) dr \quad M = \int \psi'_e(r, R_e) \cdot \mu_e \cdot \psi''_e(r, R_e) dr \int \psi'_v(R) \cdot \psi''_v(R) dR + \int \psi'_v(R) \cdot \mu_n \cdot \psi''_v(R) dR \int \psi'_e(r, R_e) \psi''_e(r, R_e) dr$$

Because different electronic wavefunctions must be orthogonal to each other, hence $\int \psi'_e(r, R_e) \psi''_e(r, R_e) dr$ is zero, the second part of the integral should be zero.

The transition moment integral can be simplified as

$$M = \int \psi'_e(r, R_e) \cdot \mu_e \cdot \psi''_e(r, R_e) dr \int \psi'_v(R) \cdot \psi''_v(R) dR \quad M = \int \psi'_e(r, R_e) \cdot \mu_e \cdot \psi''_e(r, R_e) dr \int \psi'_v(R) \cdot \psi''_v(R) dR$$

The above equation is of great importance because the first integral defines the electronic selection rules, while the second integral is the basis of vibrational selection rules.

Electronic Selection Rules

In atoms

Atoms are described by the primary quantum number n , angular momentum quantum number L , spin quantum number S , and total angular momentum quantum number J . Based on Russell-Saunders approximation of electron coupling, the atomic term symbol can be represented as $^{2S+1}L_J$.

1. The total spin cannot change, $\Delta S=0$;
2. The change in total orbital angular momentum can be $\Delta L=0, \pm 1$, but $L=0 \leftrightarrow L=0$ transition is not allowed;
3. The change in the total angular momentum can be $\Delta J=0, \pm 1$, but $J=0 \leftrightarrow J=0$ transition is not allowed;
4. The initial and final wavefunctions must change in parity. Parity is related to the orbital angular momentum summation over all electrons $\sum l_i$, which can be even or odd; only even \leftrightarrow odd transitions are allowed.
 - A_g for allowed transitions. Therefore, only $g \leftrightarrow u$ transition is allowed.

Vibrational Selection rules

1. Transitions with $\Delta v=\pm 1, \pm 2, \dots$ are all allowed for anharmonic potential, but the intensity of the peaks become weaker as Δv increases.
2. $v=0$ to $v=1$ transition is normally called the fundamental vibration, while those with larger Δv are called overtones.
3. $\Delta v=0$ transition is allowed between the lower and upper electronic states with energy E_1 and E_2 are involved, i.e. $(E_1, v''=n) \rightarrow (E_2, v'=n)$, where the double prime and prime indicate the lower and upper quantum state.

The geometry of vibrational wavefunctions plays an important role in vibrational selection rules. For diatomic molecules, the vibrational wavefunction is symmetric with respect to all the electronic states. Therefore, the Franck-Condon integral is always totally symmetric for diatomic molecules. The vibrational selection rule does not exist for diatomic molecules.

For polyatomic molecules, the nonlinear molecules possess $3N-6$ normal vibrational modes, while linear molecules possess $3N-5$ vibrational modes. Based on the harmonic oscillator model, the product of $3N-6$ normal mode wavefunctions contribute to the total vibrational wavefunction, i.e.

$$\psi_{\text{vib}} = \prod_{i=1}^{3N-6} \psi_i^{v_i}$$

where each normal mode is represented by the wavefunction $\psi_i^{v_i}$. Comparing to the Franck-Condon factor for diatomic molecules with single vibrational overlap integral, a product of $3N-6$ ($3N-5$ for linear molecules) overlap integrals needs to be evaluated. Based on the symmetry of each normal vibrational mode, polyatomic vibrational wavefunctions can be totally symmetric or non-totally symmetric. If a normal mode is totally symmetric, the vibrational wavefunction is totally symmetric with respect to all the vibrational quantum number v . If a normal mode is non-totally symmetric, the vibrational wavefunction alternates between symmetric and non-symmetric wavefunctions as v alternates between even and odd number.

If a particular normal mode in both the upper and lower electronic state is totally symmetric, the vibrational wavefunction for the upper and lower electronic state will be symmetric, resulting in the totally symmetric integrand in the Franck-Condon integral. If the vibrational wavefunction of either the lower or upper electronic state is non-totally symmetric, the Franck-Condon integrand will be non-totally symmetric.

We will use CO_2 as an example to specify the vibrational selection rule. CO_2 has four vibrational modes as a linear molecule. The vibrational normal modes are illustrated in the figure below:

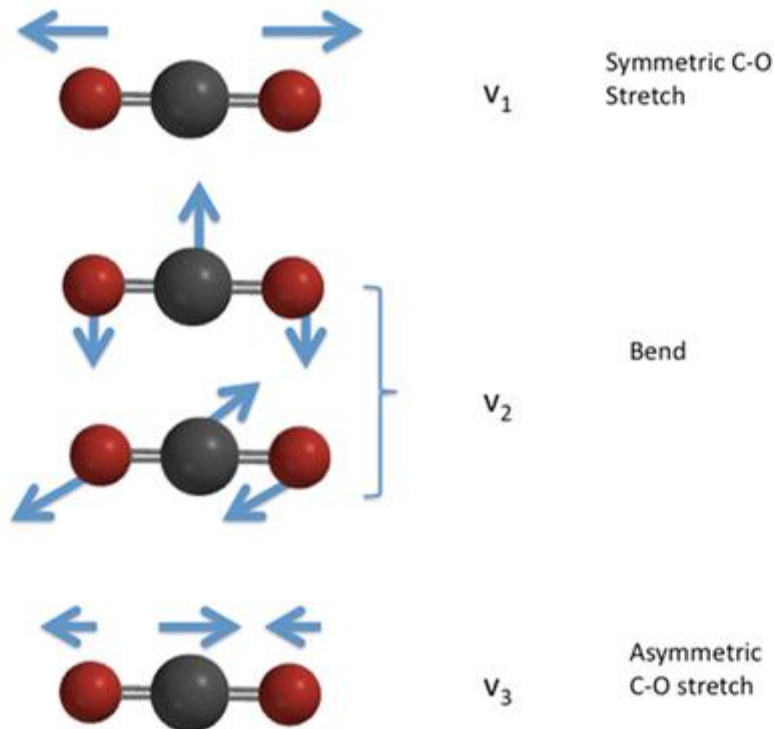


Fig. 1 Vibrational modes of CO_2

The vibrational wavefunction for the totally symmetric C-O stretch, ν_1 , is totally symmetric with respect to all the vibrational quantum numbers. However, the vibrational wavefunctions for the doubly degenerate bending modes, ν_2 , and the antisymmetric C-O stretch, ν_3 , are non-totally symmetric. Therefore, the vibrational wavefunctions are totally symmetric for even vibrational quantum numbers ($\nu=0, 2, 4\dots$), while the wavefunctions remain non-totally symmetric for ν odd ($\nu=1, 3, 5\dots$).

Therefore, any value of $\Delta\nu_1$ is possible between the upper and lower electronic state for mode ν_1 . On the other hand, modes ν_2 and ν_3 include non-totally symmetric vibrational wavefunctions, so the vibrational quantum number can only change evenly, such as $\Delta\nu=\pm\pm 2, \pm\pm 4$, etc..

Franck-Condon Principle

Franck-Condon principle was proposed by German physicist James Franck (1882-1964) and U.S. physicist Edward U. Condon (1902-1974) in 1926. This principle states that when an electronic transition takes place, the time scale of this transition is so fast compared to nucleus motion that we can consider the nucleus to be static, and the vibrational transition from one vibrational state to another state is more likely to happen if these states have a large overlap. It successfully explains the reason why certain peaks in a spectrum are strong while others are weak (or even not observed) in absorption spectroscopy.

$$M = \int \psi' e(r, R_e) \cdot \mu e \cdot \psi'' e(r, R_e) dr \int \psi' v(R) \cdot \psi'' v(R) dR \quad M = \int \psi e'(r, R_e) \cdot \mu e \cdot \psi e''(r, R_e) dr \int \psi v'(R) \cdot \psi v''(R) dR$$

The second integral in the above equation is the vibrational overlap integral between one eigenstate and another eigenstate. In addition, the square of this integral is called the Franck-Condon factor:

$$\text{Franck-Condon Factor} = \left| \int \psi' v \psi'' v dR \right|^2 \quad \text{Franck-Condon Factor} = \left| \int \psi v' \psi v'' dR \right|^2$$

It governs the vibrational transition contribution to the transition probability and shows that in order to have a large vibrational contribution, the vibrational ground state and excited state must have a strong overlap.

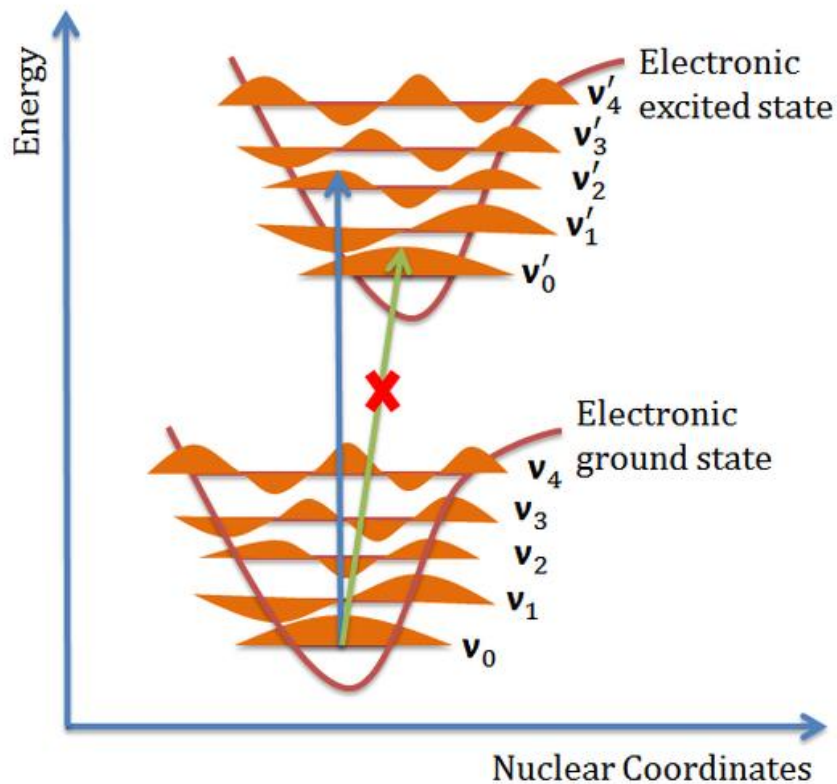


Fig. 2 Franck-Condon energy diagram

The above figure shows the Franck-Condon principle energy diagram, since electronic transition time scale is small compared to nuclear motion, the vibrational transitions are favored when the vibrational transition have the smallest change of nuclear coordinate, which is a vertical transition in the figure above. The electronic eigenstates favors the vibrational transition $v=0$ in the ground electronic state to $v''=2$ in the excited electronic state, while peak intensity of $v=0$ to $v''=0$ transition is expected to be low because the overlap between the $v=0$ wavefunction and $v''=0$ wavefunction is very low.

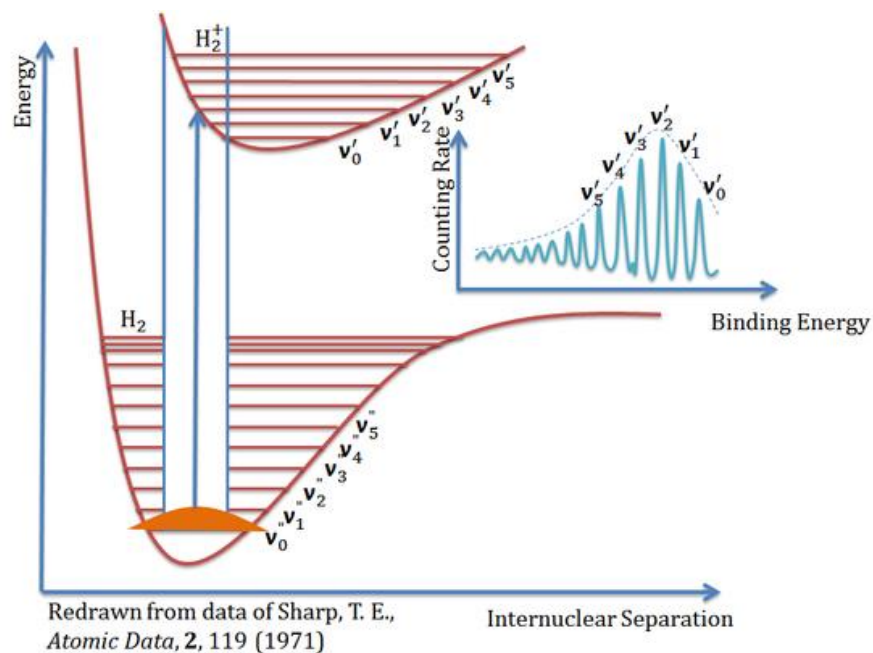


Fig. 3 Photoelectron spectrum of the ionization of H_2

The figure above is the photoelectron spectrum of the ionization of hydrogen molecule (H_2), it is also a beautiful example to formulate the Franck-Condon principle. It shows the appropriate energy curves and the vibrational energy levels, and with the help of the Franck-Condon principle, the transition between ground vibrational state v_0 and excited vibrational state v_2' is expected to be the most intense peak in the spectrum.

Vibronic Coupling

Why can some electronic-forbidden transitions be observed as weak bands in spectrum? It can be explained by the interaction between the electronic and vibrational transitions. The word "vibronic" is the combination of the words "vibrational" and "electronic." Because the energy required for one electronic state to another electronic state (electronic transition, usually in the UV-Vis region) is larger than one vibrational state to another vibrational state (vibrational transition, usually in the IR region), sometimes energy (a photon) can excite a molecule to an excited electronic and vibrational state. The bottom figure shows the pure electronic transition (no vibronic coupling) and the electronic transition couples with the vibrational transition (vibronic coupling).

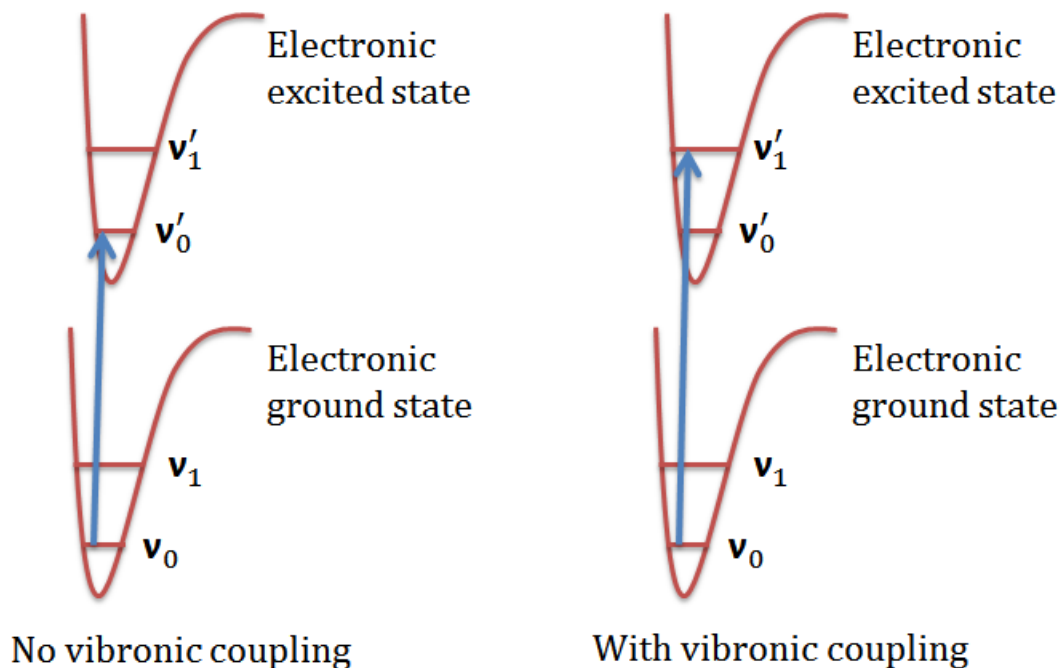


Fig. 4 Pure electronic transition and the electronic transition couples with the vibrational transition

We now can go back to the original question: Why can some electronic-forbidden transitions be observed as weak bands in spectrum? For example, the d-d transitions in the octahedral transition metal complexes are Laporte forbidden (same symmetry, parity forbidden), but they can be observed in the spectrum and this phenomenon can be explained by vibronic coupling.

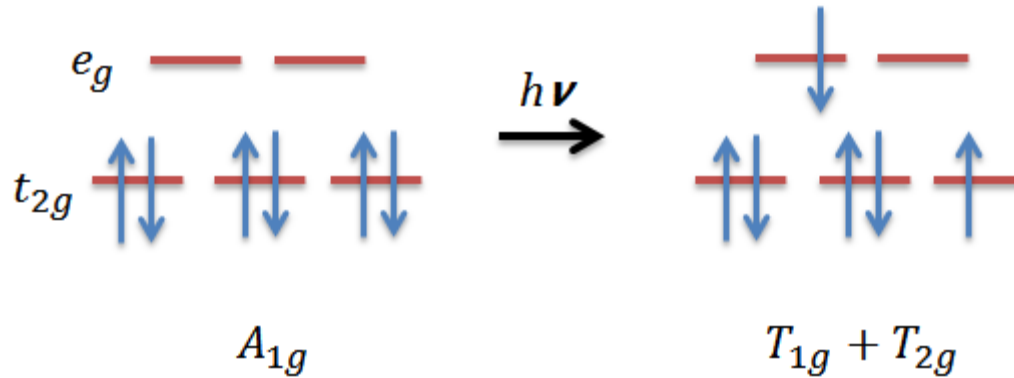
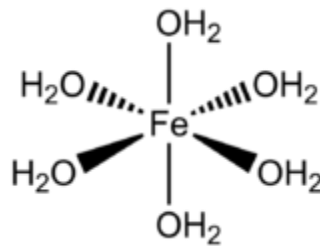


Fig. 5 e_g and t_{2g} molecular orbitals of $\text{Fe}(\text{OH}_2)_6^{2+}$



Now we consider the $\text{Fe}(\text{OH}_2)_6^{2+}$ complex which has low spin d^6 as ground state (see figure above). Let's examine the one-electron excitation from t_{2g} molecular orbital to e_g molecular orbital. The octahedral complex has O_h symmetry and therefore the ground state has A_{1g} symmetry from the character table. The symmetry of the excited state, which is the direct product of all singly occupied molecular orbitals (e_g and t_{2g} in this case):

$$\Gamma t_{2g} \otimes \Gamma e_g = T_{1g} + T_{2g} \quad \Gamma t_{2g} \otimes \Gamma e_g = T_{1g} + T_{2g}$$

The transition moment integral for the electronic transition can be written as

$$M^{\rightarrow} = \int \psi' * \mu^{\rightarrow} \psi d\tau \quad M \rightarrow = \int \psi' * \mu \rightarrow \psi d\tau$$

where ψ is the electronic ground state and ψ' is the electronic excited state. The condition for the electronic transition to be allowed is to make the transition moment integral nonzero. The μ^{\rightarrow} is the transition moment operator, which is the symmetry of the x^{\wedge} , y^{\wedge} , z^{\wedge} operators from the character table. For octahedral symmetry, these operators are degenerate and have T_{1u} symmetry. Therefore, we can see that both ${}^1T_{1g} \leftarrow {}^1A_{1g}$ and ${}^1T_{2g} \leftarrow {}^1A_{1g}$ are electronically forbidden by the direct product (do not contain the totally symmetric A_{1g}):

$$T_{1g} \times T_{1u} \times A_{1g} = A_{1u} + E_u + T_{1u} + T_{2u} \quad T_{1g} \times T_{1u} \times A_{1g} = A_{1u} + E_u + T_{1u} + T_{2u}$$

$$T_{2g} \times T_{1u} \times A_{1g} = A_{2u} + E_u + T_{1u} + T_{2u}$$

For octahedral complex, there are 15 vibrational normal modes. From the O_h character table we can get these irreducible representations:

$$\Gamma_{\text{vib}} = a_{1g} + e_g + 2t_{1u} + 2t_{2g} + 2t_{2u}$$

When we let the vibrational transition to couple with the electronic transition, the transition moment integral has the form:

$$M^{\rightarrow} = \int \psi^* e' \psi' v' \mu^{\rightarrow} \psi e \psi v d\tau \quad M^{\rightarrow} = \int \psi e' \psi v' \mu^{\rightarrow} \psi e \psi v d\tau$$

For the vibronic coupling to be allowed, the transition moment integral has to be nonzero. Use these vibrational symmetries of the octahedral complex to couple with the electronic transition:

$$A_{1g} \times \{T_{1g} \times T_{1u} \times A_{1g}\} = A_{1u} + E_u + T_{1u} + T_{2u}$$

$$E_g \times \{T_{1g} \times T_{1u} \times A_{1g}\} = E_g \times \{A_{1u} + E_u + T_{1u} + T_{2u}\} = A_{1u} + A_{2u} + 2E_u + 2T_{1u} + 2T_{2u}$$

$$T_{1u} \times \{T_{1g} \times T_{1u} \times A_{1g}\} = T_{1u} \times \{A_{1u} + E_u + T_{1u} + T_{2u}\} = A_{1g} + \dots$$

$$T_{2g} \times \{T_{1g} \times T_{1u} \times A_{1g}\} = T_{2g} \times \{A_{1u} + E_u + T_{1u} + T_{2u}\} = A_{1u} + A_{2u} + 2E_u + 3T_{1u} + 4T_{2u}$$

$$T_{2u} \times \{T_{1g} \times T_{1u} \times A_{1g}\} = T_{2u} \times \{A_{1u} + E_u + T_{1u} + T_{2u}\} = A_{1g} + \dots$$

Since the t_{1u} and t_{2u} representation can generate the totally symmetric representation in the integrand. Therefore, we can see that t_{1u} and t_{2u} can couple with the electronic transition to form the allowed vibronic transition. Therefore, the d-d transition band for $\text{Fe}(\text{OH}_2)_6^{2+}$ complex can be observed through vibronic coupling.

Rotational Selection rules

1. Transitions with $\Delta J = \pm 1$ are allowed;

Photons do not have any mass, but they have angular momentum. The conservation of angular momentum is the fundamental criteria for spectroscopic transitions. As a result, the total angular momentum has to be conserved after a molecule absorbs or emits a photon. The rotational selection rule relies on the fact that photon has one unit of quantized angular momentum. During

the photon emission and absorption process, the angular momentum J cannot change by more than one unit.

Let's consider a single photon transition process for a diatomic molecule. The rotational selection rule requires that transitions with $\Delta J = \pm 1$ are allowed. Transitions with $\Delta J = +1$ are defined as R branch transitions, while those with $\Delta J = -1$ are defined as P branch transitions. Rotational transitions are conventionally labeled as P or R with the rotational quantum number J of the lower electronic state in the parentheses. For example, R(2) specifies the rotational transition from $J=2$ in the lower electronic state to $J=3$ in the upper electronic state.

2. $\Delta J = 0$ transitions are allowed when two different electronic or vibrational states are involved: $(X'', J''=m) \rightarrow (X', J'=m)$.

The Q branch transitions will only take place when there is a net orbital angular momentum in one of the electronic states. Therefore, Q branch does not exist for $1\Sigma \leftrightarrow 1\Sigma$ or $1\Sigma \leftrightarrow 1\Sigma$ electronic transitions because $\Sigma\Sigma$ electronic state does not possess any net orbital angular momentum. On the other hand, the Q branch will exist if one of the electronic states has angular momentum. In this situation, the angular momentum of the photon will cancel out with the angular momentum of the electronic state, so the transition will take place without any change in the rotational state.

The schematic of P, Q, and R branch transitions are shown below:

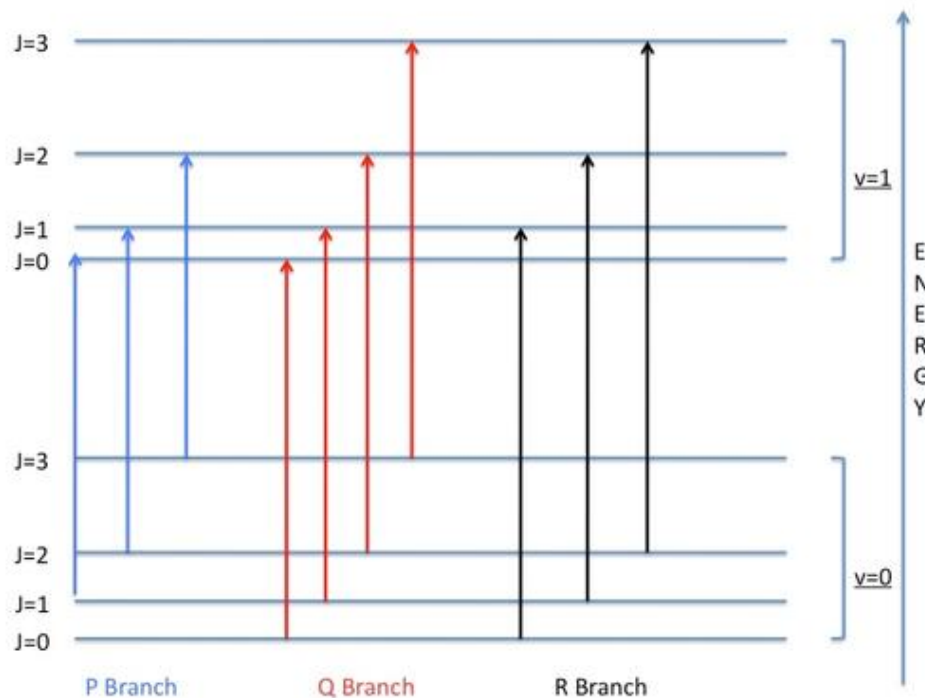


Fig. 6 Schematic diagram of P, Q, and R branch transitions

With regard to closed-shell non-linear polyatomic molecules, the selection rules are more complicated than diatomic case. The rotational quantum number J remains a good quantum number as the total angular momentum if we don't consider the nuclear spin. Under the effect of single photon transition, the change of J is still limited to a maximum of ± 1 based on the conservation of angular momentum. However, the possibility of Q branch is greatly enhanced irrelevant to the symmetry of the lower and upper electronic states. The rotational quantum number K is introduced along the inertial axis. For polyatomic molecules with symmetric top geometry, the transition moment is polarized along inertial axis. The selection rule becomes $\Delta K=0$.

While doing calculation of Racah parameter and Dq value of Cr^{+3} doped sample how to consider stokes shift influence?

Im using the following equation

$$E(^4T_2) = 10Dq$$

$$Dq/B = (15 (\Delta E/Dq - 8)) / ((\Delta E/Dq)^2 - 10 \Delta E/Dq)$$

Optical Rotatory Dispersion and Circular Dichroism

Optical rotations usually are measured at just one wavelength, namely 589.3nm, simply because sodium-vapor lamps provide an especially convenient source of monochromatic light. Measurements at other wavelengths are less easily made without specialized instruments, with which relatively few laboratories are currently equipped. Nevertheless, much information has been obtained about structure, conformation, and configuration of organic compounds from measurements of optical rotation as a function of wavelength (i.e., **optical rotatory dispersion**).

Like other phenomena involving interactions between electromagnetic radiation and organic molecules, as in infrared, ultraviolet, and nmr spectroscopy, optical rotatory dispersion curves often are quite sensitive to small changes in structure. As an example, the rotatory dispersion curves for enantiomers of *cis*- and *trans*-10-methyl-2-decalones, 1616 and 1717, are reproduced in Figure 19-7:

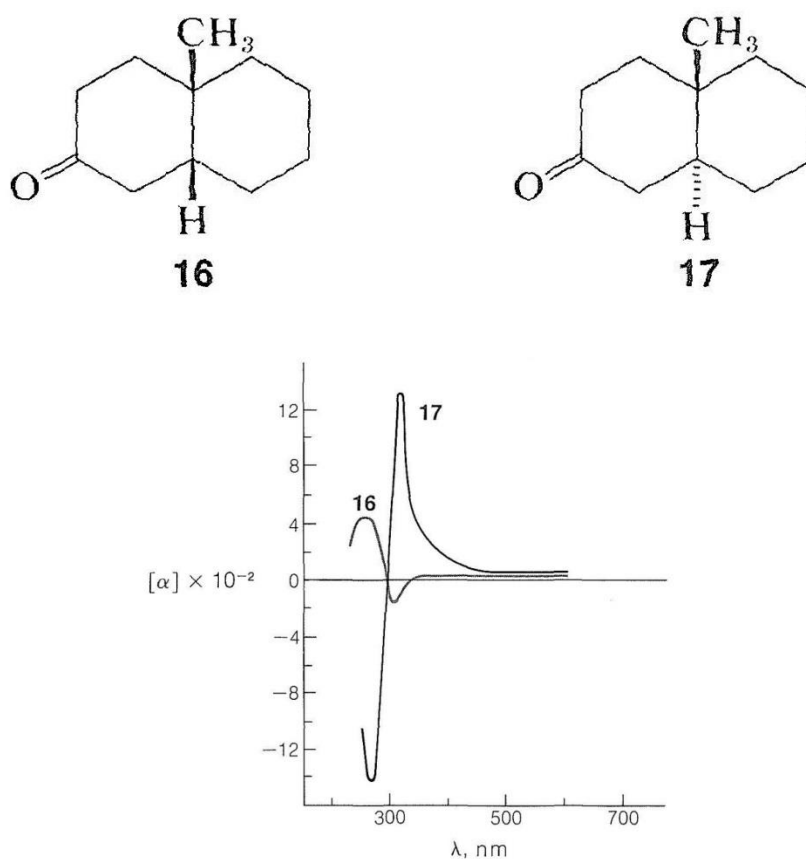


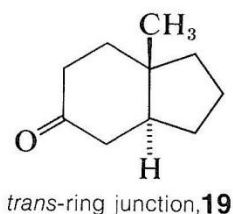
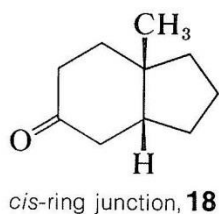
Figure 19-7: Rotatory dispersion curves for *cis*-10-methyl-2-decalone, 1616, and *trans*-10-methyl-2-decalone 1717. (By permission from C. Djerassi, *Optical Rotatory Dispersion*, McGraw-Hill Book Co., New York, 1960.)

Only a small positive rotation is observed for the particular enantiomers at the wavelength of the sodium line (589.3nm) compared to the large, both positive and negative, rotations found at wavelengths between 270nm and 400nm. If we measure the rotations as a function of wavelength and if, as we approach shorter wavelengths, the rotation rises to a *maximum* before changing sign, as it does with the trans isomer, 1717, then the compound is said to exhibit a **positive Cotton effect**. The opposite behavior, as with the cis isomer, 1616, is called a **negative Cotton effect**. The wavelength at the center point for the very rapid change in rotation for 1717 is 300nm and corresponds to the $n \rightarrow \pi^*$ absorption maximum of the carbonyl group in the ultraviolet absorption curve of the same compound. Thus excitation of the carbonyl group by absorption of ultraviolet light and strong rotatory dispersion of polarized light are associated phenomena. In fact, when a substance exhibits a Cotton effect, not only does it transmit clockwise and counterclockwise circularly polarized light with unequal velocities (Section 19-1), it also absorbs the two forms of light unequally.

This means that the molar extinction coefficients of the two enantiomers (ϵ_l and ϵ_r) are unequal in circularly polarized light. These differences in absorption (ϵ_l and ϵ_r) can be measured as a function of wavelength, and the curves obtained are called **circular dichroism** curves. They have positive or negative signs (Cotton effect) just as for optical rotatory dispersion curves.

Most of the research on optical rotatory dispersion to date has been with optically active ketones because the carbonyl chromophore conveniently has a weak absorption band in the 300nm region. Compounds with chromophores that absorb light *strongly* in the ultraviolet usually are unsatisfactory for rotatory dispersion measurements because insufficient incident light is transmitted to permit measurement of optical rotation. Weak absorption bands below about 210nm have not been exploited because of experimental difficulties in making the necessary measurements.

Many rotatory dispersion curves have been obtained for optically active ketones derived from steroids and triterpenes, which are monocyclic, bicyclic, and open-chain compounds. Enough data have been accumulated so that the various shapes and magnitudes of the curves are recognized as characteristic of particular structural features. A good illustration is provided by the rotatory dispersion curves for the *cis*- and *trans*-8-methylhydrindan-5-ones, 1818 and 1919, which are shown in Figure 19-8:



Charge transfer spectra 14

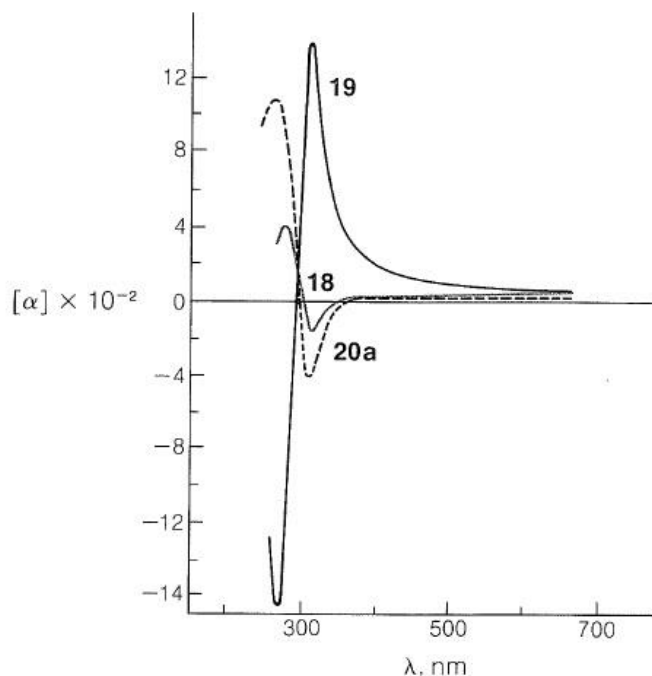
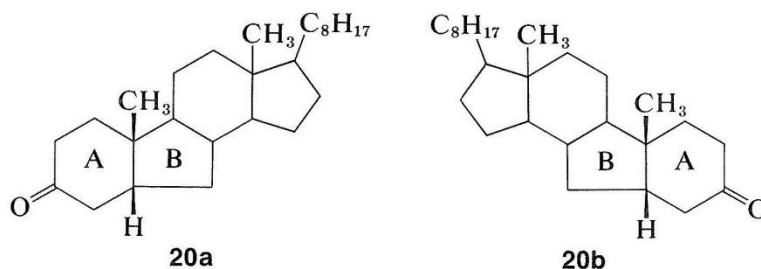


Figure 19-8: Rotatory dispersion curves for *trans*-8-methylhydrindan-5-one, 19, *cis*-8-methylhydrindan-5-one, 18, and BB-norcoprostan-3-one, 20a. (By permission from C. Djerassi, *Optical Rotatory Dispersion*, McGraw-Hill Book Co., New York, 1960.)

The remarkable differences in these curves are due to changes in the environment of the carbonyl groups arising from the different configurations of the hydrogens at the ring junctions. Because the rotatory dispersion curve of the closely related structure 20a is very similar to that of the *cis*-hydrindanone, 18, the rings labeled AA and BB in 20a can be inferred also to be *cis* oriented (see Figure 19-8):

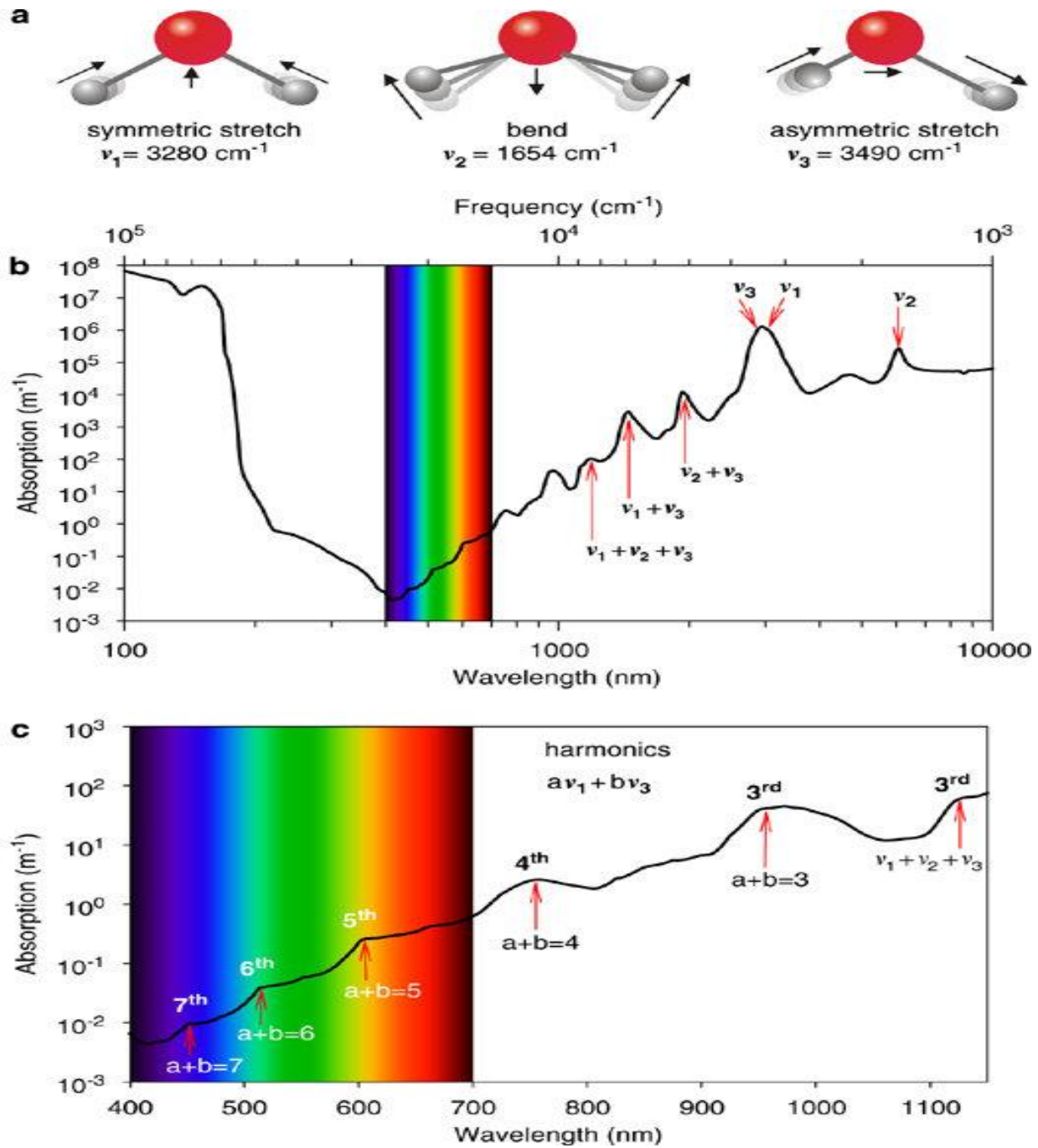


Rotatory dispersion curves often are helpful in establishing configurations; thus the relative configurations of compounds 18 and 20a must be the same because, if they were not, the two curves would resemble mirror images of one another. Therefore, if the absolute configuration of 18 corresponds to the formula shown, then compound 20a has the configuration shown and not 20b.

UNIT-II

IR and Raman spectroscopy

Simple vibration notation of H₂O



The three vibrational modes of the water molecule and their fundamental frequencies in liquid water: symmetric stretching (ν_1), bending (ν_2) and asymmetric stretching (ν_3). The atoms move in the directions indicated by arrows. (b) Absorption spectrum of pure water (Hale and Querry, 1973; Segelstein, 1981; Pope and Fry, 1997). Peaks in the absorption spectrum correspond to the fundamental frequencies and higher harmonics of the vibrations of the water molecules. (c) Absorption spectrum of pure water in the visible and infrared region. Shoulders in the absorption spectrum correspond to the third, fourth, fifth, sixth and seventh harmonics of the symmetric and asymmetric stretch vibrations, as indicated

Water, H₂O (C_{2v})

O-H symmetric stretching (a ₁)	O-H asymmetric stretching (b ₂)	H-O-H bending (a ₁)
3585 cm ⁻¹ (IR intensity = 0.17) (Raman active)	3506 cm ⁻¹ (IR intensity = 1.0) (Raman active)	1885 cm ⁻¹ (IR intensity = 0.15) (Raman active)

Vibrational modes of molecules Normal modes of vibration: Diatomic molecules can perform only one single vibration motion. The number of possible vibrational modes of multiatomic molecules can be calculated in the following way: each single atom can move to 3N spatial coordinates for N number of atoms. Therefore a system of N points of mass has 3N degrees of freedom available. In three of these movements, however, the atoms do not shift themselves relative to one another, but they all move in the same direction, thereby simultaneously changing the position of the center of mass. Degree of freedom: The number of vibrational degrees of freedom is showing by $Z=3N-6$ for nonlinear molecules and $Z = 3N-5$ for linear molecules. A linear three atomic molecule like CO₂ has 4, a nonlinear three atomic molecule like H₂O has 3, NH₃, NH₄ and N₂O₄ have 6, 9 and 12 independent vibrational coordinates, respectively. Types of vibrations: All atoms of a molecule oscillate with the same frequency and in phase. There are stretching- (change of bond length) and deformation-vibrations (change of bond angle) existing. They can be symmetric and antisymmetric.

Note : For a polyatomic molecule, some normal modes of vibration are spectroscopically active and some are not. The cross selection rule defines that the displacement of a normal mode must cause change in the dipole moment in order to be spectroscopically active in infrared.

Carbon Dioxide, CO₂

C-O asymmetric stretching		C-O symmetric stretching	
2565	cm ⁻¹	1480	cm ⁻¹
(IR intensity = 1.0)		(IR inactive)	
(Raman inactive)		(Raman active)	
O-C-O bending		O-C-O bending	
526	cm ⁻¹	526	cm ⁻¹
(IR intensity = 0.038)		(IR intensity = 0.038)	
(Raman inactive)		(Raman inactive)	

Water, H₂O (C_{2v})

O-H symmetric stretching	O-H asymmetric stretching	H-O-H bending
(a ₁)	(b ₂)	(a ₁)
3585 cm ⁻¹	3506 cm ⁻¹	1885 cm ⁻¹
(IR intensity = 0.17)	(IR intensity = 1.0)	(IR intensity = 0.15)
(Raman active)	(Raman active)	(Raman active)

Examples:

Normal modes of vibration of CO₂ :

Normal mode of vibration of H₂O:

Vibration Wave number cm-1 Vibrational mode

Vibration	Wave number cm-1	Vibrational mode
V1	1340	symmetric C=O stretching

		vibration
V2	2349	antisymmetric C=O stretching vibration
V3a V3b	667 667	deformation vibration, two-fold degenerate
V3a V3b	667 667	

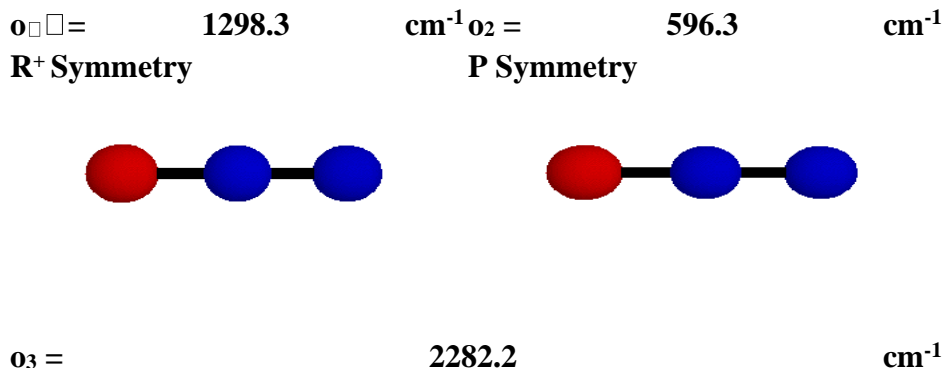
Normal mode of vibration of H₂O:

Vibration	Wave number cm ⁻¹	Vibrational mode
V1	3657	symmetric stretching vibration
V2	1595	antisymmetric deformation vibration
V3	3756	antisymmetric deformation vibration

Characteristic Vibrations of N₂O (C_{∞v} symmetry)

N₂O (nitrous oxide) is a linear molecule with many similarities to CO₂ (albeit with less symmetry). It is a minor contributor to the Earth's greenhouse effect.

According to the IPCC, an increase of 46 ppb (17%) in the atmospheric abundance of N₂O from 1750 to 2000 amounts to a radiative forcing ≈0.15Watts/m². All three of the modes shown here are infrared-active to some degree, making them capable of absorbing and scattering infrared heat radiation from the Earth before it can escape to space. The normal modes depicted below were modeled using hybrid density functional theory (B3LYP) and the cc-pVTZ basis set. Harmonic frequencies calculated by Zúñiga et al. (2003, *J. Mol. Spectrosc.* 217:43-58) are also shown. These are based on a force-field model fitted to spectroscopic measurements.



R⁺ Symmetry



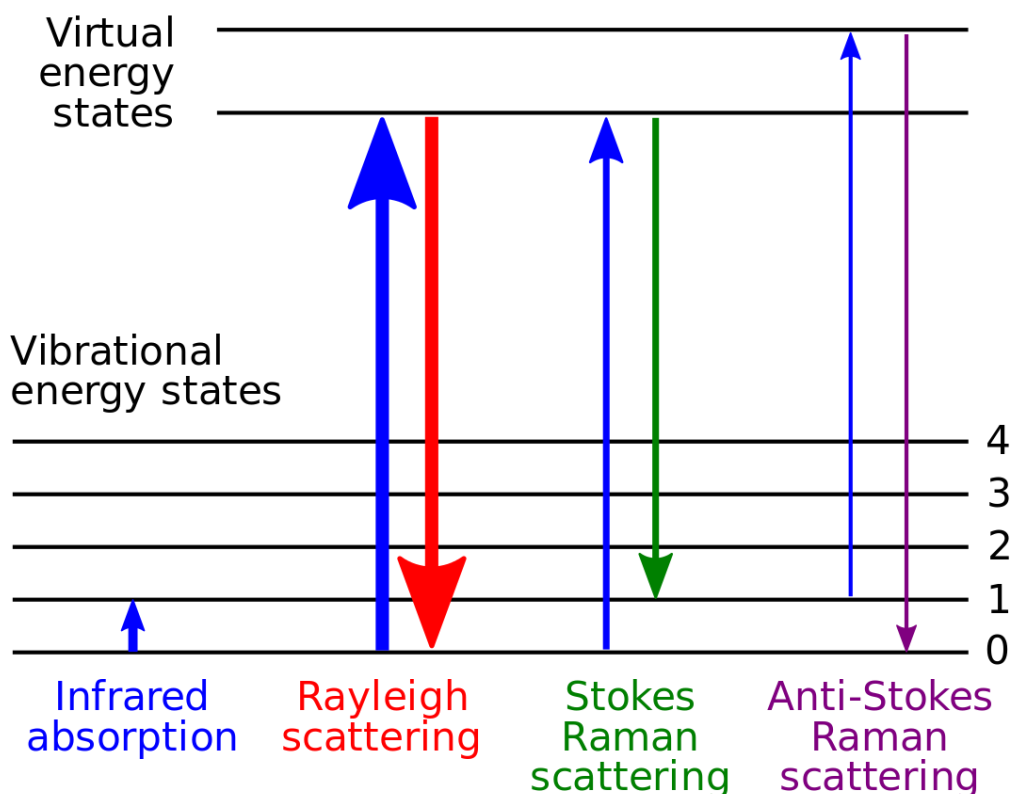
Raman selection rule

Selection rule There are certain rules on the basis of which we decide whether the transition between energy level is allowed or forbidden. For rotational Raman spectra, the selection rule is: $\Delta J = 0, \pm 2$ Where, J is rotational quantum number.

Case 1: If $\Delta J = 0$ This shows that there is no change in the rotational quantum number. In this case, the frequency of the incident and scattered radiation is same i.e. the scattering is Rayleigh scattering.

Case 2: $\Delta J = -2$ This corresponds to anti-stokes Raman lines. Here the scattered radiations have more frequency than the incident radiation.

Case 3: $\Delta J = +2$ This corresponds to stokes Raman lines. Here the scattered radiations have less frequency than the incident radiation.



Isotope Effects in Vibrational Spectroscopy

This page provides an overview of how an isotope can affect the frequencies of the vibrational modes of a molecule. Isotopic substitution is a useful technique due to the fact that the normal modes of an isotopically substituted molecule are different than the normal modes of an unsubstituted molecule, leading to different corresponding vibrational frequencies for the substituted atoms. Vibrational spectroscopy is done in the infrared region of the electromagnetic spectrum, which ranges from around 10^{-6} to 10^{-3} meters. IR and Raman spectroscopy observe the vibrations of molecules, displaying the normal and local modes of the molecule in the spectra. Isotopes are atoms that share the same number of protons but differ in the number of neutrons contained in the nucleus, thus giving these atoms different mass numbers. The specific mass of each atom will affect the reduced mass of the overall molecule, therefore changing the vibrational frequencies of that molecule.

Diatomics

A diatomic molecule, as seen in Figure 11, contains two atoms, which can either be composed of the same or different elements. It is easier to focus on these types of molecules when analyzing and calculating vibrational frequencies because they are simpler systems than polyatomic

molecules. Whether or not the diatomic consists of the same or different elements, a diatomic molecule will have only one vibrational frequency. This singular normal mode is because of the diatomic's linear symmetry, so the only vibration possible occurs along the bond connecting the two atoms.

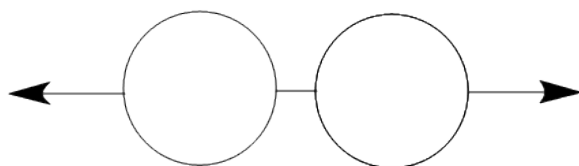


Figure 11: Diagram of a diatomic molecule with the only possible vibration it can undergo.

Normal Modes

Normal modes describe the possible movements/vibrations of each of the atoms in a system. There are many different types of vibrations that molecules can undergo, like stretching, bending, wagging, rocking, and twisting, and these types can either be out of plane, asymmetric, symmetric, or degenerate. Molecules have $3n$ possible movements due to their 3-dimensionality, where n is equal to the number of atoms in the molecule. Three movements are subtracted from the total because they are saved for the displacement of the center of mass, which keeps the distance and angles between the atoms constant. Another 3 movements are subtracted from the total because they are for the rotations about the 3 principle axes. This means that for nonlinear molecules, there are $3n - 6$ normal modes possible. Linear molecules, however, will have $3n - 5$ normal modes because it is not possible for internuclear axis rotation, meaning there is one less possible rotation for the molecule. This explain why diatomic molecules only have 1 vibrational frequency, because $3(2) - 5 = 1$.

Molecular vibrations are often thought of as masses attached by a spring (Figure 22),

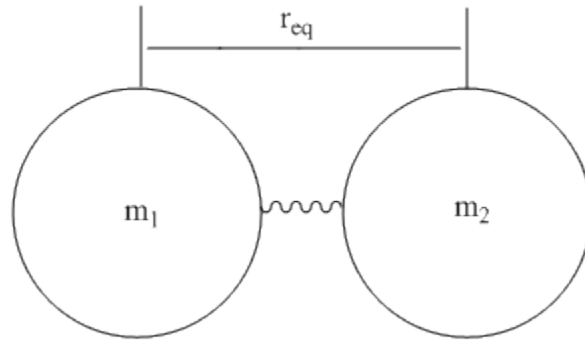


Figure 22: Representation of a diatomic molecule as masses attached by a spring separated by an equilibrium distance of r_{eq} .

and Hook's law can be applied

$$F = -kx$$

where

- F is the resulting force,
- x is the displacement of the mass from equilibrium ($x = r - r_{eq}$), and
- k is the force constant, defined as

$$k = \left(\frac{\partial^2 V(r)}{\partial r^2} \right)_{r_{eq}}$$

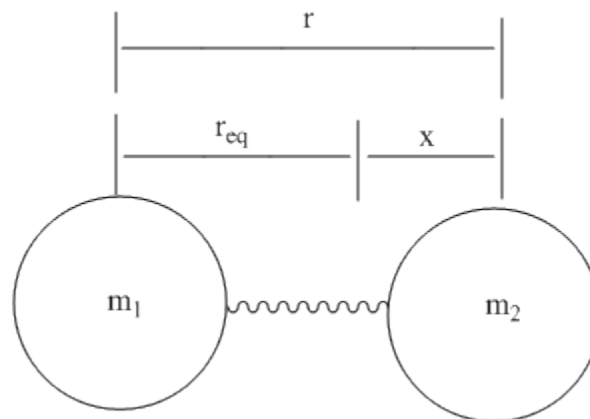


Figure 33: Depiction of the diatomic when the atoms undergo a vibration and increase their separation by a distance x .

in which $V(r) = \frac{1}{2}k(r - r_{eq})^2$, which comes from incorporating Hook's law to the harmonic oscillator. The diatomic molecule is thought of as two masses (m_1 and m_2) on a spring, they will have a reduced mass, μ , so their vibrations can be mathematically analyzed.

$$\mu = \frac{m_1 m_2}{m_1 + m_2}$$

When an atom in a molecule is changed to an isotope, the mass number will be changed, so μ will be affected, but k will not (mostly). This change in reduced mass will affect the vibrational modes of the molecule, which will affect the vibrational spectrum.

Vibrational energy levels, ν_e , are affected by both k and μ , and is given by

$$\nu_e = \frac{1}{2\pi} \sqrt{\frac{k}{\mu}}$$

These vibrational energy levels correspond to the peaks which can be observed in IR and Raman spectra. IR spectra observe the asymmetric stretches of the molecule, while Raman spectra observe the symmetric stretches.

Effects on Experimental Results

When an atom is replaced by an isotope of larger mass, μ increases, leading to a smaller ν_e and a downshift (smaller wavenumber) in the spectrum of the molecule. Taking the diatomic molecule HCl, if the hydrogen is replaced by its isotope deuterium, μ is doubled and therefore ν_e will be decreased by $2^{-1/2}$. Deuterium substitution leads to an isotopic ratio of 1.35-1.41 for the frequencies corresponding to the hydrogen/deuterium vibrations. There will also be a decrease by $2^{-1/2}$ in the band width and integrated band width for the vibrational spectra of the substituted molecule. Isotopic substitution will affect the entire molecule (to a certain extent), so it is not only the vibrational modes for the substituted atom that will change, but rather the vibrational modes of all the atoms of the molecule. The change in frequency for the atoms not directly involved in the substitution will not display as large a change, but a downshift can still occur.

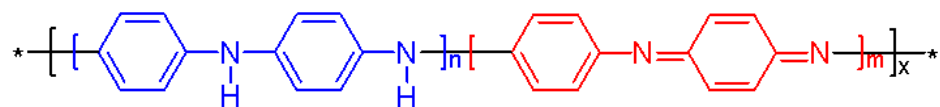


Figure 44: Structure of polyaniline.

When polyaniline (Figure 44) is fully deuterated, the vibrational peaks will downshift slightly. The following data was summarized from Quillard *et al.*

Type of vibration	Nondeuterated (frequency, cm^{-1})	Deuterated (frequency, cm^{-1})

C-C stretch	1626	1599
C-C stretch	1581	1560
C-H bend – benzenoid ring	1192	876
C-H bend – quinoid ring	1166	856
N-H bend	1515	1085

Changing hydrogen to deuterium leads to the largest effect in a vibrational spectrum since the mass is doubled. Other isotopic substitutions will also lead to a shift in the vibrational energy level, but because the mass change is not as significant, μ will not change by much, leading to a smaller change in ν . This smaller change in vibrational frequency is seen in the sulfur substitution of sulfur hexafluoride (Figure 55:), from ^{32}S to ^{34}S . The frequencies as reported by Kolomiitsova *et al.* are shown below.

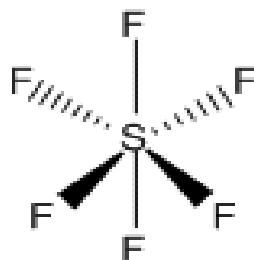


Figure 55: Structure of sulfur hexafluoride.

Vibration assignment	$^{32}\text{SF}_6$ (frequency, cm^{-1})	$^{34}\text{SF}_6$ (frequency, cm^{-1})
v3v3	939.3	922.2
v4v4	613.0	610.3

These two examples show the consistency of downshifted vibrational frequencies for atoms substituted with an isotope of higher mass.

Applications

Substituting atoms with isotopes has been shown to be very useful in determining normal mode vibrations of organic molecules. When analyzing the spectrum of a molecule, isotopic substitution can help determine the vibrational modes specific atoms contribute to. Those normal modes can be assigned to the peaks observed in the spectrum of the molecule. There are specific CH_3 rocks and torsions, as well as CH bends that can be identified in the spectrum upon deuterium substitution. Other torsion bands from hydroxyl and amine groups can also be assigned when hydrogen is replaced with deuterium. Experimental data has also shown that using deuterium substitution can help with symmetry assignments and the identification of metal hydrides.

Isotopic substitution can also be used to determine the force constants of the molecule. Calculations can be done using the frequencies of the normal modes in determining these values, based on both calculated frequencies and experimental frequencies.

Researchers have also attempted to contribute peak shape changes and splits in peaks of vibrational spectra to naturally occurring isotopes in molecules. It has been shown, however, that the shape of a peak is not related to the size of the atom, so substitution to an atom of larger mass will not affect the peak shape in the molecule's spectrum. As previously stated, isotopic substitution of atoms of higher mass will not have a significant enough effect on the shifts in frequencies for the corresponding vibrations, so analyzing the frequency shifts of smaller mass isotopes, like deuterium and ^{13}C is necessary.

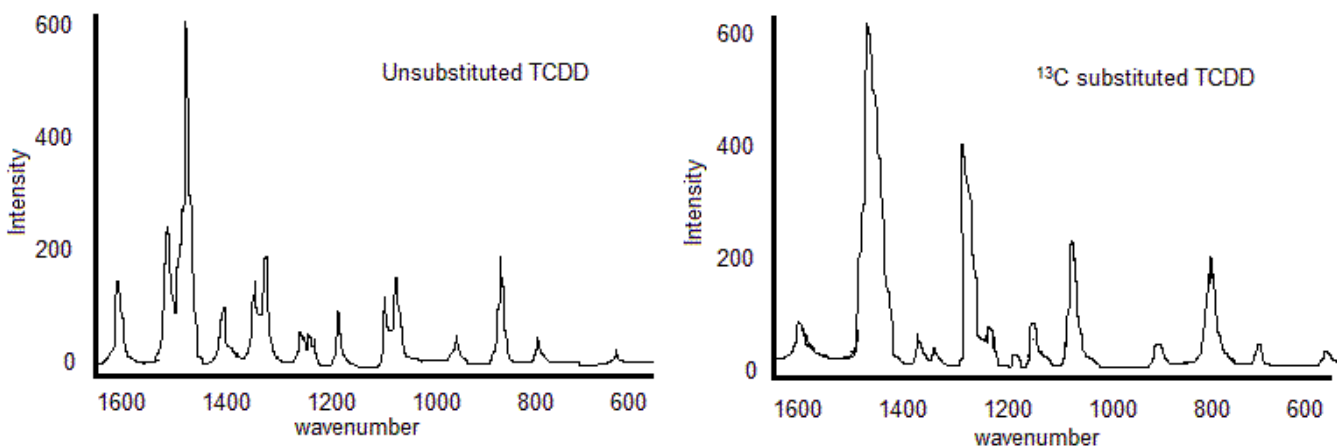


Figure 66: Spectra of unsubstituted and substituted TCDD depicting the isotopic ^{13}C effects.

As depicted in the rough representation of the vibrational spectra of the molecule tetrachlorinated dibenzodioxin (TCDD), the ^{13}C substituted TCDD spectrum is slightly downshifted compared to the unsubstituted TCDD spectrum. Although the shifts and split peaks do occur in the spectra of isotopically substituted molecules, not all observed peaks can be attributed to the isotope. This is

because the intensities of the peaks shown are not large enough to relate to the natural abundance of the ^{13}C isotope, and not all peaks can be accounted for by the substitution.

Applications

RAMAN SPECTROSCOPY APPLICATION IN INORGANIC SYSTEMS

X-ray diffraction (XRD) has been developed into a standard method of determining structure of solids in inorganic systems. Compared to XRD, it is usually necessary to obtain other information (NMR, electron diffraction, or UV-Visible) besides vibrational information from IR/Raman in order to elucidate the structure. Nevertheless, vibrational spectroscopy still plays an important role in inorganic systems. For example, some small reactive molecules only exist in gas phase and XRD can only be applied for solid state. Also, XRD cannot distinguish between the following bonds: $-\text{CN}$ vs. $-\text{NC}$, $-\text{OCN}$ vs. $-\text{NCO}$, $-\text{CNO}$ vs. $-\text{ONC}$, $-\text{SCN}$ vs. $-\text{NCS}$. [7] Furthermore, IR and Raman are fast and simple analytical method, and are commonly used for the first approximation analysis of an unknown compound.

Raman spectroscopy has considerable advantages over IR in inorganic systems due to two reasons. First, since the laser beam used in RS and the Raman-scattered light are both in the visible region, glass (Pyrex) tubes can be used in RS. On the other hand, glass absorbs infrared radiation and cannot be used in IR. However, some glass tubes, which contain rare earth salts, will give rise to fluorescence or spikes. Thus, using of glass tubes in RS still need to be careful. Secondly, since water is a very weak Raman scatter but has a very broad signal in IR, aqueous solution can be directly analyzed using RS.

Raman Spectroscopy and IR have different selection rules. RS detects the polarizability change of a molecule, while IR detects the dipole momentum change of a molecule. Principle about the RS and IR can be found at Chemwiki Infrared Theory and Raman Theory. Thus, some vibration modes that are active in Raman may not be active IR, vice versa. As a result, both of Raman and IR spectrum are provided in the structure study. As an example, in the study of Xenon Tetrafluoride. There are 3 strong bands in IR and solid Raman shows 2 strong bands and 2 weaker bands. These information indicates that Xenon Tetrafluoride is a planar molecule and has a symmetry of D_{4h} . [8] Another example is the application of Raman Spectroscopy in homonuclear diatomic molecules. Homonuclear diatomic molecules are all IR inactive, fortunately, the vibration modes for all the homonuclear diatomic molecules are always Raman Spectroscopy active.

Raman Spectroscopy Application in Organic Systems

Unlike inorganic compounds, organic compounds have less elements mainly carbons, hydrogens and oxygens. And only a certain function groups are expected in organic spectrum.

Thus, Raman and IR spectroscopy are widely used in organic systems. Characteristic vibrations of many organic compounds both in Raman and IR are widely studied and summarized in many literature. [5] Qualitative analysis of organic compounds can be done base on the characteristic vibrations table.

Table 1: Characteristic frequencies of some organic function group in Raman and IR

Vibration	Region(cm^{-1})	Raman intensity	IR intensity
v(O-H)	3650~3000	Weak	strong
v(N-H)	3500~3300	Medium	medium
v(C=O)	1820~1680	strong~weak	very strong
v(C=C)	1900~1500	very strong~medium	0~weak

“RS is similar to IR in that they have regions that are useful for functional group detection and fingerprint regions that permit the identification of specific compounds.”[1] While from the different selection rules of Raman Spectroscopy and IR, we can get the Mutual Exclusion rule [5], which says that for a molecule with a center of symmetry, no mode can be both IR and Raman Spectroscopy active. So, if we find a strong bond which is both IR and Raman Spectroscopy active, the molecule doesn't have a center of symmetry.

Non-classical Raman Spectroscopy

Although classical Raman Spectroscopy has been successfully applied in chemistry, this technique has some major limitations as follows[5]:

1. The probability for photon to undergo Raman Scattering is much lower than that of Rayleigh scattering, which causes low sensitivity of Raman Spectroscopy technique. Thus, for low concentration samples, we have to choose other kinds of techniques.
2. For some samples which are very easily to generate fluorescence, the fluorescence signal may totally obscure the Raman signal. We should consider the competition between the Raman Scattering and fluorescence.
3. In some point groups, such as C_6 , D_6 , D_{6h} , C_{4h} , D_{2h} , there are some vibrational modes that is neither Raman or IR active.
4. The resolution of the classical Raman Spectroscopy is limited by the resolution of the monochromator.

In order to overcome the limitations, special techniques are used to modify the classical Raman Spectroscopy. These non-classical Raman Spectroscopy includes: Resonance Raman Spectroscopy, surface enhanced Raman Spectroscopy, and nonlinear coherent Raman techniques, such as hyper Raman spectroscopy

Resonance Raman Scattering (RRS)

The resonance effect is observed when the photon energy of the exciting laser beam is equal to the energy of the allowed electronic transition. Since only the allowed transition is affected, (in terms of group theory, these are the totally symmetric vibrational ones.), only a few Raman bands are enhanced (by a factor of 10^6). As a result, RRS can increase the resolution of the classical Raman Spectroscopy, which makes the detection of dilution solution possible (concentrations as low as 10^{-3} M). RRS is extensively used for biological molecules because of its ability to selectively study the local environment. As an example, the Resonance Raman labels are used to study the biologically active sites on the bond ligand. RRS can also be used to study the electronic excited state. For example, the excitation profile which is the Raman intensity as a function of incident laser intensity can tell the interaction between the electronic states and the vibrational modes. Also, it can be used to measure the atomic displacement between the ground state and the excited state.

Surface Enhanced Raman Scattering (SERS)

At 1974, Fleischmann discovered that pyridine adsorbed onto silver electrodes showed enhanced Raman signals. This phenomenon is now called surface enhanced Raman Scattering (SERS). Although the mechanism of SERS is not yet fully understood, it is believed to result from an enhancement either of transition polarizability, α , or the electric field, E, by the interaction with the rough metallic support.

Unlike RRS, SERS enhances every band in the Raman spectrum and has a high sensitivity. Due to the high enhancement (by a factor of 10^{10-11}), the SERS results in a rich spectrum and is an ideal tool for trace analysis and in situ study of interfacial process. Also, it is a better tool to study highly diluted solutions. A concentration of 4×10^{-12} M was reported by Kneipp using SERS. [5]

Nonlinear Raman Spectroscopy

In a nonlinear process, the output is not linearly proportional to its input. This happens when the perturbation become large enough that the response to the perturbation doesn't follows the perturbation's magnitude. Nonlinear Raman Spectroscopy includes: Hyper Raman spectroscopy, coherent anti-Stokes Raman Spectroscopy, coherent Stokes Raman spectroscopy, stimulated Raman gain and inverse Raman spectroscopy. Nonlinear Raman spectroscopy is more sensitive than classical Raman spectroscopy and can effectively reduce/remove the influence of fluorescence. The following paragraph will focus on the most useful nonlinear Raman spectroscopy---coherent anti-Stokes Raman Spectroscopy (CARS):

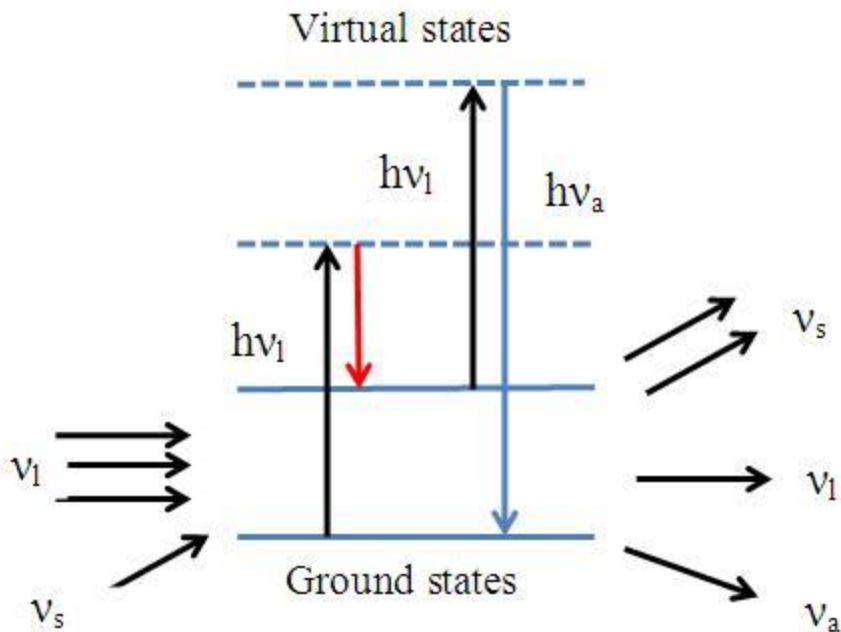


Figure 3: Schematic representation of coherent anti-Stokes Raman. ν is the frequency of the light. The subscript 1 represents laser light; s represents Stoke scattering light; a represents anti-Stoke scattering light.

Figure 3) The two laser sources generate a coherent beam at frequency ν_3 . There is a signal enhancement when ν_3 equal the anti-Stokes scattering (ν_a), and the vibrational transition equals to the energy difference between two light sources. Since CARS signal is at anti-Stoke region (a higher energy region than fluorescence), the influence of fluorescence is eliminated. Thus, CARS is very useful for molecules with high fluorescence effect, for example, some biological molecules. Another important advantage of CARS is that the resolution is no longer limited by the monochromator as in classical Raman because only the anti-Stokes frequency is studied in CARS. High-resolution CARS has been developed as a tool for small-time scale process, such as photochemical analysis and chemical kinetics studies.

UNIT –III

Interpreting NMR spectra

Chemical Shift

The different local chemical environments surrounding any particular nuclei causes them to resonate at slightly different frequencies. This is a result of a nucleus being more or less shielded than another. This is called the chemical shift (δ). One factor that affects chemical shift is the changing of electron density from around a nucleus, such as a bond to an electronegative group. Hydrogen bonding also changes the electron density in ^1H NMR, causing a larger shift. These frequency shifts are miniscule in comparison to the fundamental NMR frequency differences, on a scale of Hz as compared to MHz. For this reason chemical shifts (δ) are described by the unit ppm on an NMR spectra, 4.7.34.7.3, where H_{ref} = the resonance frequency of the reference, H_{sub} = resonance frequency of the substance, and H_{machine} = operating frequency of the spectrometer.

$$\delta = (H_{\text{ref}} - H_{\text{sub}}) / H_{\text{machine}} \times 10^6 \quad (4.7.3) \quad (4.7.3) \quad \delta = (H_{\text{ref}} - H_{\text{sub}}) / H_{\text{machine}} \times 10^6$$

Since the chemical shift (δ in ppm) is reported as a relative difference from some reference frequency, so a reference is required. In ^1H and ^{13}C NMR, for example, tetramethylsilane (TMS, $\text{Si}(\text{CH}_3)_4$) is used as the reference. Chemical shifts can be used to identify structural properties in a molecule based on our understanding of different chemical environments. Some examples of where different chemical environments fall on a ^1H NMR spectra are given in Table 4.7.14.7.1.

Functional Group	Chemical Shift Range (ppm)
Alkyl (e.g. methyl- CH_3)	~ 1
Alkyl adjacent to oxygen ($-\text{CH}_2-\text{O}$)	3 - 4
Alkene ($=\text{CH}_2$)	~ 6
Alkyne (C-H)	~ 3
Aromatic	7 - 8

In Figure 4.7.34.7.3, an ^1H NMR spectra of ethanol, we can see a clear example of chemical shift. There are three sets of peaks that represent the six hydrogens of ethanol ($\text{C}_2\text{H}_6\text{O}$). The presence of three sets of peaks means that there are three different chemical environments that the hydrogens can be found in: the terminal methyl (CH_3) carbon's three hydrogens, the two hydrogens on the methylene (CH_2) carbon adjacent to the oxygen, and the single hydrogen on the

oxygen of the alcohol group (OH). Once we cover spin-spin coupling, we will have the tools available to match these groups of hydrogens to their respective peaks.

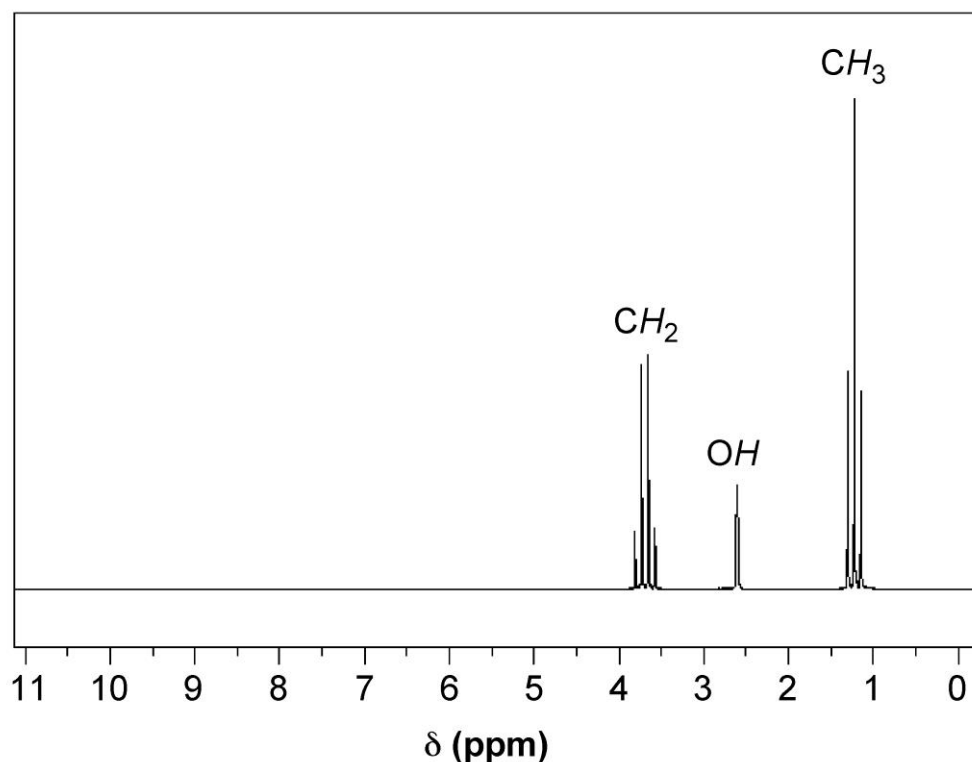


Figure 4.7.34.7.3: A ¹H NMR spectra of ethanol (CH₃CH₂OH).

Spin-spin Coupling

Another useful property that allows NMR spectra to give structural information is called spin-spin coupling, which is caused by spin coupling between NMR active nuclei that are not chemically identical. Different spin states interact through chemical bonds in a molecule to give rise to this coupling, which occurs when a nuclei being examined is disturbed or influenced by a nearby nuclear spin. In NMR spectra, this effect is shown through peak splitting that can give direct information concerning the connectivity of atoms in a molecule. Nuclei which share the same chemical shift do not form splitting peaks in an NMR spectra.

In general, neighboring NMR active nuclei three or fewer bonds away lead to this splitting. The splitting is described by the relationship where n neighboring nuclei result in $n+1$ peaks, and the area distribution can be seen in Pascal's triangle (Figure 4.7.44.7.4). However, being adjacent to a strongly electronegative group such as oxygen can prevent spin-spin coupling. For example a doublet would have two peaks with intensity ratios of 1:1, while a quartet would have four peaks of relative intensities 1:3:3:1. The magnitude of the observed spin splitting depends on many factors and is given by the coupling constant J , which is in units of Hz.

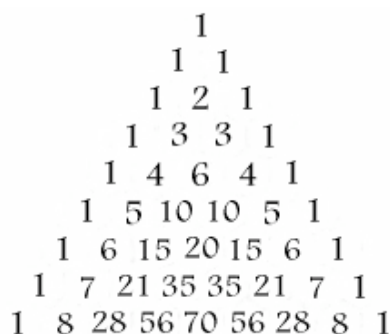


Figure 4.7.44.7.4: Pascal's triangle.

Referring again to Figure 4.7.44.7.4, we have a good example of how spin-spin coupling manifests itself in an NMR spectra. In the spectra we have three sets of peaks: a quartet, triplet, and a singlet. If we start with the terminal carbon's hydrogens in ethanol, using the $n+1$ rule we see that they have two hydrogens within three bonds (i.e., H-C-C-H), leading us to identify the triplet as the peaks for the terminal carbon's hydrogens. Looking next at the two central hydrogens, they have four NMR active nuclei within three bonds (i.e., H-C-C-H), but there is no quintet on the spectra as might be expected. This can be explained by the fact that the single hydrogen bonded to the oxygen is shielded from spin-spin coupling, so it must be a singlet and the two central hydrogens form the quartet. We have now interpreted the NMR spectra of ethanol by identifying which nuclei correspond to each peak.

Peak Intensity

Mainly useful for proton NMR, the size of the peaks in the NMR spectra can give information concerning the number of nuclei that gave rise to that peak. This is done by measuring the peak's area using integration. Yet even without using integration the size of different peaks can still give relative information about the number of nuclei. For example a singlet associated with three hydrogen atoms would be about 3 times larger than a singlet associated with a single hydrogen atom.

This can also be seen in the example in Figure 4.7.34.7.3. If we integrated the area under each peak, we would find that the ratios of the areas of the quartet, singlet, and triplet are approximately 2:1:3, respectively.

Limitations of NMR

Despite all of its upsides, there are several limitations that can make NMR analysis difficult or impossible in certain situations. One such issue is that the desired isotope of an element that is needed for NMR analysis may have little or no natural abundance. For example the natural abundance of ^{13}C , the active isotope for carbon NMR, is about 11%, which works well for

analysis. However, in the case of oxygen the active isotope for NMR is ^{17}O , which is only 0.035% naturally abundant. This means that there are certain elements that can essentially never be measured through NMR.

Another problem is that some elements have an extremely low magnetic moment, μ . The sensitivity of NMR machines is based on the magnetic moment of the specific element, but if the magnetic moment is too low it can be very difficult to obtain an NMR spectra with enough peak intensity to properly analyze.

NMR Spin Coupling

The Basis of Spin Coupling

Nuclear magnetic resonance (NMR) signals arise when nuclei absorb a certain radio frequency and are excited from one spin state to another. The exact frequency of electromagnetic radiation that the nucleus absorbs depends on the magnetic environment around the nucleus. This magnetic environment is controlled mostly by the applied field, but is also affected by the magnetic moments of nearby nuclei. Nuclei can be in one of many spin states Figure 4.7.54.7.5, giving rise to several possible magnetic environments for the observed nucleus to resonate in. This causes the NMR signal for a nucleus to show up as a multiplet rather than a single peak.

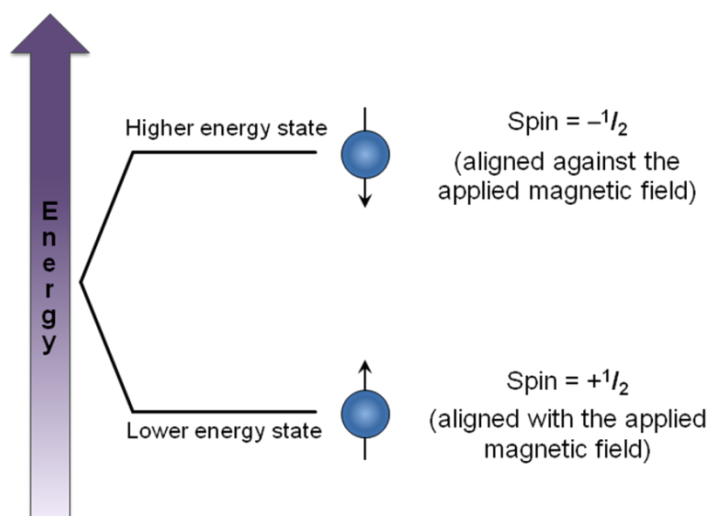


Figure 4.7.54.7.5 The different spin states of a nucleus ($I = 1/2$) in a magnetic field. These different states increase or decrease the effective magnetic field experienced by a nearby nucleus, allowing for two distinct signals.

When nuclei have a spin of $I = 1/2$ (as with protons), they can have two possible magnetic moments and thus split a single expected NMR signal into two signals. When more than one nucleus affects the magnetic environment of the nucleus being examined, complex multiplets

form as each nucleus splits the signal into two additional peaks. If those nuclei are magnetically equivalent to each other, then some of the signals overlap to form peaks with different relative intensities. The multiplet pattern can be predicted by Pascal's triangle (Figure 4.7.64.7.6), looking at the n^{th} row, where n = number of nuclei equivalent to each other but *not* equivalent to the one being examined. In this case, the number of peaks in the multiplet is equal to $n + 1$

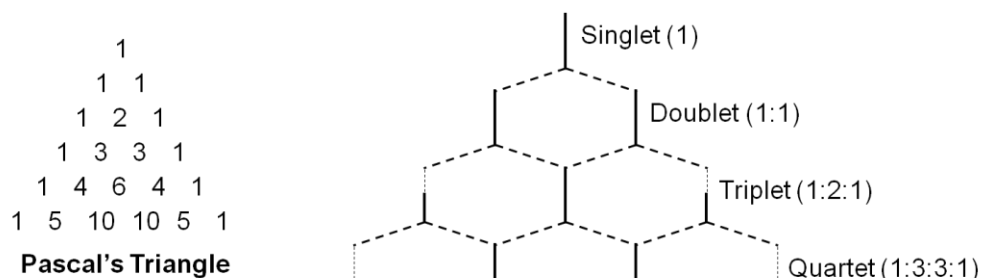


Figure 4.7.64.7.6 Pascal's triangle predicts the number of peaks in a multiplet and their relative intensities.

When there is more than one type of nucleus splitting an NMR signal, then the signal changes from a multiplet to a group of multiplets (Figure 4.7.74.7.7). This is caused by the different coupling constants associated with different types of nuclei. Each nucleus splits the NMR signal by a different width, so the peaks no longer overlap to form peaks with different relative intensities.

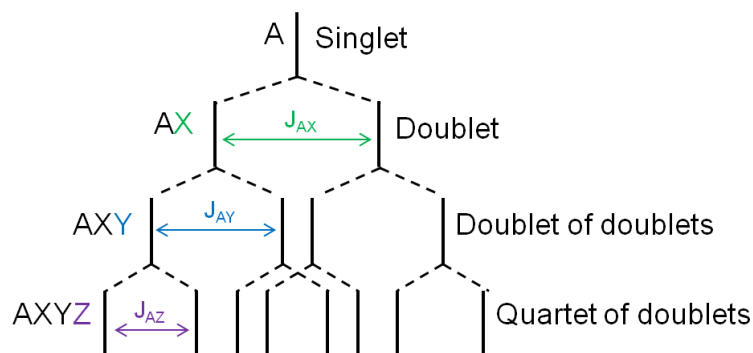


Figure 4.7.74.7.7 The splitting tree of different types of multiplets.

When nuclei have $I > 1/2$, they have more than two possible magnetic moments and thus split NMR signals into more than two peaks. The number of peaks expected is $2I + 1$, corresponding to the number of possible orientations of the magnetic moment. In reality however, some of these peaks may be obscured due to quadrupolar relaxation. As a result, most NMR focuses on $I = 1/2$ nuclei such as ^1H , ^{13}C , and ^{31}P .

Multiplets are centered around the chemical shift expected for a nucleus had its signal not been split. The total area of a multiplet corresponds to the number of nuclei resonating at the given frequency.

Spin Coupling in molecules

Looking at actual molecules raises questions about which nuclei can cause splitting to occur. First of all, it is important to realize that only nuclei with $I \neq 0$ will show up in an NMR spectrum. When $I = 0$, there is only one possible spin state and obviously the nucleus cannot flip between states. Since the NMR signal is based on the absorption of radio frequency as a nucleus transitions from one spin state to another, $I = 0$ nuclei do not show up on NMR. In addition, they do not cause splitting of other NMR signals because they only have one possible magnetic moment. This simplifies NMR spectra, in particular of organic and organometallic compounds, greatly, since the majority of carbon atoms are ^{12}C , which have $I = 0$.

For a nucleus to cause splitting, it must be close enough to the nucleus being observed to affect its magnetic environment. The splitting technically occurs through bonds, not through space, so as a general rule, only nuclei separated by three or fewer bonds can split each other. However, even if a nucleus is close enough to another, it may not cause splitting. For splitting to occur, the nuclei must also be non-equivalent. To see how these factors affect real NMR spectra, consider the spectrum for chloroethane (Figure 4.7.84.7.8).

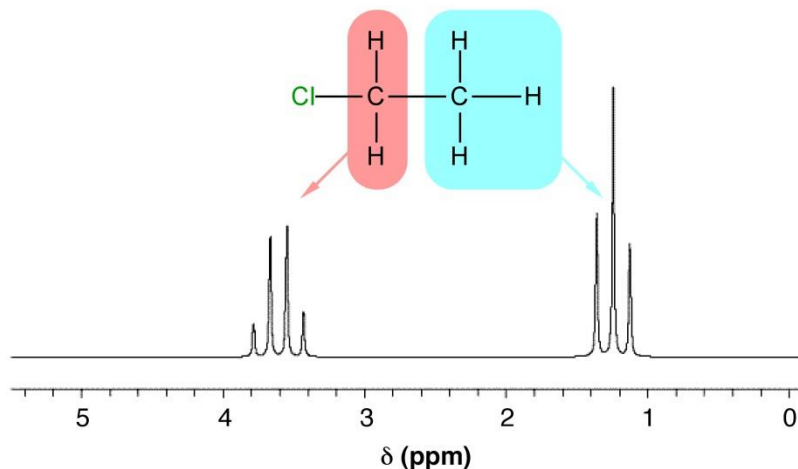


Figure 4.7.84.7.8 The NMR spectrum for chloroethane. Adapted from A. M. Castillo, L. Patiny, and J. Wist. *J. Magn. Reson.*, 2010, **209**, 123.

Notice that in Figure 4.7.84.7.8 there are two groups of peaks in the spectrum for chloroethane, a triplet and a quartet. These arise from the two different types of $I \neq 0$ nuclei in the molecule, the protons on the methyl and methylene groups. The multiplet corresponding to the CH_3 protons has a relative integration (peak area) of three (one for each proton) and is split by the two

methylene protons ($n = 2$), which results in $n + 1$ peaks, i.e., 3 which is a triplet. The multiplet corresponding to the CH_2 protons has an integration of two (one for each proton) and is split by the three methyl protons ($n = 3$) which results in $n + 1$ peaks, i.e., 4 which is a quartet. Each group of nuclei splits the other, so in this way, they are *coupled*.

Coupling Constants

The difference (in Hz) between the peaks of a multiplet is called the *coupling constant*. It is particular to the types of nuclei that give rise to the multiplet, and is independent of the field strength of the NMR instrument used. For this reason, the coupling constant is given in Hz, not ppm. The coupling constant for many common pairs of nuclei are known (Table 4.7.34.7.3), and this can help when interpreting spectra.

Coupling constants are sometimes written nJ to denote the number of bonds (n) between the coupled nuclei. Alternatively, they are written as $J(\text{H-H})$ or J_{HH} to indicate the coupling is between two hydrogen atoms. Thus, a coupling constant between a phosphorous atom and a hydrogen would be written as $J(\text{P-H})$ or J_{PH} . Coupling constants are calculated empirically by measuring the distance between the peaks of a multiplet, and are expressed in Hz.

Coupling constants may be calculated from spectra using frequency or chemical shift data. Consider the spectrum of chloroethane shown in Figure 4.7.54.7.5 and the frequency of the peaks (collected on a 60 MHz spectrometer) give in Table 4.7.44.7.4.

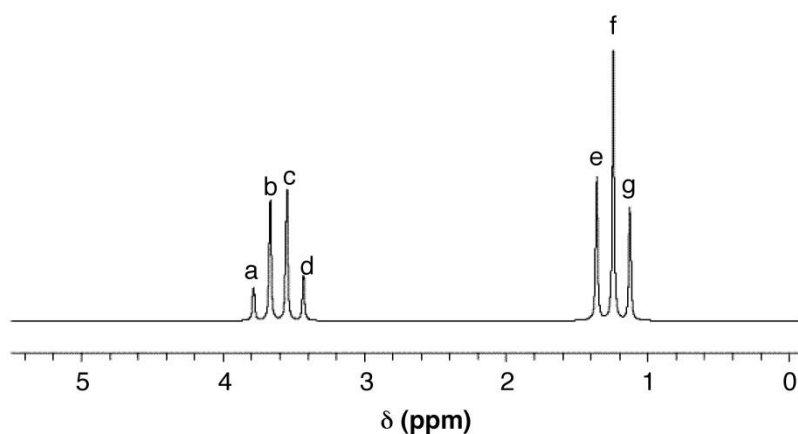


Figure 4.7.54.7.5 ${}^1\text{H}$ NMR spectrum of chloroethane. Peak positions for labeled peaks are given in Table 4.7.44.7.4.

Peak Label	$\delta\delta$ (ppm)	ν (Hz)
A	3.7805	226.83
B	3.6628	219.77
C	3.5452	212.71
D	3.4275	205.65
E	1.3646	81.88
F	1.2470	74.82
G	1.1293	67.76

Table 4.7.44.7.4 Chemical shift in ppm and Hz for all peaks in the ^1H NMR spectrum of chloroethane. Peak labels are given in Figure 4.7.54.7.5.

To determine the coupling constant for a multiplet (in this case, the quartet in Figure 4.7.34.7.3, the difference in frequency (ν) between each peak is calculated and the average of this value provides the coupling constant in Hz. For example using the data from Table 4.7.44.7.4:

$$\text{Frequency of peak c} - \text{frequency of peak d} = 212.71 \text{ Hz} - 205.65 \text{ Hz} = 7.06 \text{ Hz}$$

$$\text{Frequency of peak b} - \text{frequency of peak c} = 219.77 \text{ Hz} - 212.71 \text{ Hz} = 7.06 \text{ Hz}$$

$$\text{Frequency of peak a} - \text{frequency of peak b} = 226.83 \text{ Hz} - 219.77 \text{ Hz} = 7.06 \text{ Hz}$$

$$\text{Average: } 7.06 \text{ Hz}$$

$$\therefore J(\text{H-H}) = 7.06 \text{ Hz}$$

In this case the difference in frequency between each set of peaks is the same and therefore an average determination is not strictly necessary. In fact for 1st order spectra they should be the same. However, in some cases the peak picking programs used will result in small variations, and thus it is necessary to take the trouble to calculate a true average.

To determine the coupling constant of the same multiplet using chemical shift data (δ), calculate the difference in ppm between each peak and average the values. Then multiply the chemical shift by the spectrometer field strength (in this case 60 MHz), in order to convert the value from ppm to Hz:

$$\text{Chemical shift of peak c} - \text{chemical shift of peak d} = 3.5452 \text{ ppm} - 3.4275 \text{ ppm} = 0.1177 \text{ ppm}$$

Chemical shift of peak b - chemical shift of peak c = 3.6628 ppm – 3.5452 ppm = 0.1176 ppm

Chemical shift of peak a - chemical shift of peak b = 3.7805 ppm – 3.6628 ppm = 0.1177 ppm

Average: 0.1176 ppm

Average difference in ppm x frequency of the NMR spectrometer = 0.1176 ppm x 60 MHz = 7.056 Hz

$\therefore J(\text{H-H}) = 7.06 \text{ Hz}$

Second-Order Coupling

When coupled nuclei have similar chemical shifts (more specifically, when $\Delta\nu$ is similar in magnitude to J), *second-order coupling* or *strong coupling* can occur. In its most basic form, second-order coupling results in “roofing” (Figure 4.7.64.7.6). The coupled multiplets point to or lean toward each other, and the effect becomes more noticeable as $\Delta\nu$ decreases. The multiplets also become off-centered with second-order coupling. The midpoint between the peaks no longer corresponds exactly to the chemical shift.

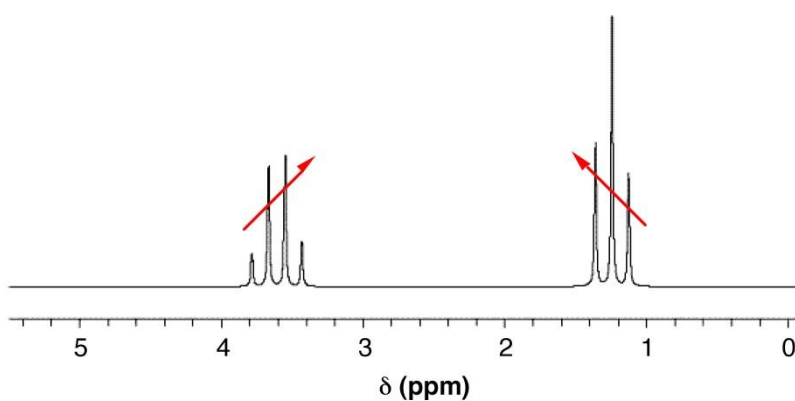


Figure 4.7.64.7.6 Roofing can be seen in the NMR spectrum of chloroethane. Adapted from A. M. Castillo, L. Patiny, and J. Wist, *J. Magn. Reson.*, 2010, **209**, 123.

In more drastic cases of strong coupling (when $\Delta\nu \approx J$), multiplets can merge to create deceptively simple patterns. Or, if more than two spins are involved, entirely new peaks can appear, making it difficult to interpret the spectrum manually. Second-order coupling can often be converted into first-order coupling by using a spectrometer with a higher field strength. This works by altering the $\Delta\nu$ (which is dependent on the field strength), while J (which is independent of the field strength) stays the same.

Phosphorus-31 nuclear magnetic resonance (^{31}P NMR) is conceptually the same as proton (^1H) NMR. The ^{31}P nucleus is useful in NMR spectroscopy due to its relatively high gyromagnetic ratio (17.235 MHz T $^{-1}$). For comparison, the gyromagnetic ratios of ^1H and ^{13}C are (42.576 MHz T $^{-1}$) and (10.705 MHz T $^{-1}$), respectively. Furthermore, ^{31}P has a 100% natural isotopic abundance. Like the ^1H nucleus, the ^{31}P nucleus has a nuclear spin of $1/2$ which makes spectra relatively easy to interpret. ^{31}P NMR is an excellent technique for studying phosphorus containing compounds, such as organic compounds and metal coordination complexes.

Differences Between ^1H and ^{31}P NMR

There are certain significant differences between ^1H and ^{31}P NMR. While ^1H NMR spectra is referenced to tetramethylsilane [$\text{Si}(\text{CH}_3)_4$], the chemical shifts in ^{31}P NMR are typically reported relative to 85% phosphoric acid ($\delta = 0$ ppm), which is used as an external standard due to its reactivity. However, trimethyl phosphite, $\text{P}(\text{OCH}_3)_3$, is also used since unlike phosphoric acid its shift ($\delta = 140$ ppm) is not dependent on concentration or pH. As in ^1H NMR, positive chemical shifts correspond to a downfield shift from the standard. However, prior to the mid-1970s, the convention was the opposite. As a result, older texts and papers report shifts using the opposite sign. Chemical shifts in ^{31}P NMR commonly depend on the concentration of the sample, the solvent used, and the presence of other compounds. This is because the external standard does not take into account the bulk properties of the sample. As a result, reported chemical shifts for the same compound could vary by 1 ppm or more, especially for phosphate groups ($\text{P}=\text{O}$). ^{31}P NMR spectra are often recorded with all proton signals decoupled, i.e., $^{31}\text{P}\{-^1\text{H}\}$, as is done with ^{13}C NMR. This gives rise to single, sharp signals per unique ^{31}P nucleus. Herein, we will consider both coupled and decoupled spectra.

Interpreting Spectra

As in ^1H NMR, phosphorus signals occur at different frequencies depending on the electron environment of each phosphorus nucleus. In this section we will study a few examples of phosphorus compounds with varying chemical shifts and coupling to other nuclei.

Different Phosphorus Environments and their Coupling to ^1H

Consider the structure of 2,6,7-trioxa-1,4-diphosphabicyclo[2.2.2]octane [$\text{P}_\alpha(\text{OCH}_2)_3\text{P}_\beta$] shown in Figure 4.7.84.7.8. The subscripts α and β are simply used to differentiate the two phosphorus nuclei. According to Table 1, we expect the shift of P_α to be downfield of the phosphoric acid standard, roughly around 125 ppm to 140 ppm and the shift of P_β to be upfield of the standard, between -5 ppm and -70 ppm. In the decoupled spectrum shown in Figure 4.7.84.7.8, we can assign the phosphorus shift at 90.0 ppm to P_α and the shift at -67.0 ppm to P_β .

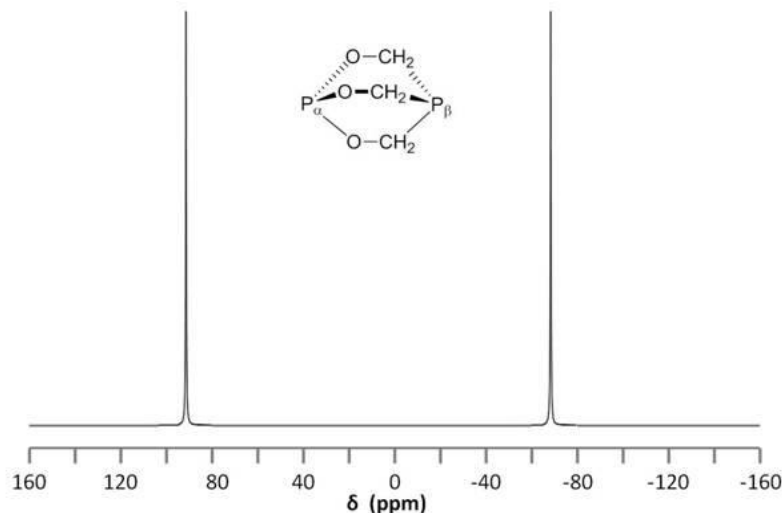


Figure 4.7.84.7.8 Structure and decoupled ^{31}P spectrum ($^{31}\text{P}-\{^1\text{H}\}$) of $\text{P}_\alpha(\text{OCH}_2)_3\text{P}_\beta$.

Figure 4.7.94.7.9 shows the coupling of the phosphorus signals to the protons in the compound. We expect a stronger coupling for P_β because there are only two bonds separating P_β from H, whereas three bonds separate P_α from H ($J_{\text{PCH}} > J_{\text{POCH}}$). Indeed, $J_{\text{PCH}} = 8.9$ Hz and $J_{\text{POCH}} = 2.6$ Hz, corroborating our peak assignments above.

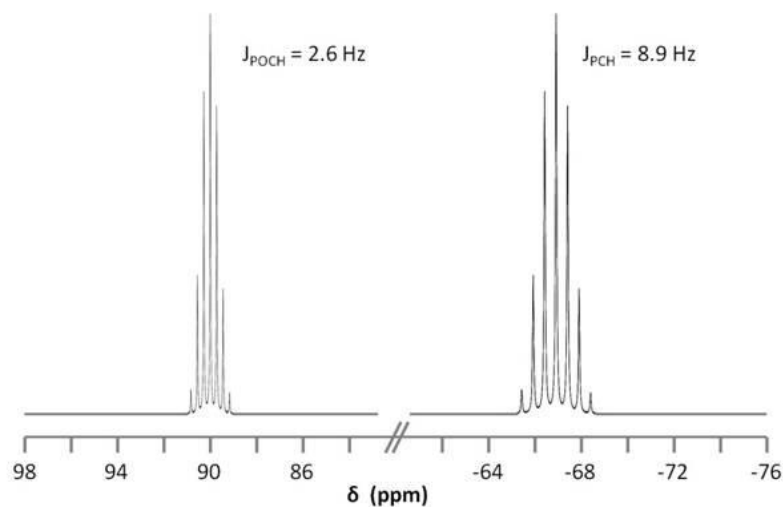


Figure 4.7.94.7.9 The ^{31}P spin coupled spectrum of $\text{P}_\alpha(\text{OCH}_2)_3\text{P}_\beta$.

Finally, Figure 4.7.104.7.10 shows the ^1H spectrum of $\text{P}_\alpha(\text{OCH}_2)_3\text{P}_\beta$ (Figure 4.7.114.7.11), which shows a doublet of doublets for the proton signal due to coupling to the two phosphorus nuclei.

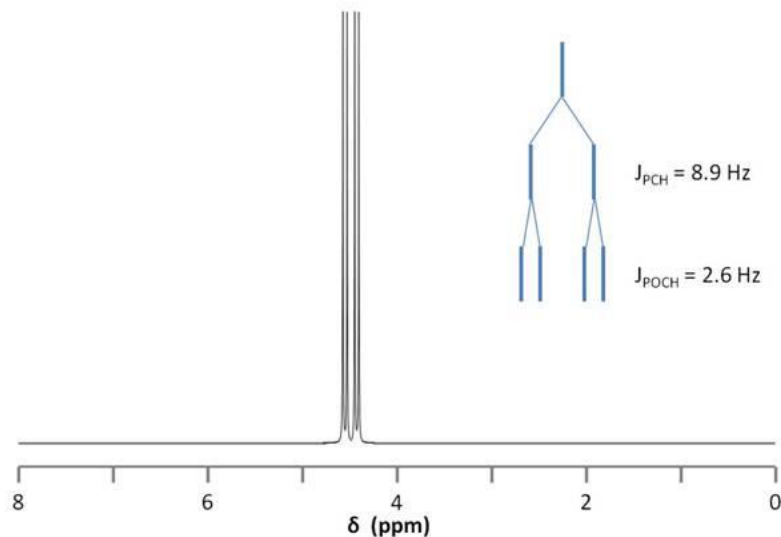


Figure 4.7.104.7.10 ^1H spectrum of $\text{P}_\alpha(\text{OCH}_2)_3\text{P}_\beta$ and proton splitting pattern due to phosphorus.

As suggested by the data in Figure 4.7.74.7.7 we can predict and observe changes in phosphorus chemical shift by changing the coordination of P. Thus for the series of compounds with the structure shown in Figure 4.7.114.7.11 the different chemical shifts corresponding to different phosphorus compounds are shown in Table 4.7.34.7.3.

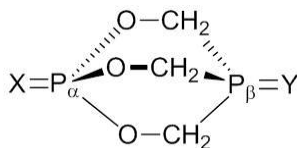


Figure 4.7.114.7.11 Structure of $[\text{XP}_\alpha(\text{OCH}_2)_3\text{P}_\beta\text{Y}]$.

X	Y	P_α chemical shift (ppm)	P_β chemical shift (ppm)
-	-	90.0	-67.0
O	O	-18.1	6.4
S	-	51.8	-70.6

Table 4.7.54.7.5 ^{31}P chemical shifts for variable coordination of $[\text{XP}_\alpha(\text{OCH}_2)_3\text{P}_\beta\text{Y}]$ (Figure 4.7.114.7.11). Data from K. J. Coskran and J. G. Verkade, *Inorg. Chem.*, 1965, **4**, 1655.

Coupling to Fluorine

^{19}F NMR is very similar to ^{31}P NMR in that ^{19}F has spin $1/2$ and is a 100% abundant isotope. As a result, ^{19}F NMR is a great technique for fluorine-containing compounds and allows observance of P-F coupling. The coupled ^{31}P and ^{19}F NMR spectra of ethoxybis(trifluoromethyl)phosphine,

$\text{P}(\text{CF}_3)_2(\text{OCH}_2\text{CH}_3)$, are shown in Figure 4.7.114.7.11. It is worth noting the splitting due to $J_{\text{PCF}} = 86.6 \text{ Hz}$.

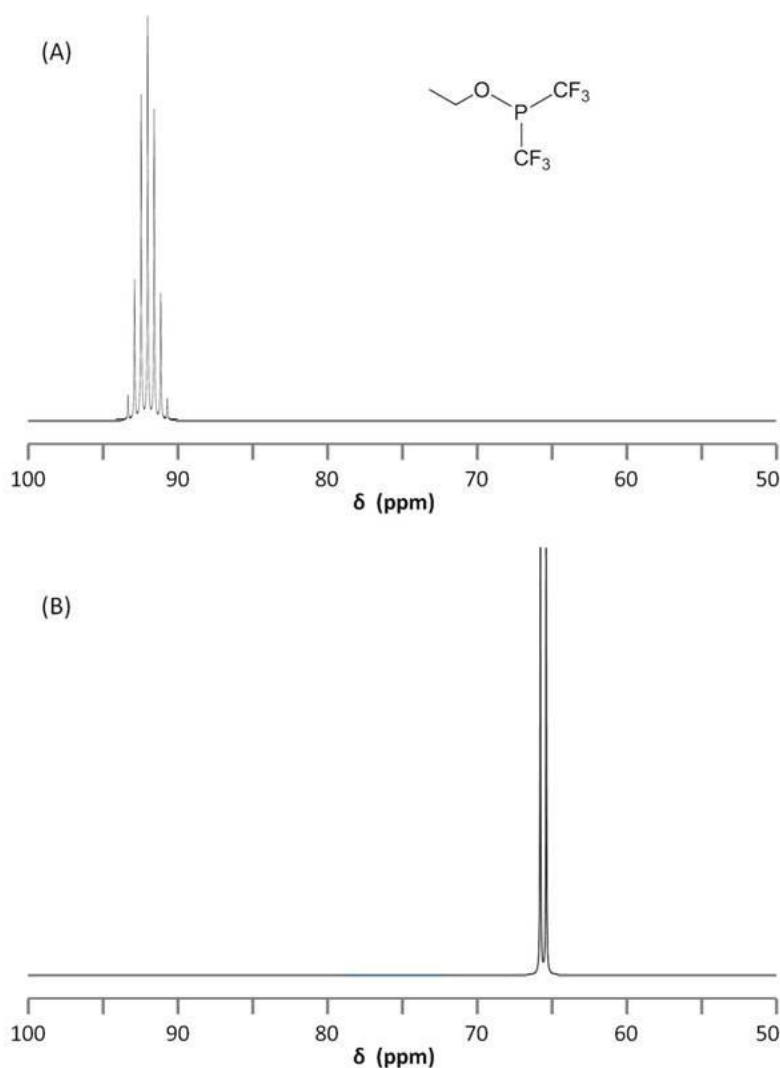


Figure 4.7.114.7.11 Structure, $^{31}\text{P}\{-^1\text{H}\}$ spectrum (A), and $^{19}\text{F}\{-^1\text{H}\}$ spectrum (B) for $\text{P}(\text{CF}_3)_2(\text{OCH}_2\text{CH}_3)$. Data from K. J. Packer, *J. Chem. Soc.*, 1963, 960.

$^{31}\text{P} - ^1\text{H}$ Coupling

Consider the structure of dimethyl phosphonate, $\text{OPH}(\text{OCH}_3)_2$, shown in Figure 4.7.124.7.12. As the phosphorus nucleus is coupled to a hydrogen nucleus bound directly to it, that is, a coupling separated by a single bond, we expect J_{PH} to be very high. Indeed, the separation is so large (715 Hz) that one could easily mistake the split peak for two peaks corresponding to two different phosphorus nuclei.

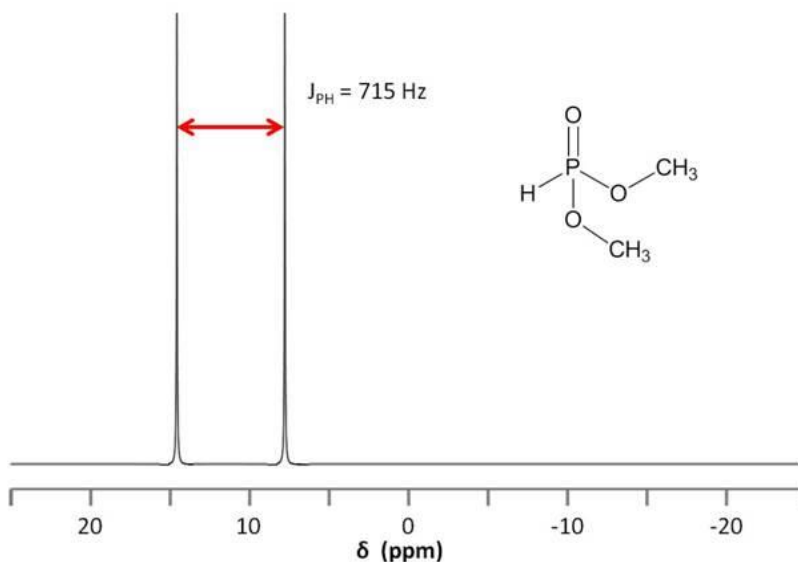


Figure 4.7.124.7.12 Structure and ^{31}P NMR spectrum of $\text{OPH}(\text{OCH}_3)_2$ with only the OCH_3 protons decoupled.

This strong coupling could also lead us astray when we consider the ^1H NMR spectrum of dimethyl phosphonate (Figure 4.7.134.7.13). Here we observe two very small peaks corresponding to the phosphine proton. The peaks are separated by such a large distance and are so small relative to the methoxy doublet (ratio of 1:1:12), that it would be easy to confuse them for an impurity. To assign the small doublet, we could decouple the phosphorus signal at 11 ppm, which will cause this peak to collapse into a singlet.

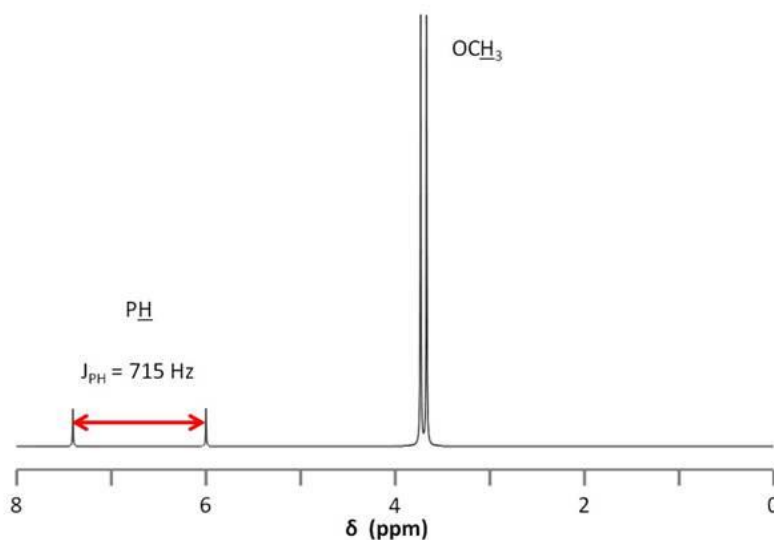


Figure 4.7.134.7.13 ^1H spectrum of $\text{OPH}(\text{OCH}_3)_2$.

³¹P NMR Applications

Assaying Sample Purity

³¹P NMR spectroscopy gives rise to single sharp peaks that facilitate differentiating phosphorus-containing species, such as starting materials from products. For this reason, ³¹P NMR is a quick and simple technique for assaying sample purity. Beware, however, that a “clean” ³¹P spectrum does not necessarily suggest a pure compound, only a mixture free of phosphorus-containing contaminants.

³¹P NMR can also be used to determine the optical purity of a chiral sample. Adding an enantiomer to the chiral mixture to form two different diastereomers will give rise to two unique chemical shifts in the ³¹P spectrum. The ratio of these peaks can then be compared to determine optical purity.

Monitoring Reactions

As suggested in the previous section, ³¹P NMR can be used to monitor a reaction involving phosphorus compounds. Consider the reaction between a slight excess of organic diphosphine ligand and a nickel(0) *bis*-cyclooctadiene, Figure 4.7.154.7.15.

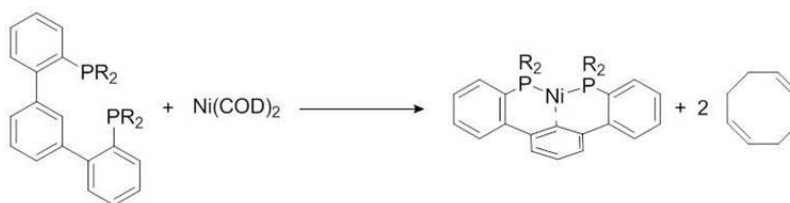


Figure 4.7.154.7.15 Reaction between diphosphine ligand and nickel

The reaction can be followed by ³¹P NMR by simply taking a small aliquot from the reaction mixture and adding it to an NMR tube, filtering as needed. The sample is then used to acquire a ³¹P NMR spectrum and the procedure can be repeated at different reaction times. The data acquired for these experiments is found in Figure 4.7.164.7.16. The changing in ³¹P peak intensity can be used to monitor the reaction, which begins with a single signal at -4.40 ppm, corresponding to the free diphosphine ligand. After an hour, a new signal appears at 41.05 ppm, corresponding to the diphosphine nickel complex. The downfield peak grows as the reaction proceeds relative to the upfield peak. No change is observed between four and five hours, suggesting the conclusion of the reaction.

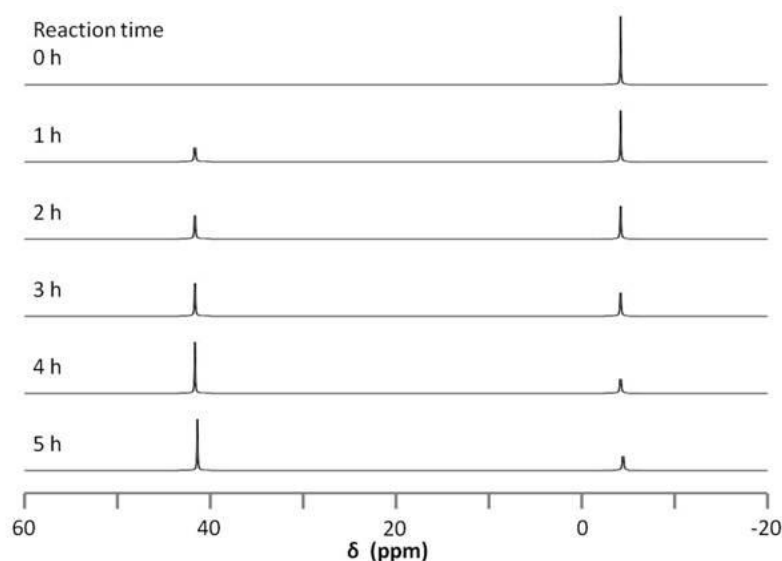


Figure 4.7.164.7.16 $^{31}\text{P}\{-^1\text{H}\}$ NMR spectra of the reaction of diphosphine ligand with nickel(0) *bis*-cyclooctadiene to make a diphosphine nickel complex over time.

There are a number of advantages for using ^{31}P for reaction monitoring when available as compared to ^1H NMR:

- There is no need for a deuterated solvent, which simplifies sample preparation and saves time and resources.
- The ^{31}P spectrum is simple and can be analyzed quickly. The corresponding ^1H NMR spectra for the above reaction would include a number of overlapping peaks for the two phosphorus species as well as peaks for both free and bound cyclooctadiene ligand.
- Purification of product is also easy assayed.

^{31}P NMR does not eliminate the need for ^1H NMR characterization, as impurities lacking phosphorus will not appear in a ^{31}P experiment. However, at the completion of the reaction, both the crude and purified products can be easily analyzed by both ^1H and ^{31}P NMR spectroscopy.

Measuring Epoxide Content of Carbon Nanomaterials

One can measure the amount of epoxide on nanomaterials such as carbon nanotubes and fullerenes by monitoring a reaction involving phosphorus compounds in a similar manner to that described above. This technique uses the catalytic reaction of methyltrioxorhenium (Figure 4.7.174.7.17). An epoxide reacts with methyltrioxorhenium to form a five membered ring. In the presence of triphenylphosphine (PPh_3), the catalyst is regenerated, forming an alkene and triphenylphosphine oxide (OPPh_3). The same reaction can be applied to carbon nanostructures and used to quantify the amount of epoxide on the nanomaterial. Figure 4.7.184.7.18 illustrates the quantification of epoxide on a carbon nanotube.

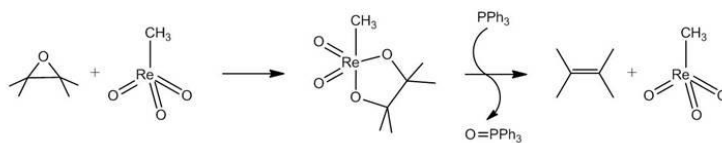


Figure 4.7.174.7.17

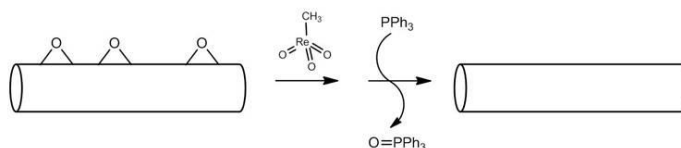


Figure 4.7.184.7.18

Because the amount of initial PPh_3 used in the reaction is known, the relative amounts of PPh_3 and OPPh_3 can be used to stoichiometrically determine the amount of epoxide on the nanotube. ^{31}P NMR spectroscopy is used to determine the relative amounts of PPh_3 and OPPh_3 (Figure 4.7.194.7.19).

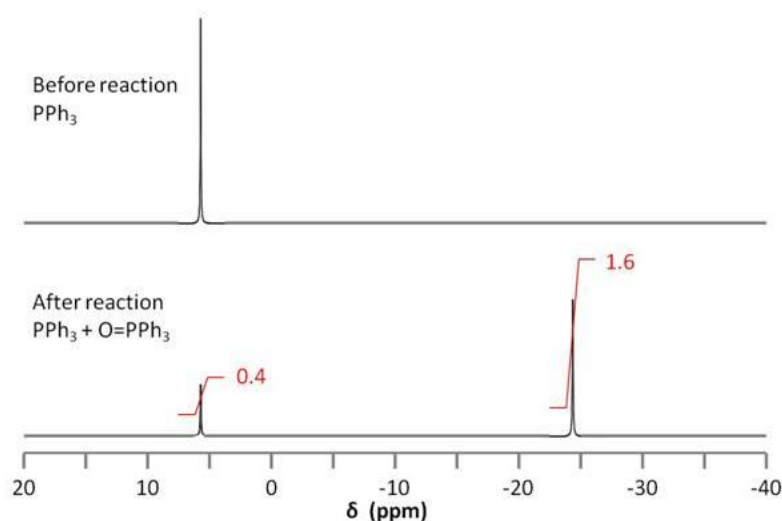


Figure 4.7.194.7.19 ^{31}P spectrum of experiment before addition of Re complex (top) and at the completion of experiment (bottom).

The integration of the two ^{31}P signals is used to quantify the amount of epoxide on the nanotube according to 4.7.44.7.4.

Moles of Epoxide = $\frac{\text{area of OPPH}_3 \text{ peak}}{\text{area of PPh}_3 \text{ peak}} \times \text{moles PPh}_3$ (4.7.4) (4.7.4)
 Moles of Epoxide = $\frac{\text{area of OPPH}_3 \text{ peak}}{\text{area of PPh}_3 \text{ peak}} \times \text{moles PPh}_3$

Thus, from a known quantity of PPh_3 , one can find the amount of OPPh_3 formed and relate it stoichiometrically to the amount of epoxide on the nanotube. Not only does this experiment allow for such quantification, it is also unaffected by the presence of the many different species present in the experiment. This is because the compounds of interest, PPh_3 and OPPh_3 , are the only ones that are characterized by ^{31}P NMR spectroscopy.

paramagnetic Chemical Exchange Saturation Transfer

Strengths of PARACEST

PARACEST addresses the two complications that arise with CEST. Application of a radio frequency pulse close to the bulk water signal will result in some off-resonance saturation of the water. This essentially limits power which enhances CEST effect. Furthermore, a slow exchange condition less than the saturation frequency difference ($\Delta\omega$) means that a very slow exchange rate is required for diamagnetic CEST agents of this sort. Both problems can be alleviated by using an agent that has a larger chemical shift separation such as paramagnetic species. Figure 4.7.68 shows the broad $\Delta\omega$ of Eu^{3+} complex.

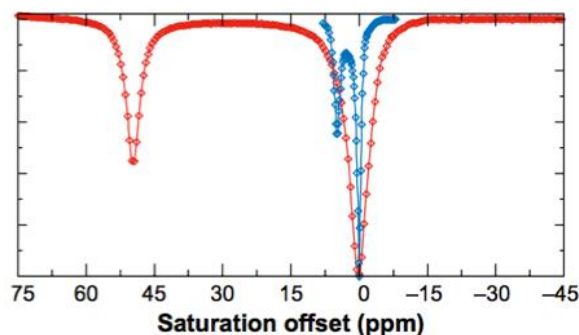


Figure 4.7.68 Eu^{3+} complex broadens the chemical shift leading to a larger saturation frequency difference that can easily be detected. Red spectral line represents $\text{EuDOTA}-(\text{glycine ethyl ester})_4$. Blue spectral line represents barbituric acid. Adapted from A. D. Sherry and M. Woods, *Annu. Rev. Biomed. Eng.*, 2008, **10**, 391.

Selection of Lanthanide Species

Based on the criteria established in 4.7.22, we see that only Eu^{3+} , Tb^{3+} , Dy^{3+} , and Ho^{3+} are effective lanthanide CEST agents at the most common MRI power level (1.5 T). However, given stronger field strengths the Table 4.7.84.7.8 suggests more CEST efficiency. With exception of Sm^{3+} , all other lanthanide molecules have shifts far from water peak providing a large $\Delta\omega$ that is desired of CEST agents. This table should be considered before design of a PARACEST experiment. Furthermore, this table eludes the relationship between power of the saturation pulse and the observed CEST effect. Referring to the following 4.7.234.7.23, we see

that for increased saturation pulse we notice increased CEST effect. In fact, varying B_1 levels changes saturation offset. The higher the B_1 frequency the higher the signal intensity of the saturation offset. As such, it is important to select a proper saturation pulse before experimentation.

Complex	T_m at 298 K (μs)	$\delta \text{ } ^1\text{H}$ (ppm)	$\Delta\omega\tau_a$ at 1.5 T	$\Delta\omega\tau_a$ at 4.7 T	$\Delta\omega\tau_a$ at 11.75 T
Pr^{3+}	20	-60	0.5	1.5	3.8
Nd^{3+}	80	-32	1.0	3.2	8.0
Sm^{3+}	320	-4	0.5	1.6	4.0
Eu^{3+}	382	50	7.7	24.0	60.0
Tb^{3+}	31	-600	7.5	23.4	58.5
Dy^{3+}	17	-720	4.9	15.4	38.5
Ho^{3+}	19	-360	2.8	8.6	21.5
Er^{3+}	9	200	0.7	2.3	5.7
Tm^{3+}	3	500	0.6	1.9	4.7
Yb^{3+}	3	200	0.2	0.5	1.9

Table 4.7.84.7.8 The chemical shifts and proton lifetime values for various lanthanide metals in a lanthanide DOTA-4AmCE complex (Figure 4.7.684.7.68).

Based on the criteria established in 4.7.224.7.22, we see that only Eu^{3+} , Tb^{3+} , Dy^{3+} , and Ho^{3+} are effective lanthanide CEST agents at the most common MRI power level (1.5 T). However, given stronger field strengths the Table 4.7.94.7.9 suggests more CEST efficiency. With exception of Sm^{3+} , all other lanthanide molecules have shifts far from water peak providing a large $\Delta\omega$ that is desired of CEST agents. This table should be considered before design of a PARACEST experiment. Furthermore, this table eludes the relationship between power of the saturation pulse and the observed CEST effect. Referring to the following 4.7.234.7.23, we see that for increased saturation pulse we notice increased CEST effect. In fact, varying B_1 levels changes saturation offset. The higher the B_1 frequency the higher the signal intensity of the saturation offset. As such, it is important to select a proper saturation pulse before experimentation.

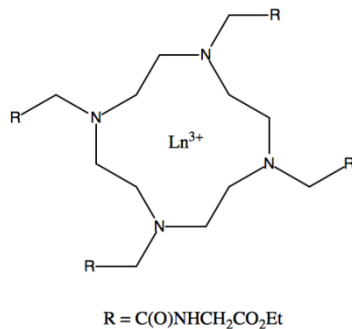


Figure 4.7.69 Structure of lanthanide DOTA-4AmCE complex.

$$\Delta\omega \cdot \tau\alpha = 12\pi B_1 \quad (4.7.22) \quad \Delta\omega \cdot \tau\alpha = 12\pi B_1$$

$$\tau\alpha = 12\pi B_1 \quad (4.7.23) \quad \tau\alpha = 12\pi B_1$$

Running a PARACEST Experiment

Two types of experiments can be run to quantify PARACEST. The first produces quantifiable Z-spectral data and is typically run on 400 MHz spectrometers with a B1 power between 200-1000 KHz and an irradiation time between 2 and 6 seconds based on the lanthanide complex. Imaging experiments are typically performed on either clinical scanners or small bore MRI scanner at room temperature using a custom surface coil. Imaging experiments usually require the following sequence of steps:

1. Bulk water spectra are collected from PARACEST using a 2 second presaturation pulse at a desired power level based on lanthanide complex.
2. Following base scan, the saturation frequency is stepped between ± 100 ppm (relative to the bulk water frequency at 0 ppm) in 1 ppm increments. The scanning frequency can be altered to include a wider scan if lanthanide complex has a larger chemical shift difference.
3. Following collection of data, the bulk water signal is integrated using a Matlab program. The difference between the integrated signals measured at equivalent positive and negative saturation frequencies are plotted and subtracted using the following 4.7.24 and mapped to produce gradient images.
4. To create a CEST Image the data set is first filtered to improve signal-to-noise ratio and normalized with phantom data by subtraction and color-coded.
5. For data tools to perform CEST Imaging analysis. Please refer to the following links for free access to open source software tools: .

$$S_{\text{sat}}(-\Delta\omega) - S_{\text{sat}}(\Delta\omega) S_0 \quad (4.7.24)$$

UNIT-IV

EPR: Theory.

COMPARISON BETWEEN EPR AND NMR

EPR is fundamentally similar to the more widely familiar method of NMR spectroscopy, with several important distinctions. While both spectroscopies deal with the interaction of electromagnetic radiation with magnetic moments of particles, there are many differences between the two spectroscopies:

1. EPR focuses on the interactions between an external magnetic field and the unpaired electrons of whatever system it is localized to, as opposed to the nuclei of individual atoms.
2. The electromagnetic radiation used in NMR typically is confined to the radio frequency range between 300 and 1000 MHz, whereas EPR is typically performed using microwaves in the 3 - 400 GHz range.
3. In EPR, the frequency is typically held constant, while the magnetic field strength is varied. This is the reverse of how NMR experiments are typically performed, where the magnetic field is held constant while the radio frequency is varied.
4. Due to the short relaxation times of electron spins in comparison to nuclei, EPR experiments must often be performed at very low temperatures, often below 10 K, and sometimes as low as 2 K. This typically requires the use of liquid helium as a coolant.
5. EPR spectroscopy is inherently roughly 1,000 times more sensitive than NMR spectroscopy due to the higher frequency of electromagnetic radiation used in EPR in comparison to NMR.

It should be noted that advanced pulsed EPR methods are used to directly investigate specific couplings between paramagnetic spin systems and specific magnetic nuclei. The most widely application is Electron Nuclear Double Resonance (ENDOR). In this method of EPR spectroscopy, both microwave and radio frequencies are used to perturb the spins of electrons and nuclei simultaneously in order to determine very specific couplings that are not attainable through traditional continuous wave methods.

Origin of the EPR Signal

An electron is a negatively charged particle with certain mass, it mainly has two kinds of movements. The first one is spinning around the nucleus, which brings orbital magnetic moment. The other is "spinning" around its own axis, which brings spin magnetic moment. Magnetic moment of the molecule is primarily contributed by unpaired electron's spin magnetic moment.

$$M_S = S(S+1) \hbar^2 \pi \quad (\text{EPR.1})$$

- M_S is the total spin angular momentum,
- S is the spin quantum number and
- \hbar is Planck's constant.

In the z direction, the component of the total spin angular momentum can only assume two values:

$$M_{SZ} = m_S \hbar^2 \pi \quad (\text{EPR.2})$$

The term m_s have $(2S + 1)$ different values: $+S, (S - 1), (S - 2), \dots, -S$. For single unpaired electron, only two possible values for m_s are $+1/2$ and $-1/2$.

The magnetic moment, μ_e is directly proportional to the spin angular momentum and one may therefore write

$$\mu_e = -g_e \mu_B M_S \quad (\text{EPR.3})$$

The appearance of negative sign due to the fact that the magnetic momentum of electron is collinear, but **antiparallel** to the spin itself. The term $(g_e \mu_B)$ is the magnetogyric ratio. The Bohr magneton, μ_B , is the magnetic moment for one unit of quantum mechanical angular momentum:

$$\mu_B = \frac{eh^2}{4\pi m_e} \quad (\text{EPR.4})$$

where e is the electron charge, m_e is the electron mass, the factor g_e is known as the free electron g-factor with a value of 2.002 319 304 386 (one of the most accurately known physical constant). This magnetic moment interacts with the applied magnetic field. The interaction between the magnetic moment (μ) and the field (B) is described by

$$E = -\mu \cdot B \quad (\text{EPR.5})$$

For single unpaired electron, there will be two possible energy states, this effect is called Zeeman splitting.

$$E_{+1/2} = +g_e \mu_B B \quad (\text{EPR.6})$$

$$E_{-1/2} = -g_e \mu_B B \quad (\text{EPR.7})$$

In the absence of external magnetic field,

$$E_{+1/2} = E_{-1/2} = 0 \quad (\text{EPR.8})$$

However, in the presence of external magnetic field (Figure 1), the difference between the two energy states can be written as

$$\Delta E = h\nu = g\mu_B B$$

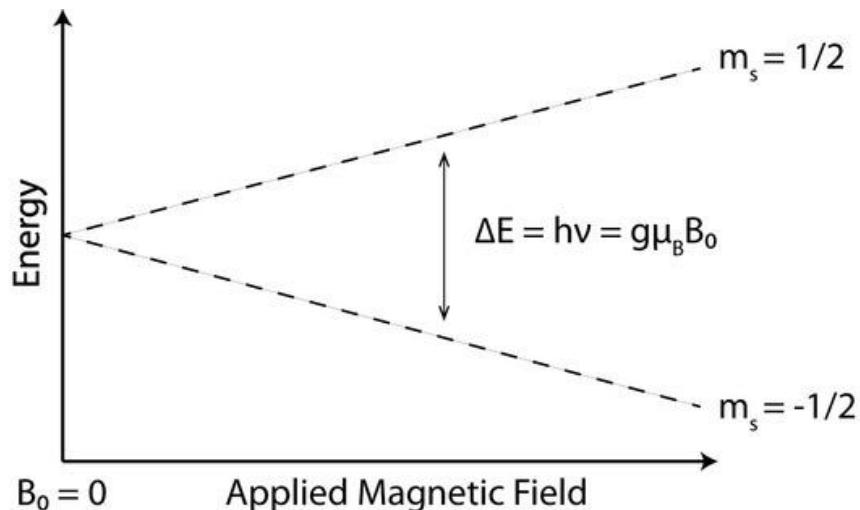


Figure 1: Energy levels for an electron spin ($M_s = \pm 1/2$) in an applied magnetic field B .

With the intensity of the applied magnetic field increasing, the energy difference between the energy levels widens until it matches with the microwave radiation, and results in absorption of photons. This is the fundamental basis for EPR spectroscopy. EPR spectrometers typically vary the magnetic field and hold the microwave frequency. EPR spectrometers are available in several frequency ranges, and X band is currently the most commonly used.

<i>Table 1: Different Microwave bands for EPR Spectroscopy</i>			
Microwave band	Frequency/GHz	Wavelength/cm	B (electron)/Tesla
S	3.0	10.0	0.107
X	9.5	3.15	0.339
K	23	1.30	0.82
Q	35	0.86	1.25
W	95	0.315	3.3

Energy Level Structure and the g-factor

EPR is often used to investigate systems in which electrons have both orbital and spin angular momentum, which necessitates the use of a scaling factor to account for the coupling between the two momenta. This factor is the g-factor, and it is roughly equivalent in utility how chemical

shift is used in NMR. The g factor is associated with the quantum number J, the total angular momentum, where $J=L+S$.

$$g_J = \frac{J(J+1)(g_L + g_s) + (L(L+1) - S(S+1))(g_L - g_s)}{2J(J+1)} \quad (\text{EPR.10})$$

Here, g_L is the orbital g value and g_s is the spin g value. For most spin systems with angular and spin magnetic momenta, it can be approximated that g_L is exactly 1 and g_s is exactly 2. This equation reduces to what is called the Landé formula:

$$g_J = \frac{3}{2} - \frac{S(S+1) - L(L+1)}{2J(J+1)} \quad (\text{EPR.11})$$

And the resultant electronic magnetic dipole is:

$$\mu_J = -g_J \mu_B J \quad (\text{EPR.12})$$

In practice, these approximations do not always hold true, as there are many systems in which J-coupling does occur, especially in transition metal clusters where the unpaired spin is highly delocalized over several nuclei. But for the purposes of an elementary examination of EPR theory it is useful for the understanding of how the g factor is derived. In general this is simply referred to as the **g-factor** or the **Landé g-factor**.

The g-factor for a free electron with zero angular momentum still has a small quantum mechanical corrective g value, with $g = 2.0023193$. In addition to considering the total magnetic dipole moment of a paramagnetic species, the g-value takes into account the local environment of the spin system. The existence of local magnetic fields produced by other paramagnetic species, electric quadrupoles, magnetic nuclei, ligand fields (especially in the case of transition metals) all can change the effective magnetic field that the electron experiences such that

$$B_{\text{eff}} = B_0 + B_{\text{local}} \quad (\text{EPR.13})$$

These local fields can either:

1. be induced by the applied field, and hence have magnitude dependence on B_0 or are
2. permanent and independent of B_0 other than in orientation.

In the case of the first type, it is easiest to consider the effective field experienced by the electron as a function of the applied field, thus we can write:

$$B_{\text{eff}} = B_0(1 - \sigma) \quad (\text{EPR.14})$$

where σ is the shielding factor that results in decreasing or increasing the effective field. The g-factor must then be replaced by a variable g factor g_{eff} such that:

$$B_{\text{eff}} = B_0 \cdot (g_{\text{eff}}) \quad (\text{EPR.15})$$

Many organic radicals and radical ions have unpaired electrons with L near zero, and the total angular momentum quantum number J becomes approximately S . As a result, the g -values of these species are typically close to 2. In stark contrast, unpaired spins in transition metal ions or complexes typically have larger values of L and S , and their g values diverge from 2 accordingly.

After all of this, the energy levels that correspond to the spins in an applied magnetic field can now be written as:

$$E_{ms} = m_s g \mu_B B_0 \quad (\text{EPR.16})$$

And thus the energy difference associated with a transition is given as:

$$\Delta E_{ms} = \Delta m_s g \mu_B B_0 \quad (\text{EPR.17})$$

Typically, EPR is performed perpendicular mode, where the magnetic field component of the microwave radiation is oriented perpendicular to the magnetic field created by the magnet. Here, the selection rule for allowed EPR transitions is $\Delta m_s = \pm 1$, so the energy of the transition is simply:

$$\Delta E_{ms} = g \mu_B B_0 \quad (\text{EPR.18})$$

There is a method called Parallel Mode EPR in which the microwaves are applied parallel to the magnetic field, changing the selection rule to $\Delta m_s = \pm 2$. This is more fully explained in the Parallel Mode EPR: Theory module.

Electron/Nuclear Zeeman Interactions using Operators

Using the Hamiltonians derived in the last section, we can develop hamiltonians for the perturbed case in which an external magnetic field is introduced. For the simple case of the hydrogen atom with $S=1/2$ and $I=1/2$, interaction with a strong magnetic field oriented along the z -direction will be considered. Using the operator form, the Hamiltonian takes the form:

$$\hat{H} = -B \mu^z \quad (\text{EPR.39})$$

Here, the electron magnetic moment operator μ_{ez} is proportional to the electron spin operator. Likewise, the nuclear magnetic moment operator μ_{nz} is proportional to the nuclear spin operator I_z . Therefore,

$$\mu^z = \gamma_e S^z = -g \mu_B S^z \quad (\text{EPR.40})$$

$$\mu^{\wedge}nz = \gamma n I^{\wedge}zh = +gn\mu n I^{\wedge}z \text{ (EPR.41)}$$

Now the electron and nuclear spin Hamiltonians can be defined as:

$$H^{\wedge}e = g_e \mu_B S_z^{\wedge} \text{ (EPR.42)}$$

$$H^{\wedge}n = -gn\mu n I_z^{\wedge} \text{ (EPR.43)}$$

We now have a quantum mechanical framework for the energies of electronic and nuclear spin states that will be further useful in developing a description of the interactions between the magnetic moments of the two classes of particles.

Nuclear Hyperfine Structure

According to the figure 1, we should observe one spectra line in a paramagnetic molecule, but in reality, we usually observe more than one split line. The reason for that is hyperfine interactions, which results from interaction of the magnetic moment of the unpaired electron and the magnetic nuclei. The hyperfine patterns are highly valuable when it comes to determine the spatial structure of paramagnetic species and identify the paramagnetic species. As a result, nuclear spins act as probes which are sensitive to the magnetitude and direction of the field due to the unpaired electron.

In general, there are two kinds of hyperfine interactions between unpaired electron and the nucleus. The first is the interaction of two dipoles. We refer it as the anisotropic or dipolar hyperfine interaction, which is the interaction between electron spin magnetic moment and the nuclei magnetic moment, and it depends on the shape of electronic orbital and the average distance of electron and nucleus. This interaction can help us to determine the possible position of a paramagnetic species in a solid lattice.

The second interaction is known as the Fermi contact interaction, and only takes the electrons in s orbital into consideration, since p, d and f orbitals have nodal planes passing through the nucleus. We refer to this type of interaction as isotropic, which depends on the presence of a finite unpaired electron spin density at the position of the nucleus, not on the orientation of the paramagnetic species in the magnetic field.

$$A = -83\pi (\mu_n \cdot \mu_e) \cdot |\psi(0)|^2 \text{ (EPR.44)}$$

A is the isotropic hyperfine coupling constant and is related to the unpaired spin density, μ_n is the nuclear magnetic moment, μ_e is the electron magnetic moment and $\Psi(0)$ is the electron wavefunction at the nucleus. The Fermi contact interaction happens in s orbital when electron density is not zero. Thus nuclear hyperfine spectra not only includes the interaction of nuclei and

their positions in the molecule but also the extent to which part or all of the molecule is free to reorientate itself according to the direction of the applied magnetic field.

Isotropic Hyperfine Interaction

In the case of one unpaired electron, the spin hamiltonian can be written as below for the isotropic part of nuclear hyperfine interaction.

$$H = H_{EZ} - H_{NZ} - H_{HFS} \quad (\text{EPR.45})$$

EZ means electron Zeeman, NZ means nuclear Zeeman and HFS represents hyperfine interaction. The equation can also be written as

$$H^{\wedge} = g\mu_B H S_Z - g_N \mu_N N \cdot B I_Z + h \cdot S \cdot a I \quad (\text{EPR.46})$$

The term $aS \cdot I$ is introduced by Fermi contact interaction. I is the nucleus spin, H is the external field. Since μ_B is much larger than μ_N , the equation can take the form as:

$$H^{\wedge} = g\mu_B H S_Z + h \cdot S \cdot a I \quad (\text{EPR.47})$$

When one unpaired electron interacts with one nucleus, the number of EPR lines is $2I+1$. When one unpaired electron interacts with N equivalent nuclei, the number of EPR lines is $2NI+1$. When one electron interacts with nonequivalent nuclei (N_1, N_2, \dots), the number of EPR lines is

$$\prod_{i=1}^k (2N_i I_i + 1)$$

In the case of DPPH, $I=1/2$ and two nitrogen nuclei are equivalent. $2NI+1=5$, we can get five lines: 1:2:3:2:1.

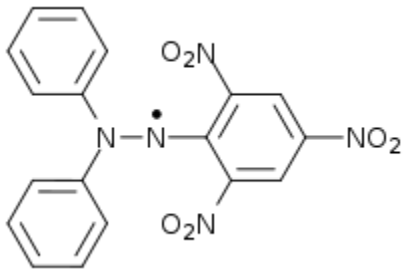


Figure 2: DPPH

The table below shows the relative intensities of the lines according to unpaired electrons interacting with multiple equivalent nuclei.

Number of Equivalent Nuclei	Relative Intensities
1	1:1
2	1:2:1
3	1:3:3:1
4	1:4:6:4:1
5	1:5:10:10:5:1
6	1:6:15:20:15:6:1

We can observe that increasing number of nuclei leads to the complexity of the spectrum, and spectral density depends on the number of nuclei as equation shown below:

$$\text{Spectral density EPR} = \sum_{k=1}^N |a_k| N_i (EPR.49)$$

a is the isotropic hyperfine coupling constant.

The g Anisotropy

From the below equation, we can calculate g in this way:

$$\Delta E = h\nu = g\mu_B B (EPR.50)$$

If the energy gap is not zero, g factor can be remembered as:

$$g \approx 114 \nu [\text{GHZ}] / B [\text{T}] (EPR.51)$$

The g factor is not necessarily isotropic and needs to be treated as a tensor g . For a free electron, g factor is close to 2. If electrons are in the atom, g factor is no longer 2, spin orbit coupling will shift g factor from 2. If the atom are placed at an electrostatic field of other atoms, the orbital energy level will also shift, and the g factor becomes anisotropic. The anisotropies lead to line broadening in isotropic ESR spectra. The Electron-Zeeman interaction depends on the absolute orientation of the molecule with respect to the external magnetic field. Anisotropic is very important for free electrons in non-symmetric orbitals (p,d).

In a more complex spin system, Hamiltonian is required to interpret as below:

$$H^s = \mu_B B^{\vec{r}} \cdot g \cdot S^{\vec{r}} + \sum_i I^{\vec{r}} \cdot A_i \cdot S^{\vec{r}} (EPR.52)$$

g and A_i are 3×3 matrices representing the anisotropic Zeeman and nuclear hyperfine interactions, thus it is more accurate to describe g -factor as a tensor like:

$$g = g_x \sin 2\alpha \cdot \cos 2\beta + g_y \sin 2\alpha \cdot \cos 2\beta + g_z \cos 2\alpha (EPR.53)$$

Alpha and beta is the angle between magnetic field with respect to principle axis of g tensor. If $g_x = g_y$, it can be expressed as:

$$g = g_x \cdot \sin 2\alpha + g_z \cos 2\alpha \quad (\text{EPR.54})$$

Thus, we can identify the g tensor by measuring the angular dependence in the above equation.

Spin Relaxation Mechanisms

The excess population of lower state over upper state for a single spin system is very small as we can calculate from the following example. With the temperature of 298K in a magnetic field of 3000G, $N_{\text{upper}}/N_{\text{lower}} = 0.9986$, which means the populations of the two energy levels are almost equal, yet the slight excess in the lower level leads to energy absorption. In order to maintain a population excess in the lower level, the electrons from the upper level give up the hv energy to return to the lower level to satisfy the Maxwell–Boltzmann law. The process of this energy releasing is called spin relaxation process, of which there are two types, known as spin–lattice relaxation and spin–spin relaxation.

Spin-lattice relaxation

this implies interaction between the species with unpaired electrons, known as "spin system" and the surrounding molecules, known as "lattice". The energy is dissipated within the lattice as vibrational, rotational or translational energy. The spin lattice relaxation is characterized by a relaxation time T_{1e} , which is the time for the spin system to lose $1/e^{\text{th}}$ of its excess energy. Rapid dissipation of energy (short T_{1e}) is essential if the population difference of the spin states is to be maintained. Slow spin-lattice relaxation, which is of frequent occurrence in systems containing free radicals, especially at low temperatures, can cause saturation of the spin system. This means that the population difference of the upper and lower spin states approaches zero, and EPR signal ceases.

Spin-spin relaxation

Spin-spin relaxation or Cross relaxation, by which energy exchange happens between electrons in a higher energy spin state and nearby electrons or magnetic nuclei in a lower energy state, without transferring to the lattice. The spin–spin relaxation can be characterized by spin-spin relaxation time T_{2e} .

When both spin–spin and spin–lattice relaxations contribute to the EPR signal, the resonance line width (ΔB) can be written as

$$\Delta B \propto 1/T_{1e} + 1/T_{2e} \quad (\text{EPR.55})$$

Hyperfine Splitting

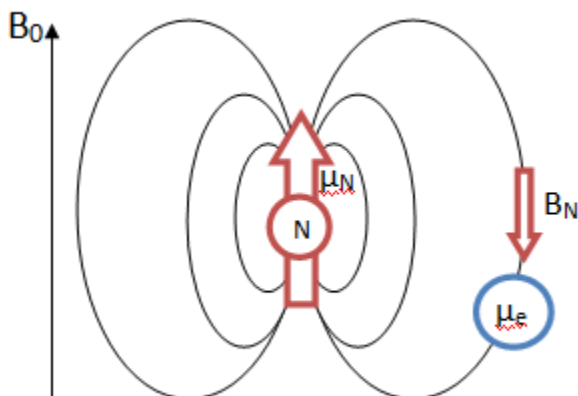


Figure 11. B is magnetic field, μ is dipole moment, 'N' refers to the nucleus, 'e' refers to the electron

This spin interaction in turn causes splitting of the fine structure of spectral lines into smaller components called hyperfine structure. Hyperfine structure is approximately 1000 times smaller than fine structure. Figure 22 shows a comparison of fine structure with hyperfine structure splitting for hydrogen, though this is not to scale.

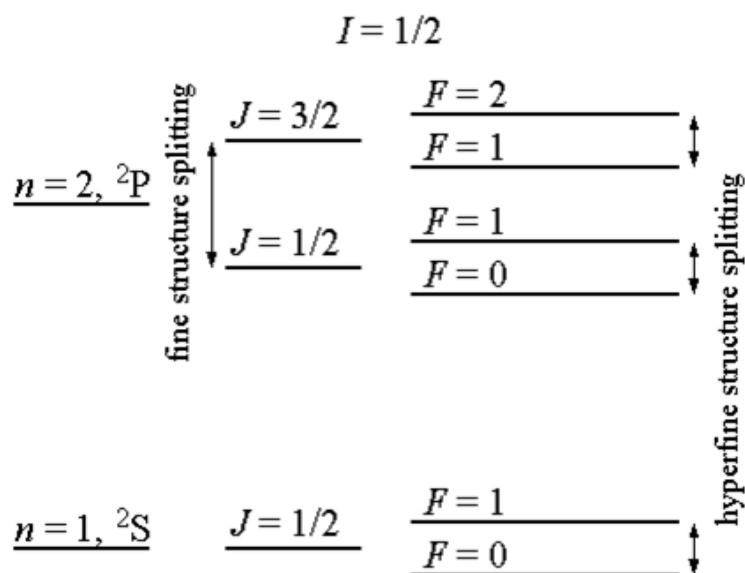


Figure 22. Splitting diagram of hydrogen

The total angular momentum of the atom is represented by F with regards to hyperfine structure. This is found simply through the relation $F=J+I$ where I is the ground state quantum number and J refers to the energy levels of the system.

Results of Nuclear-Electron Interactions

These hyperfine interactions between dipoles are especially relevant in EPR. The spectra of EPR are derived from a change in the spin state of an electron. Without the additional energy levels arising from the interaction of the nuclear and electron magnetic moments, only one line would be observed for single electron spin systems. This process is known as hyperfine splitting (hyperfine coupling) and may be thought of as a Zeeman effect occurring due to the magnetic dipole moment of the nucleus inducing a magnetic field.

The coupling patterns due to hyperfine splitting are identical to that of NMR. The number of peaks resulting from hyperfine splitting of radicals may be predicted by the following equations where M_i is the number of equivalent nuclei:

- # of peaks= $M_i I + 1$ # of peaks= $M_i I + 1$ for atoms having one equivalent nuclei
- # of peaks= $(2M_1 I_1 + 1)(2M_2 I_2 + 1) \dots$ # of peaks= $(2M_1 I_1 + 1)(2M_2 I_2 + 1) \dots$ for atoms with multiple equivalent nuclei

For example, in the case of a methyl radical 4 lines would be observed in the EPR spectra. A methyl radical has 3 equivalent protons interacting with the unpaired electron, each with $I=1/2$ as their nuclear state yielding 4 peaks.

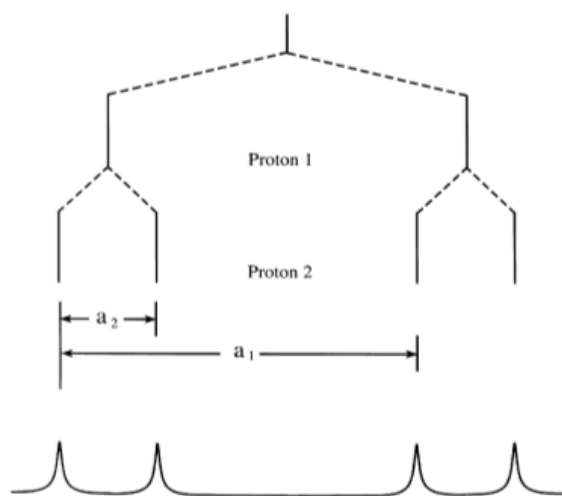


Figure 33. Approximate peaks resulting from hyperfine splitting between two nonequivalent protons

The relative intensities of certain radicals can also be predicted. When $I = 1/2$ as in the case for ^1H , ^{19}F , and ^{31}P , then the intensity of the lines produced follow Pascal's triangle. Using the methyl radical example, the 4 peaks would have relative intensities of 1:3:3:1. The following figures² show the different splitting that results from interaction between equivalent versus nonequivalent protons.

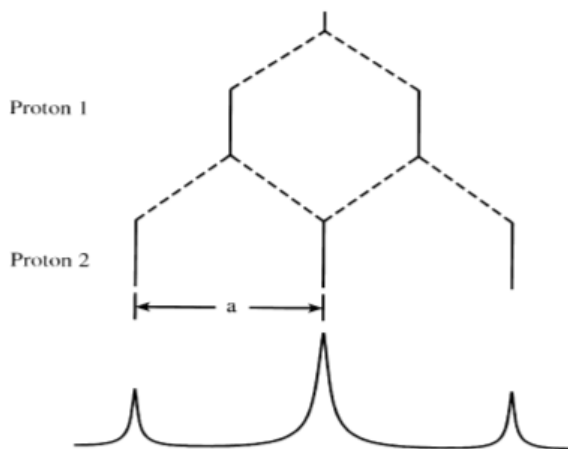


Figure 44. Approximate peaks resulting from hyperfine splitting between two equivalent protons

It is important to note that the spacing between peaks is 'a', the hyperfine coupling constant. This constant is equivalent for both protons in the equivalent system but unequal for the nonequivalent protons.

The Hyperfine Coupling Constant

The **hyperfine coupling constant** (a_i) is directly related to the distance between peaks in a spectrum and its magnitude indicates the extent of delocalization of the unpaired electron over the molecule. This constant may also be calculated. The following equation shows the total energy related to electron transitions in EPR.

$$\Delta E = g_e \mu_B M_s B + \sum_i g_N \mu_N M_I (1 - \sigma_i) + \sum_i a_i M_s M_I$$

The first two terms correspond to the Zeeman energy of the electron and the nucleus of the system, respectively. The third term is the hyperfine coupling between the electron and nucleus where a_i is the hyperfine coupling constant. Figure 55 shows splitting between energy levels and their dependence on magnetic field strength. In this figure, there are two resonances where frequency equals energy level splitting at magnetic field strengths of B_1 and B_2 .

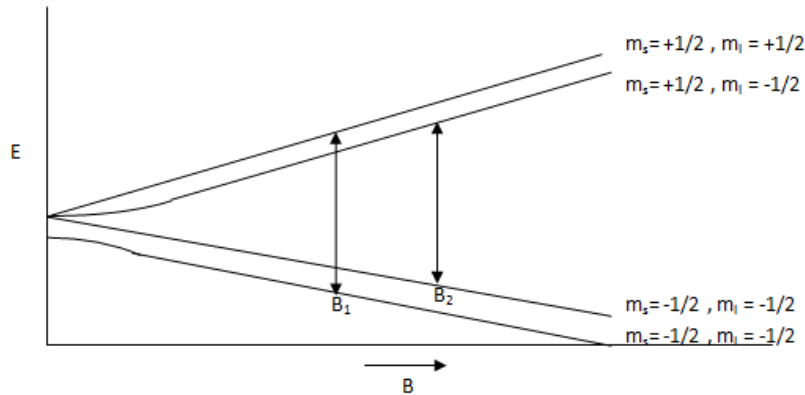


Figure 55: Splitting between energy levels and their dependence on magnetic field strength

Classes of Magnetic Materials

The origin of magnetism lies in the orbital and spin motions of electrons and how the electrons interact with one another. The best way to introduce the different types of magnetism is to describe how materials respond to magnetic fields. This may be surprising to some, but all matter is magnetic. It's just that some materials are much more magnetic than others. The main distinction is that in some materials there is no collective interaction of atomic magnetic moments, whereas in other materials there is a very strong interaction between atomic moments.

The magnetic behavior of materials can be classified into the following five major groups:

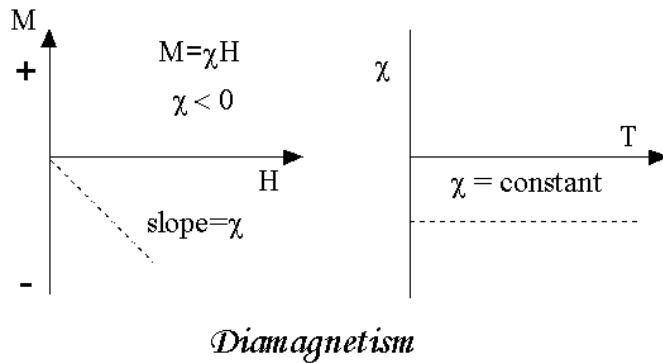
Magnetic Properties of some common minerals

Materials in the first two groups are those that exhibit no collective magnetic interactions and are not magnetically ordered. Materials in the last three groups exhibit long-range magnetic order below a certain critical temperature. Ferromagnetic and ferrimagnetic materials are usually what we consider as being magnetic (ie., behaving like iron). The remaining three are so weakly magnetic that they are usually thought of as "nonmagnetic".

1. Diamagnetism

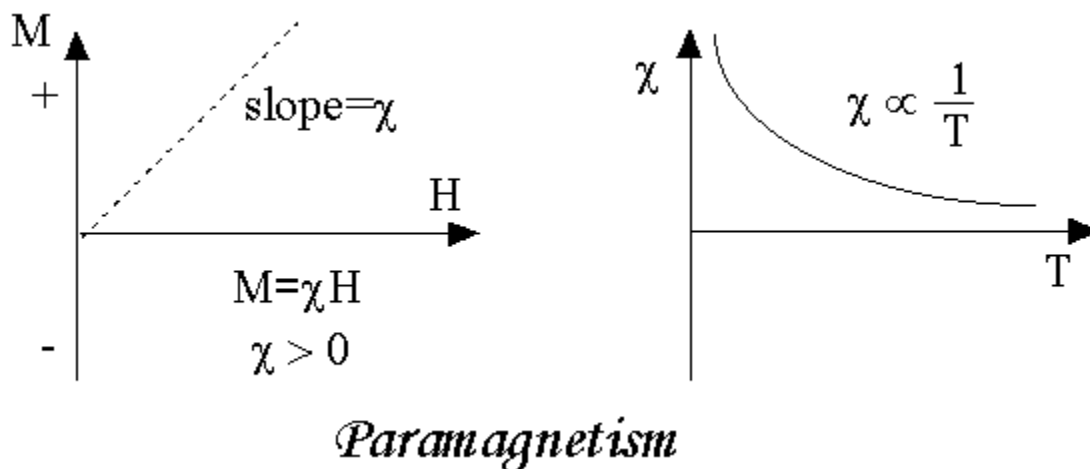
Diamagnetism is a fundamental property of all matter, although it is usually very weak. It is due to the non-cooperative behavior of orbiting electrons when exposed to an applied magnetic field. Diamagnetic substances are composed of atoms which have no net magnetic moments (ie., all the orbital shells are filled and there are no unpaired electrons). However, when exposed to a

field, a negative magnetization is produced and thus the susceptibility is negative. If we plot M vs H , we see:



2. Paramagnetism

This class of materials, some of the atoms or ions in the material have a net magnetic moment due to unpaired electrons in partially filled orbitals. One of the most important atoms with unpaired electrons is iron. However, the individual magnetic moments do not interact magnetically, and like diamagnetism, the magnetization is zero when the field is removed. In the presence of a field, there is now a partial alignment of the atomic magnetic moments in the direction of the field, resulting in a net positive magnetization and positive susceptibility.



In addition, the efficiency of the field in aligning the moments is opposed by the randomizing effects of temperature. This results in a temperature dependent susceptibility, known as the Curie Law.

At normal temperatures and in moderate fields, the paramagnetic susceptibility is small (but larger than the diamagnetic contribution). Unless the temperature is very low ($\ll 100$ K) or the field is very high paramagnetic susceptibility is independent of the applied field. Under these conditions, paramagnetic susceptibility is proportional to the total iron content. Many iron bearing minerals are paramagnetic at room temperature. Some examples, in units of $10^{-8} \text{ m}^3/\text{kg}$, include:

Montmorillonite (clay) 13

Nontronite (Fe-rich clay) 65

Biotite (silicate) 79

Siderite(carbonate) 100

Pyrite (sulfide) 30

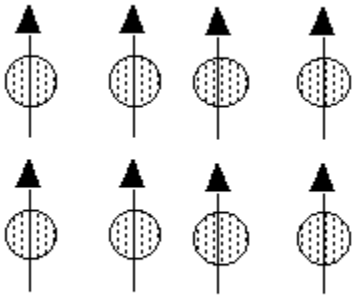
The paramagnetism of the matrix minerals in natural samples can be significant if the concentration of magnetite is very small. In this case, a paramagnetic correction may be needed.

3. Ferromagnetism

When you think of magnetic materials, you probably think of iron, nickel or magnetite. Unlike paramagnetic materials, the atomic moments in these materials exhibit very strong interactions. These interactions are produced by electronic exchange forces and result in a parallel or antiparallel alignment of atomic moments. Exchange forces are very large, equivalent to a field on the order of 1000 Tesla, or approximately a 100 million times the strength of the earth's field.

The exchange force is a quantum mechanical phenomenon due to the relative orientation of the spins of two electron.

Ferromagnetic materials exhibit parallel alignment of moments resulting in large net magnetization even in the absence of a magnetic field.

parallel alignment

The elements Fe, Ni, and Co and many of their alloys are typical ferromagnetic materials.

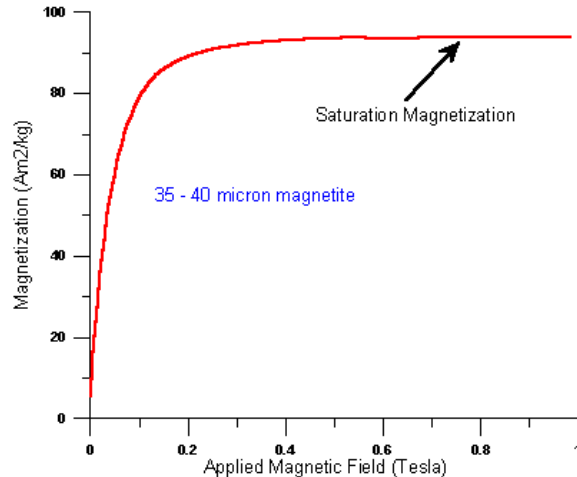
Two distinct characteristics of ferromagnetic materials are their

- (1) spontaneous magnetization and the existence of
- (2) magnetic ordering temperature

Ferromagnetism**Spontaneous Magnetization**

The spontaneous magnetization is the net magnetization that exists inside a uniformly magnetized microscopic volume in the absence of a field. The magnitude of this magnetization, at 0 K, is dependent on the spin magnetic moments of electrons.

A related term is the saturation magnetization which we can measure in the laboratory. The saturation magnetization is the maximum induced magnetic moment that can be obtained in a magnetic field (H_{sat}); beyond this field no increase in magnetization occurs.



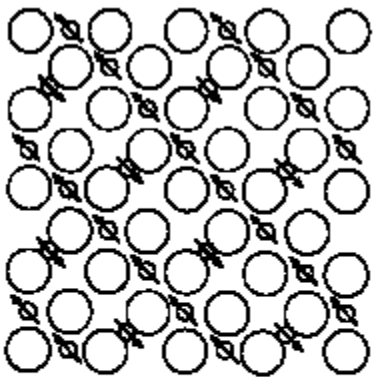
The difference between spontaneous magnetization and the saturation magnetization has to do with magnetic domains (more about domains later). Saturation magnetization is an intrinsic property, independent of particle size but dependent on temperature.

There is a big difference between paramagnetic and ferromagnetic susceptibility. As compared to paramagnetic materials, the magnetization in ferromagnetic materials is saturated in moderate magnetic fields and at high (room-temperature) temperatures:

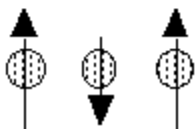
	H_{sat} Tesla	T range (K)	χ $10^{-8}\text{m}^3/\text{kg}$
paramagnets	>10	<<100	~50
ferromagnets	~1	~300	1000-10000

4. Ferrimagnetism

In ionic compounds, such as oxides, more complex forms of magnetic ordering can occur as a result of the crystal structure. One type of magnetic ordering is called ferrimagnetism. A simple representation of the magnetic spins in a ferrimagnetic oxide is shown here.



Ferrimagnetism

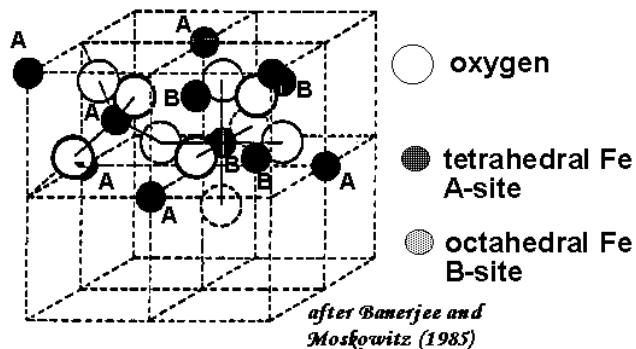


The magnetic structure is composed of two magnetic sublattices (called A and B) separated by oxygens. The exchange interactions are mediated by the oxygen anions. When this happens, the interactions are called indirect or superexchange interactions. The strongest superexchange interactions result in an antiparallel alignment of spins between the A and B sublattice.

In ferrimagnets, the magnetic moments of the A and B sublattices are not equal and result in a net magnetic moment. Ferrimagnetism is therefore similar to ferromagnetism. It exhibits all the hallmarks of ferromagnetic behavior- spontaneous magnetization, Curie temperatures, hysteresis, and remanence. However, ferro- and ferrimagnets have very different magnetic ordering.

Magnetite is a well known ferrimagnetic material. Indeed, magnetite was considered a ferromagnet until Néel in the 1940's, provided the theoretical framework for understanding ferrimagnetism.

Crystal Structure of Magnetite



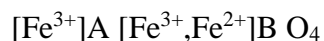
Magnetite, Fe_3O_4 crystallizes with the spinel structure. The large oxygen ions are close packed in a cubic arrangement and the smaller Fe ions fill in the gaps. The gaps come in two flavors:

tetrahedral site: Fe ion is surrounded by four oxygens

octahedral site: Fe ion is surrounded by six oxygens

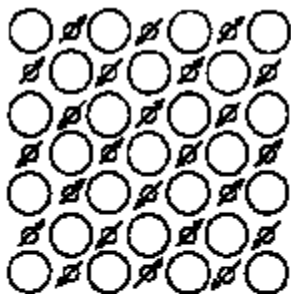
The tetrahedral and octahedral sites form the two magnetic sublattices, A and B respectively. The spins on the A sublattice are antiparallel to those on the B sublattice. The two crystal sites are very different and result in complex forms of exchange interactions of the iron ions between and within the two types of sites.

The structural formula for magnetite is

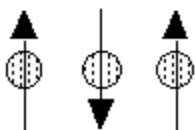


This particular arrangement of cations on the A and B sublattice is called an inverse spinel structure. With negative AB exchange interactions, the net magnetic moment of magnetite is due to the B-site Fe^{2+} .

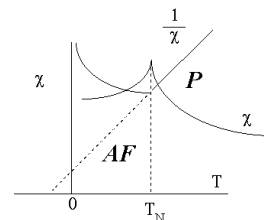
5. Antiferromagnetism



Antiferromagnetism

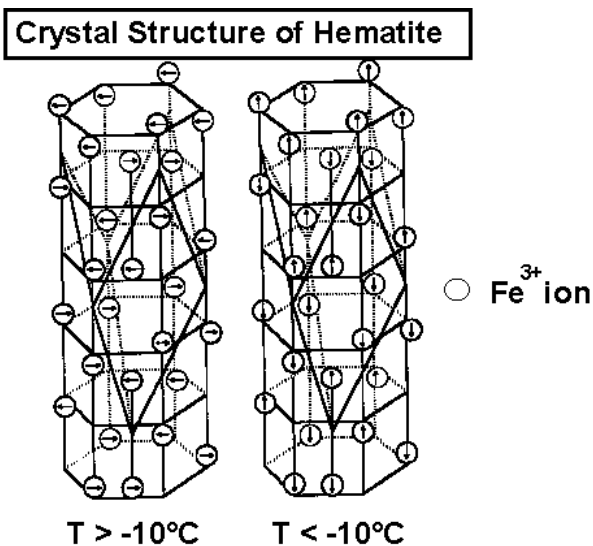


If the A and B sublattice moments are exactly equal but opposite, the net moment is zero. This type of magnetic ordering is called antiferromagnetism.

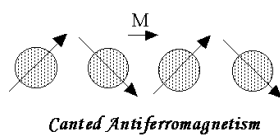


The clue to antiferromagnetism is the behavior of susceptibility above a critical temperature, called the Néel temperature (T_N). Above T_N , the susceptibility obeys the Curie-Weiss law for paramagnets but with a negative intercept indicating negative exchange interactions.

Crystal Structure of Hematite



Hematite crystallizes in the corundum structure with oxygen ions in an hexagonal close packed framework. The magnetic moments of the Fe^{3+} ions are ferromagnetically coupled within specific c-planes, but antiferromagnetically coupled between the planes.

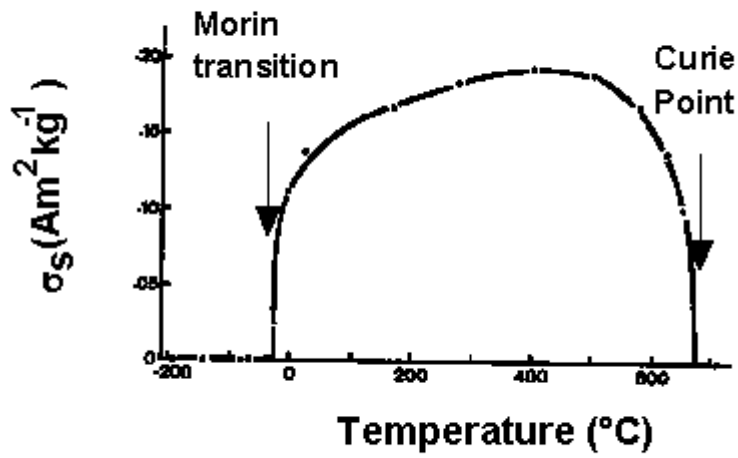


Above -10°C , the spin moments lie in the c-plan but are slightly canted. This produces a weak spontaneous magnetization within the c-plan ($\sigma_s = 0.4 \text{ Am}^2/\text{kg}$).

Below -10°C , the direction of the antiferromagnetism changes and becomes parallel to the c-axis; there is no spin canting and hematite becomes a perfect antiferromagnet.

This spin-flop transition is called the Morin transition.

Hematite



after Dunlop (1971)

Magnetic Properties of Minerals

Mineral	Composition	Magnetic Order	T_c ($^\circ\text{C}$)	σ_s (Am^2/kg)
Oxides				
Magnetite	Fe_3O_4	ferrimagnetic	575-585	90-92
Ulvospinel	Fe_2TiO_2	AFM	-153	
Hematite	$\alpha\text{Fe}_2\text{O}_3$	canted AFM	675	0.4
Ilmenite	FeTiO_2	AFM	-233	
Maghemite	$\gamma\text{Fe}_2\text{O}_3$	ferrimagnetic	~600	~80
Jacobsite	MnFe_2O_4	ferrimagnetic	300	77
Trevorite	NiFe_2O_4	ferrimagnetic	585	51
Magnesioferrite	MgFe_2O_4	ferrimagnetic	440	21

Sulfides				
Pyrrhotite	Fe ₇ S ₈	ferrimagnetic	320	~20
Greigite	Fe ₃ S ₄	ferrimagnetic	~333	~25
Troilite	FeS	AFM	305	
Oxyhydroxides				
Goethite	αFeOOH	AFM, weak FM	~120	<1
Lepidocrocite	γFeOOH	AFM(?)	-196	
Feroxyhyte	δFeOOH	ferrimagnetic	~180	<10
Metals & Alloys				
Iron	Fe	FM	770	
Nickel	Ni	FM	358	55
Cobalt	Co	FM	1131	161
Awaruite	Ni ₃ Fe	FM	620	120
Wairauite	CoFe	FM	986	235

Magnetism & Spectra of lanthanides and actinides

	config.	Ground	No. of			Observed
Ln	Ln ³⁺	State	unpaired e ⁻	Colour	$g_J \sqrt{J(J+1)}$	m_{eff}/m_B
La	4f ⁰	¹ S ₀	0	colourless	0	0
Ce	4f ¹	² F _{5/2}	1	colourless	2.54	2.3 - 2.5
Pr	4f ²	³ H ₄	2	green	3.58	3.4 - 3.6

Nd	4f ³	⁴ I _{9/2}	3	<i>lilac</i>	3.62	3.5 - 3.6
Pm	4f ⁴	⁵ I ₄	4	<i>pink</i>	2.68	-
Sm	4f ⁵	⁶ H _{5/2}	5	<i>yellow</i>	0.85	1.4 - 1.7
Eu	4f ⁶	⁷ F ₀	6	<i>pale pink</i>	0	3.3 - 3.5
Gd	4f ⁷	⁸ S _{7/2}	7	<i>colourless</i>	7.94	7.9 - 8.0
Tb	4f ⁸	⁷ F ₆	6	<i>pale pink</i>	9.72	9.5 - 9.8
Dy	4f ⁹	⁶ H _{15/2}	5	<i>yellow</i>	10.65	10.4 - 10.6
Ho	4f ¹⁰	⁵ I ₈	4	<i>yellow</i>	10.6	10.4 - 10.7
Er	4f ¹¹	⁴ I _{15/2}	3	<i>rose-pink</i>	9.58	9.4 - 9.6
Tm	4f ¹²	³ H ₆	2	<i>pale green</i>	7.56	7.1 - 7.6
Yb	4f ¹³	² F _{7/2}	1	<i>colourless</i>	4.54	4.3 - 4.9
Lu	4f ¹⁴	¹ S ₀	0	<i>colourless</i>	0	0

Magnetic Properties

Paramagnetism

see R.L. Carlin, *Magnetochemistry*, Springer, N.Y., 1986 Chapter 9 for a detailed account

- Magnetic properties have **spin & orbit contributions**

(contrast "*spin-only*" of transition metals)

- Magnetic moments of Ln³⁺ ions are generally well-described from the coupling of spin and orbital angular momenta ~ **Russell-Saunders Coupling Scheme**
- **spin orbit coupling** constants are typically **large** (ca. 1000 cm⁻¹)
- **ligand field** effects are very **small** (ca. 100 cm⁻¹)

P only ground J-state is populated

P spin-orbit coupling >>> ligand field splittings

P magnetism is essentially **independent of environment**

- Magnetic moment of a J-state is expressed by the **Landé formula**

$$\mu = g_J \sqrt{J(J+1)} \mu_B \quad g_J = \frac{3}{2} + \frac{S(S+1) - L(L+1)}{2J(J+1)}$$

Sample Landé Calculation

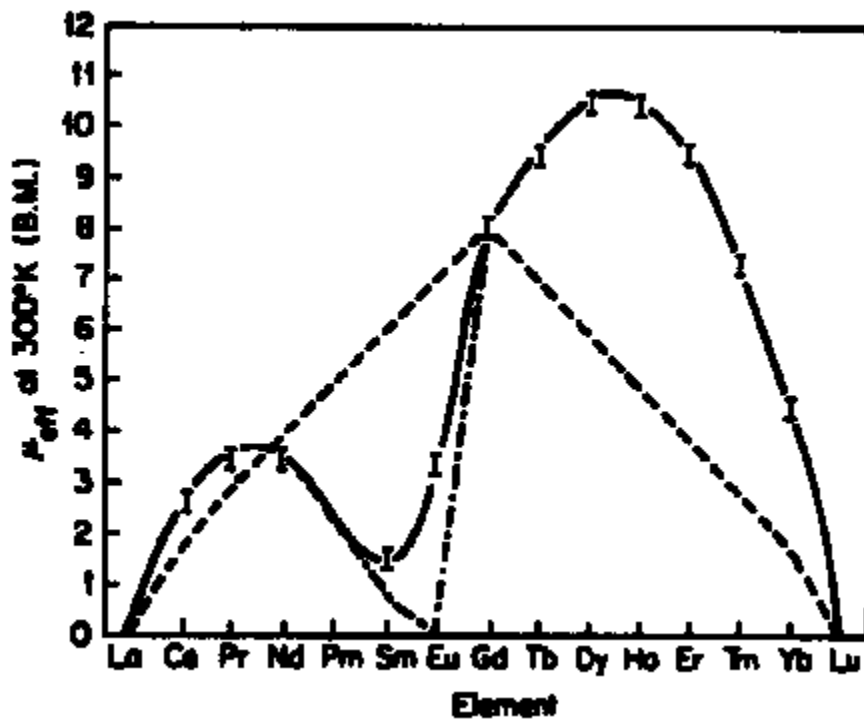
e.g $\text{Pr}^{3+} [\text{Xe}]4f^2$

- Find Ground State from Hund's Rules
 - **Maximum Multiplicity** $S = 1/2 + 1/2 = 1$ **P** $2S + 1 = 3$
 - **Maximum Orbital Angular Momentum** $L = 3 + 2 = 5$ **P** **H** state
 - **Total Angular Momentum** $J = (L + S), (L + S) - 1, \dots, |L - S| = 6, 5, 4$
 - Less than half-filled sub-shell **P** Minimum J **P** $J = 4$

{Greater than half-filled sub-shell **P** Maximum J }

Ln^{3+} Magnetic Moments compared with Theory

Experimental ——— Landé Formula -·-·- Spin-Only Formula - - -






- Landé formula fits well with observed magnetic moments for all but Sm^{III} and Eu^{III}

- Moments of Sm^{III} and Eu^{III} are altered from the Landé expression by **temperature-dependent population of low-lying excited J-state(s)**

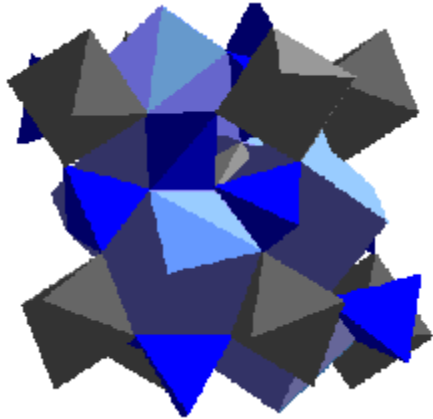
Uses of Ln^{3+} Magnetic Moments?

NMR Shift Reagents - paramagnetism of lanthanide ions is utilized to spread resonances in ^1H NMR of organic molecules that coordinate to lanthanides (*see account of $\text{Eu}(\text{fcam})_3$*)

Ferromagnetism / Anti-Ferromagnetism / Ferrimagnetism

<i>Ferromagnetism</i>	moments align in same direction	
<i>Anti-ferromagnetism</i>	moments align in opposite directions and cancel	
<i>Ferrimagnetism</i>	moments align in opposite directions leaving net residual moment	

- **Lanthanide metals and alloys** have interesting ordered magnetism effects
- **SmCo_5 permanent magnets - FERROMAGNETIC**
 - light weight
 - high saturation moments,
 - high coercivity
 - high magnetocrystalline anisotropy
 - Superior performance magnets for magnetic bearings / couplings / wavetubes & d.c. synchronous motors
- **Garnets**
 - Complex oxides $\text{A}_3\text{B}_2\text{X}_3\text{O}_{12}$
 - A site distorted cubic environment
 - B / X sites octahedral & tetrahedral sites



- **Rare Earth Garnets** *e.g.* $\text{Ln}_3\text{Fe}_5\text{O}_{12}$ and $\text{Y}_3\text{Fe}_5\text{O}_{12}$ (*yttrium iron garnet, YIG*)

FERRIMAGNETISM shows an **unusual temperature-dependence** as **T**,

- moment **∅ to zero** at the *Condensation Temperature*
- above Condensation Temperature moment **rises in the opposite direction to a maximum**
- moment then **∅ to zero** at the *Curie Temperature*. in the normal manner

Spin Crossover

Octahedral complexes with between 4 and 7 d electrons can be either high-spin or low-spin depending on the size of Δ . When the ligand field splitting has an intermediate value such that the two states have similar energies, then the two states can coexist in measurable amounts at equilibrium. Many "crossover" systems of this type have been studied, particularly for iron complexes.

The change in spin state is a transition from a low spin (LS) ground state electron configuration to a high spin (HS) ground state electron configuration of the metal's d atomic orbitals (AOs), or vice versa. The magnitude of the ligand field splitting along with the pairing energy of the complex determines whether it will have a LS or HS electron configuration. A LS state occurs because the ligand field splitting (Δ) is greater than the pairing energy of the complex (which is an unfavorable process).

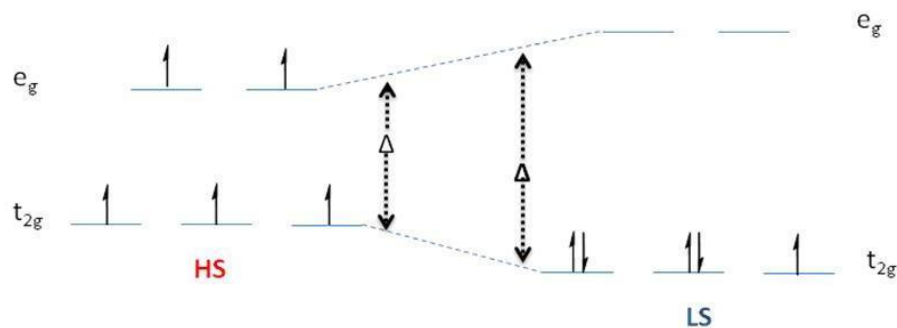
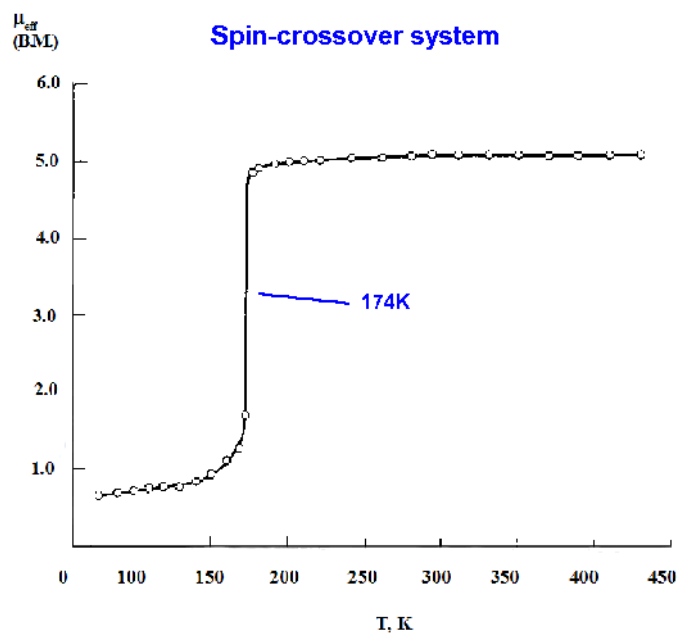


Figure 20.10.120.10.1: Diagram illustrating the dependence of the HS or LS state on Δ of the octahedral ligand field splitting and the corresponding electron configuration.

Figure 20.10.120.10.1 is a simplified illustration of the metal's d orbital splitting in the presence of an octahedral ligand field. A large splitting between the t_{2g} and e_g AOs requires a substantial amount of energy for the electrons to overcome the energy gap (Δ) to comply with Hund's Rule. Therefore, electrons will fill the lower energy t_{2g} orbitals completely before populating the higher energy e_g orbitals. Conversely, a HS state occurs with weaker ligand fields and smaller orbital splitting. In this case the energy required to populate the higher levels is substantially less than the pairing energy and the electrons fill the orbitals according to Hund's Rule by populating the higher energy orbitals before pairing with electrons in the lower lying orbitals. An example of a metal ion that can exist in either a LS or HS state is Fe^{3+} in an octahedral ligand field. Depending on the ligands that are coordinated to this complex the Fe^{3+} can attain a LS or a HS state, as in Figure 20.10.120.10.1.

In the d^6 case of $\text{Fe}(\text{phen})_2(\text{NCS})_2$, the crossover involves going from $S=2$ to $S=0$.



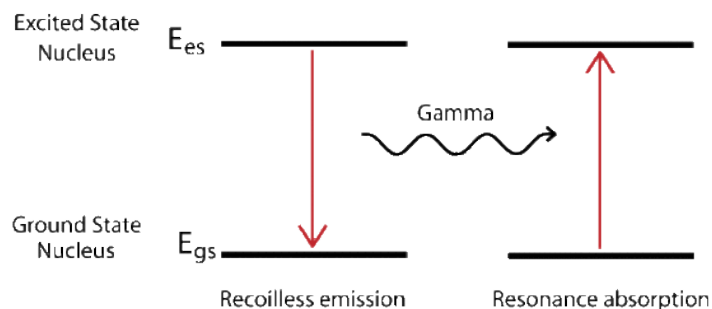
At the higher temperature the ground state is $^5T_{2g}$ while at low temperatures it changes to $^1A_{1g}$. The changeover is found at about 174 K. In solution studies, it is possible to calculate the heat of conversion from the one isomer to the other.

UNIT- V**MÖSSBAUER SPECTROSCOPY**

Mössbauer spectroscopy is a versatile technique used to study nuclear structure with the absorption and re-emission of gamma rays, part of the electromagnetic spectrum. The technique uses a combination of the Mössbauer effect and Doppler shifts to probe the hyperfine transitions between the excited and ground states of the nucleus. Mössbauer spectroscopy requires the use of solids or crystals which have a probability to absorb the photon in a recoilless manner, many isotopes exhibit Mössbauer characteristics but the most commonly studied isotope is ^{57}Fe .

Introduction

Rudolf L. Mössbauer became a physics student at Technical University in Munich at the age of 20. After passing his intermediate exams Mössbauer began working on his thesis and doctorate work in 1955, while working as an assistant lecturer at Institute for Mathematics. In 1958 at the age of 28 Mössbauer graduated, and also showed experimental evidence for recoilless resonant absorption in the nucleus, later to be called the Mössbauer Effect. In 1961 Mössbauer was awarded the Nobel Prize in physics and, under the urging of Richard Feynman, accepted the position of Professor of Physics at the California Institute of Technology.

**Mössbauer Effect**

The recoil energy associated with absorption or emission of a photon can be described by the conservation of momentum. In it we find that the recoil energy depends inversely on the mass of the system. For a gas the mass of the single nucleus is small compared to a solid. The solid or crystal absorbs the energy as phonons, quantized vibration states of the solid, but there is a probability that no phonons are created and the whole lattice acts as the mass, resulting in a recoilless emission of the gamma ray. The new radiation is at the proper energy to excite the next ground state nucleus. The probability of recoilless events increases with decreasing transition energy.

$$P_R = P \gamma(1)$$

$$P_2 \gamma = P_2 \gamma(2)$$

$$2M_{ER} = E_2 \gamma c^2(3)$$

$$E_R = E_2 \gamma^2 M c^2(4)$$

Doppler Effect

The Doppler shift describes the change in frequency due to a moving source and a moving observer. f is the frequency measured at the observer, v is the velocity of the wave so for our case this is the speed of light c , v_r is the velocity of the observer, v_s is the velocity of the source which is positive when heading away from the observer, and f_0 is the initial frequency.

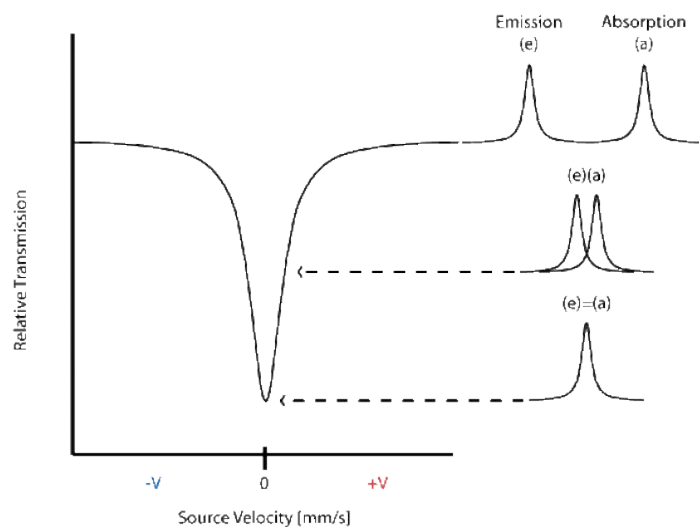
$$f = (v + v_r + v_s) f_0(5)$$

$$f = (c + v_s) f_0(6)$$

In the case where the source is moving toward a stationary observer the perceived frequency is higher. For the opposite situation where the source travels away from the observer frequencies recorded at the observer will be of lower compared to the initial wave. The energy of a photon is related to the product of Planck's constant and the frequency of the electromagnetic radiation. Thus for increasing frequencies the corresponding energy also increase, and the same is true in the reverse case where frequencies decrease and therefore energy decreases.

$$E = hc/\lambda = h\nu(7) \quad E = hc/\lambda = h\nu$$

The energy differences between hyperfine states are minimal (fractions of an eV) and the energy variation is achieved by the moving the source toward and away from the sample in an oscillating manner, commonly at a velocity of a few mm/s. The transmittance is then plotted against the velocity of the source and a peak is seen at the energy corresponding to the resonance energy.



In the above spectrum the emission and absorption are both estimated by the Lorentzian distribution.

Mössbauer Isotopes

By far the most common isotopes studied using Mössbauer spectroscopy is ^{57}Fe , but many other isotopes have also displayed a Mössbauer spectrum. Two criteria for functionality are

1. The excited state is of very low energy, resulting in a small change in energy between ground and excited state. This is because gamma rays at higher energy are not absorbed in a recoil free manner, meaning resonance only occurs for gamma rays of low energy.
2. The resolution of Mössbauer spectroscopy depends upon the lifetime of the excited state. The longer the excited state lasts the better the image.

H																	He																												
Li	Be											B	C	N	O	F	Ne																												
Na	Mg											Al	Si	P	S	Cl	Ar																												
K	Ca	Sc	Ti	V	Cr	Mn	Fe	Co	Ni	Cu	Zn	Ga	Ge	As	Se	Br	Kr																												
Rb	Sr	Y	Zr	Nb	Mo	Tc	Ru	Rh	Pd	Ag	Cd	In	Sn	Sb	Te	I	Xe																												
Cs	Ba	La	Hf	Ta	W	Re	Os	Ir	Pt	Au	Hg	Tl	Pb	Bi	Po	At	Rn																												
Fr	Ra	Ac	Rf	Db	Sg	Bh	Hs	Mt	Ds																																				
<table border="1" style="width: 100%; text-align: center;"> <tbody> <tr> <td>Ce</td><td>Pr</td><td>Nd</td><td>Pm</td><td>Sm</td><td>Eu</td><td>Gd</td><td>Tb</td><td>Dy</td><td>Ho</td><td>Er</td><td>Tm</td><td>Yb</td><td>Lu</td> </tr> <tr> <td>Th</td><td>Pa</td><td>U</td><td>Np</td><td>Pu</td><td>Am</td><td>Cm</td><td>Bk</td><td>Cf</td><td>Es</td><td>Fm</td><td>Md</td><td>No</td><td>Lr</td> </tr> </tbody> </table>																		Ce	Pr	Nd	Pm	Sm	Eu	Gd	Tb	Dy	Ho	Er	Tm	Yb	Lu	Th	Pa	U	Np	Pu	Am	Cm	Bk	Cf	Es	Fm	Md	No	Lr
Ce	Pr	Nd	Pm	Sm	Eu	Gd	Tb	Dy	Ho	Er	Tm	Yb	Lu																																
Th	Pa	U	Np	Pu	Am	Cm	Bk	Cf	Es	Fm	Md	No	Lr																																

Both conditions are met by ^{57}Fe and it is thus used extensively in Mössbauer spectroscopy. In the figure to the right the red colored boxes of the periodic table of elements indicate all elements that have isotopes visible using the Mössbauer technique.

Hyperfine Interactions

Mössbauer spectroscopy allows the researcher to probe structural elements of the nucleus in several ways, termed isomer shift, quadrupole interactions, and magnetic splitting. These are each explained by the following sections as individual graphs, but in practice Mössbauer spectrum are likely to contain a combination of all effects.

Isomer Shift

An isomeric shift occurs when non identical atoms play the role of source and absorber, thus the radius of the source, R_s , is different that of the absorber, R_a , and the same holds that the electron density of each species is different. The Coulombic interactions affects the ground and excited state differently leading to a energy difference that is not the same for the two species. This is best illustrated with the equation:

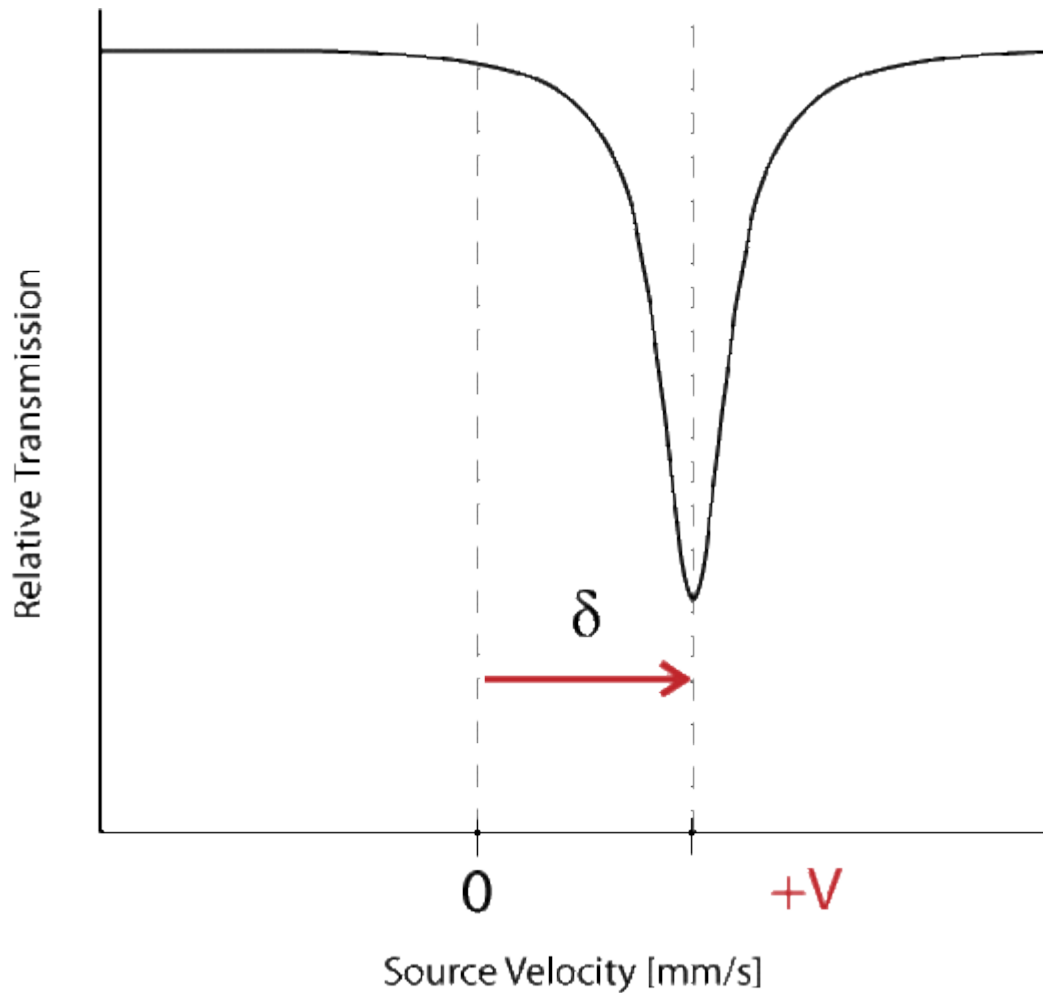
$$R_A \neq R_S \quad (8) \quad R_A \neq R_S$$

$$\rho_S \neq \rho_A \quad (9) \quad \rho_S \neq \rho_A$$

$$E_A \neq E_S \quad (10) \quad E_A \neq E_S$$

$$\delta = E_A - E_S = 23nZe^2(\rho_A - \rho_S)(R_{es}^2 - R_{gs}^2) \quad (11) \quad \delta = E_A - E_S = 23nZe^2(\rho_A - \rho_S)(R_{es}^2 - R_{gs}^2)$$

Where delta represents the change in energy necessary to excite the absorber, which is seen as a shift from the Doppler speed 0 to V_1 . The isomer shift depends directly on the s-electrons and can be influenced by the shielding p,d,f electrons. From the measured delta shift there is information about the valance state of the absorbing atom



The energy level diagram for $\delta\delta$ shift shows the change in source velocity due to different sources used. The shift may be either positive or negative.

Quadrupole Interaction

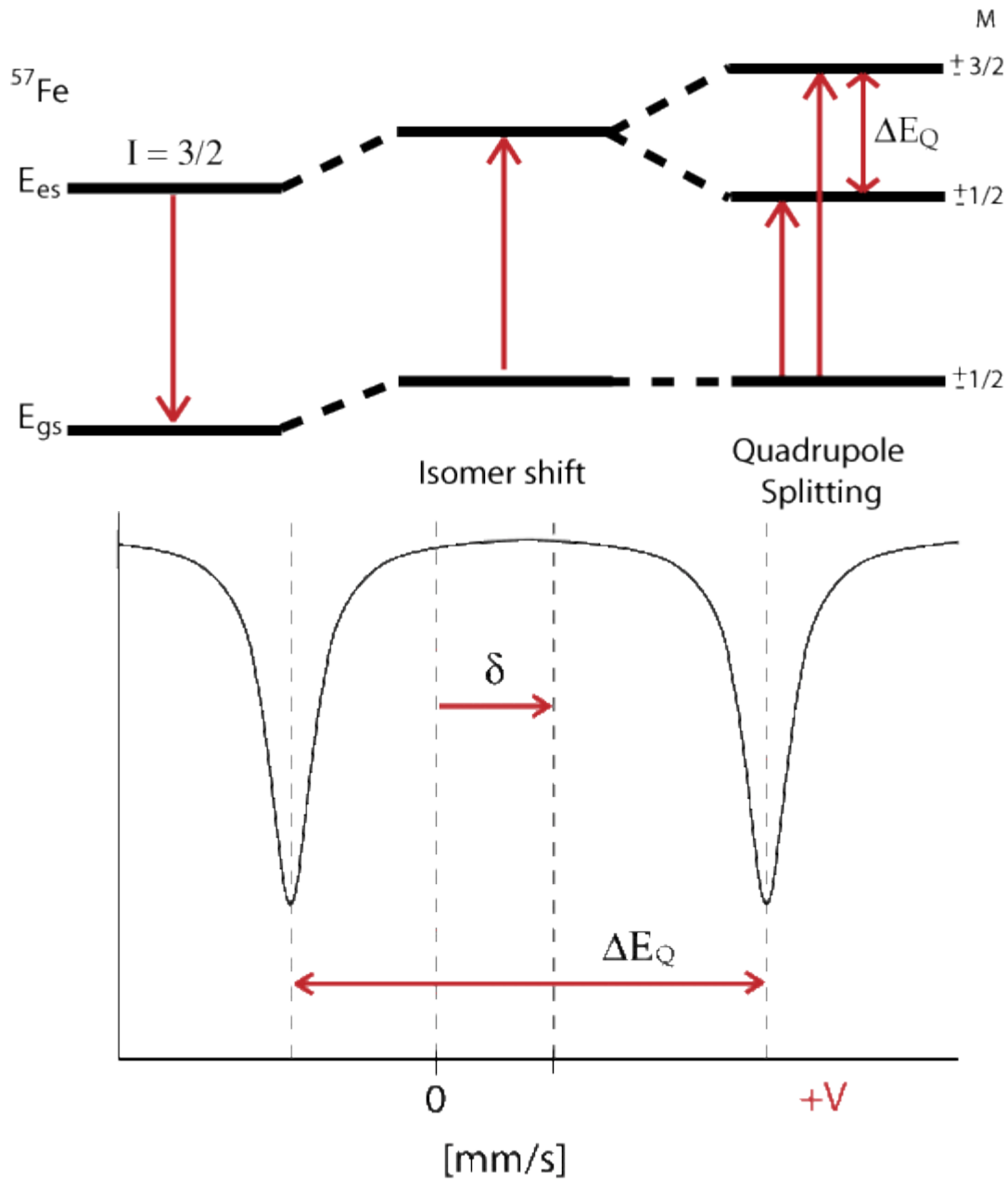
The Hamiltonian for quadrupole interaction using ^{57}Fe nuclear excited state is given by

$$H_Q = eQV_{ZZ} \frac{1}{2} [3I_z^2 - I(I+1) + \eta(I_x^2 - I_y^2)] \quad (12)$$

where the nuclear excited states are split into two degenerate doublets in the absence of magnetic interactions. For the asymmetry parameter $\eta=0$ doublets are labeled with magnetic quantum numbers $m_{es} = \pm 3/2$ and $m_{es} = \pm 1/2$, where the $m_{es} = \pm 3/2$ doublet has the higher energy. The energy difference between the doublets is thus

$$\Delta E_Q = eQV_{zz} \frac{1}{2} [3I(I+1) - 4m_{es}^2] \quad (13)$$

The energy diagram and corresponding spectrum can be seen as

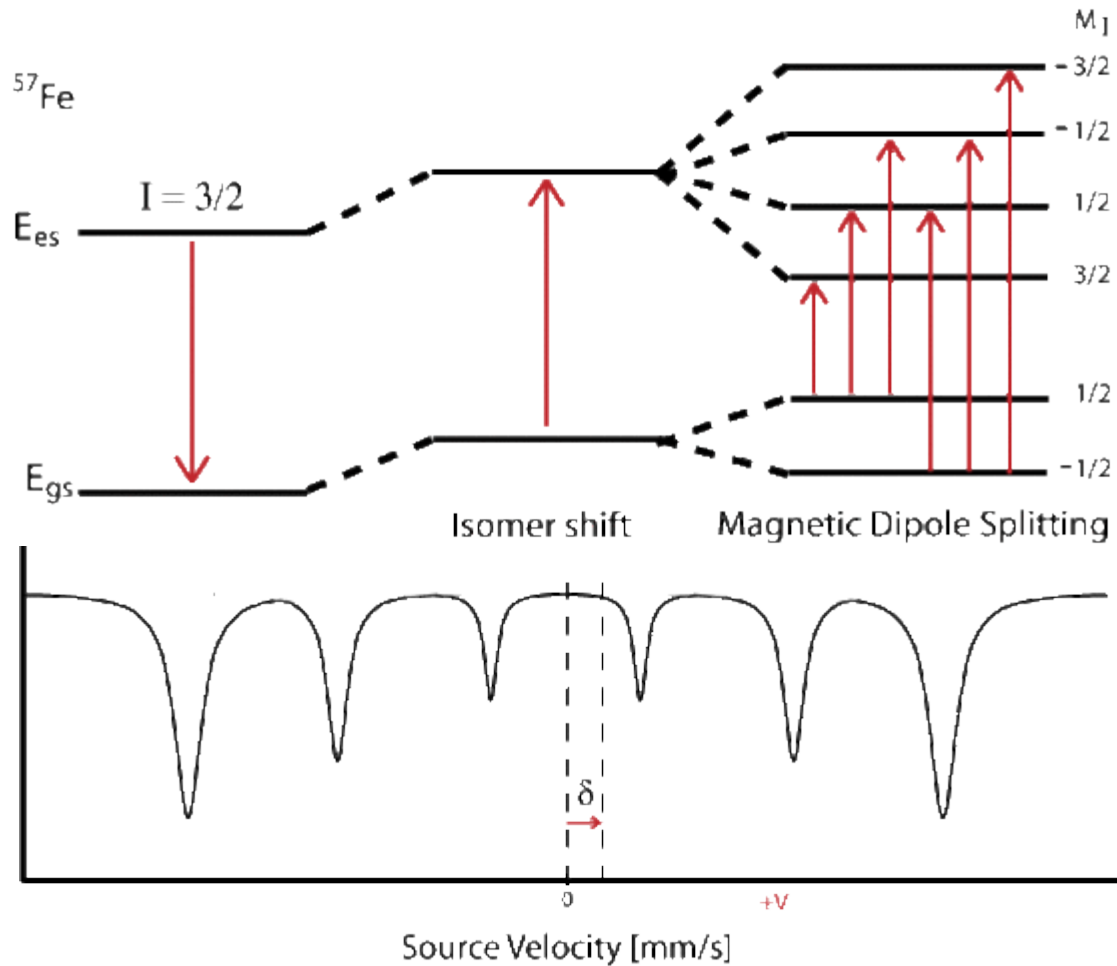


Magnetic Splitting

Magnetic splitting of seen in Mössbauer spectroscopy can be seen because the nuclear spin moment undergoes dipolar interactions with the magnetic field

$$E(mI) = -g_n \beta_n B_{eff} mI$$

where g_n is the nuclear g -factor and β_n is the nuclear magneton. In the absence of quadrupole interactions the Hamiltonian splits into equally spaced energy levels of



The allowed gamma stimulated transitions of nuclear excitation follows the magnetic dipole transition selection rule:

$$\Delta I = 1 \text{ and } \Delta m_I = 0, \pm 1$$

$$m_I(1) m_I$$

is the magnetic quantum number and the direction of β defines the nuclear quantization axis. If we assume g and A are isotropic (direction independent) where $g_x = g_y = g_z$ and B is actually a combination of the applied and internal magnetic fields:

$$H = g\beta S \cdot B + AS \cdot I - g_n \beta_n B \cdot I$$

The electronic Zeeman term is far larger than the nuclear Zeeman term, meaning the electronic term dominates the equation so $\langle S_x \rangle$ and $\langle S_y \rangle$ are approximated by 0 and

$$\langle S_z \rangle = m_s \hbar \quad (17a) \quad \langle S_z \rangle = m_s \hbar$$

and

$$\langle S_x \rangle = \langle S_y \rangle \approx 0 \quad (17b) \quad \langle S_x \rangle = \langle S_y \rangle \approx 0$$

$$H_n = A \langle S_z \rangle \cdot I - g_n \beta_n B \cdot I \quad (18) \quad H_n = A \langle S_z \rangle \cdot I - g_n \beta_n B \cdot I$$

Pulling out a $-g_n \beta_n$ followed by I leaves

$$H_n = -g_n \beta_n (-A \langle S_z \rangle + B) I \quad (19) \quad H_n = -g_n \beta_n (-A \langle S_z \rangle + B) I$$

Substituting the internal magnetic field with

$$B_{int} = -A \langle S_z \rangle \quad (20) \quad B_{int} = -A \langle S_z \rangle$$

results in a combined magnetic field term involving both the applied magnetic field and the internal magnetic field

$$H_n = -g_n \beta_n (B_{int} + B) \cdot I \quad (21) \quad H_n = -g_n \beta_n (B_{int} + B) \cdot I$$

which is simplified by using the effective magnetic field B_{eff}

$$H_n = -g_n \beta_n B_{eff} \cdot I \quad (22) \quad H_n = -g_n \beta_n B_{eff} \cdot I$$